The predicting brain

Anticipation of moving objects in human visual cortex

Wouter Schellekens

Colofon

The studies described in this thesis were performed at the Brain Center Rudolf Magnus, Department of Neurology & Neurosurgery, University Medical Center Utrecht, The Netherlands.

ISBN: 978-94-6295-182-2

Cover & lay-out by Wouter Schellekens

Printed by Proefschriftmaken.nl || Uitgeverij BOXPress

Published by Uitgeverij BOXPress, 's-Hertogenbosch

The predicting brain

anticipation of moving objects in human visual cortex

Het voorspellende brein

anticipatie van bewegende objecten in humane visuele cortex

(met een samenvatting in het Nederlands)

Proefschrift

ter verkrijging van de graad van doctor aan de Universiteit Utrecht op gezag van de rector magnificus, prof.dr. G.J. van der Zwaan, ingevolge het besluit van het college voor promoties in het openbaar te verdedigen op woensdag 13 mei 2015 des middags te 16.15 uur

door

Wouter Schellekens

geboren op 20 juni 1983
te Rotterdam

Promotor: Prof.dr. N.F. Ramsey

Copromotor: Dr. M.A.H.L.L. Raemaekers

The empires of the future are
the empires of the mind

Winston Churchill

Table of contents

1	Introduction	**9**
2	Integration of motion responses underlying directional motion anisotropy in human early visual cortical areas	**25**
3	Predictive coding for motion stimuli in human early visual cortex	**47**
4	Predictions to motion stimuli in early visual cortex: effects of motion displacement on motion predictability	**73**
5	Changes in fMRI BOLD dynamics reflect anticipation of a moving object in human early visual cortex	**95**
6	Summary and discussion	**115**
7	Nederlandse samenvatting	**133**
	List of abbreviations	**141**
	List of publications	**145**
	Curriculum Vitae	**149**
	Dankwoord	**153**

Chapter 1

Introduction

General Introduction

We hardly ever realize how much sensory information nearly constantly reaches our sensory systems. For instance when we walk through a busy street or drive home during rush hour, we are subjected to an overwhelming load of sensory information coming from a large variety of sources. We often cannot make out precise sounds or smells that reach our sensory systems, but the visual world that we perceive appears stable and coherent. The apparent visual stability is rather remarkable, given that objects move in and out of our visual field and we, the observers, move in our surroundings. As a consequence, visual input itself is highly dynamic. To complicate matters even further, visual information is projected onto the concave surface of the retina in 2D. Therefore, the retina produces a distorted and ambiguous image from the world that lies before our eyes. It is the job of the central nervous system to reconstruct the most likely origins of the retinal stimulations. Whenever the representation of any object translates across the retina, the brain is required to determine correspondence of input signals across visual space and over time. The question not only concerns what external source causes retinal stimulations, but also whether or not the same external source has already been detected at a different in point in space at a previous point in time. This information is necessary for the brain to create stable and coherent interpretations of visual motion. Differential neural responses to novel and previously detected visual motion information are central in this thesis.

Visual Cortex

The importance for the central nervous system to obtain visual stability becomes immediately apparent, when we consider the percentage of cortical surface devoted to visual input. Approximately 30% of the neocortex is related to vision, which is considerably larger than the cortical areas devoted to touch or hearing (8% and 3% respectively). The visual processing stream starts at the retina where photoreceptors transmit input through bipolar cells and interneurons to retinal ganglion cells (RCG). A retinal ganglion cell basically converts the chemical reaction in photoreceptors, as a result from photon absorptions, into a neural signal that is transmitted through the ganglion cell's axon. Immediately at this stage, the visual scenery is decomposed into smaller fractions: each RCG receives input from a specific portion of the retina and thus responds to a specific portion of the visual field. Furthermore, some RGCs respond to light increments (ON cells), whereas others respond to light decrements (OFF cells)[1,2]. The fibers from the

RGCs transmit the retinal information to the lateral geniculate nucleus (LGN), which acts as relay station of visual input, and sends most information to the occipital lobe. Many fibers coming from the LGN terminate in layer 4 of Brodmann area 17, which is positioned medio-posterior in the occipital lobe around the calcarine sulcus. This area is currently recognized as the primary visual cortex, or V1. However, the 'discovery' of the primary visual cortex did not occur until the mid-20th century. At that time there were already clear indications of visual information processing in brain areas around the calcarine sulcus from the Russo-Japanese war in 1905 and the First World War. During these wars, several neurologists noted that bullet and shrapnel wounds to specific parts at the back of the brain could cause visual field defects that were limited to very specific parts of the visual field[3–5]. However, it was the pioneering work of Hubel & Wiesel that revealed several intrinsic response properties of neurons in the primary visual cortex of a cat. Using electrophysiology, they showed that cells in V1 do not fully respond in direct relation to retinal light absorption, but that cells in V1 have a preference for stimulus orientation and/or motion direction[6,7]. Cells in the primary visual cortex receive input from a specific combination of information coming from RGCs to realize the observed stimulus preference. The number of RGCs that project to a single V1 cell is limited, which also causes V1 cells to respond to a specific limited portion of the visual field. The area of the visual field that a visual neuron responds to is referred to as the cell's receptive field, which is shaped as a Gaussian function with a cell's peak response at the center of its receptive field. For 'simple' cells, the center of a receptive field is referred to as the ON-center, whereas the area surrounding the ON-center is called the OFF-surround. Stimuli presented in a cell's OFF-surround lead to a reduction in the cell's responses. Information from different ON/OFF RGCs likely contribute to the ON/OFF antagonism found in V1 cells, although clear distinctions between ON/OFF regions were not found for all V1 cells (i.e. complex cells).

Despite limited receptive field sizes, all the cells in V1 together make up a complete topographic map of the retinal input, which is referred to as the retinotopic representation of the primary visual cortex. The retinotopic representation is neatly structured on the cortex, showing a map of each half of the visual field in the contralateral hemisphere, which is also mirrored along the horizontal meridian (i.e. lower visual field in the dorsal parts and upper visual field in ventral parts of Brodmann area 17). The fovea is represented

on the occipital pole, while more eccentric portions of the visual field (i.e. peripheral vision) are represented more anterior on the cortex. Furthermore, foveal neurons have the smallest receptive field sizes, suggesting a 'higher resolution' for the part of the visual field on which the observer focuses. Neurons in V1 are heavily interconnected, showing strongest connections between neurons that have similar orientation/direction preferences. These connections are referred to as horizontal or lateral connections and sometimes even stretch over 4 mm on the cortical surface (long range horizontal connections)[8]. Thus, visual input is spatially decomposed for further processing. But how does the brain process this mosaic of local information to obtain stable and coherent percepts?

The primary visual cortex, as the name already suggests, is not the only brain area involved in visual processing. Prior to the studies of Hubel & Wiesel, it was shown that the area lateral to V1 contained an additional retinotopic visual field representation, which was dubbed visual area II, or V2[9]. In a following study, Hubel & Wiesel investigated intrinsic response properties of V2 and additionally identified another area, visual area III (V3), lateral to V2[10]. In terms of anatomy, the visual field representations of V2 and V3 are split in 4 quadrants, whereas the retinotopic organization in V1 is only split in half (i.e. 1 half per hemisphere). Currently, more than 20 visual areas have been identified and many of them exhibit a complete or partial retinotopic representation of the visual field[11,12]. Might it be that each visual area carries out a specific task in visual information processing? Certainly, there are several visual areas that are tightly linked to a specific function in the processing of visual input. Neurons in the medial temporal area (MT) and medial superior temporal area (MST) have been demonstrated to respond specifically to motion stimuli[13–15]. Even further up the hierarchy we find cortical areas that specifically react to faces, body parts, buildings, etc.[16–18]. From this we might conclude that specific categories of visual input are processed by specific cortical areas. However, for the majority of visual areas the 1-area-1-function hypothesis has been proven difficult to demonstrate. Especially in early visual cortex (i.e. V1, V2 and V3), neurons react to all sorts of visual stimuli, although neurons' receptive field sizes increase for cortical areas higher up the processing stream[19–22]. The receptive field size increase is thought to reflect the convergence of visual information from lower-level to higher-level visual areas. Cells in extra-striate areas receive massive projections from V1 neurons[23] and single cells in

V2 have been shown to respond to combinations of visual features[24], which shows how information might be converged from V1 to V2. Nonetheless, neurons that require input of increased complexity, still respond optimally when the visual stimulus is presented within their receptive field. These types of responses are often referred to as classical receptive field effects. In addition to classical receptive field effects, the behavior of a neuron can be modulated by the output of other neurons without the necessity of a direct stimulation within its own receptive field. These extra-classical receptive field effects can account for a large variety of response modulations, such as end-inhibition or visuo-spatial attention[25,26]. Thus, the visual system is able to assess features from all sorts of visual input. But how does it keep track of the performed computations, or in other words, how does it integrate signals over space and time? In motion-rich visual sceneries many external sources can be the cause of orientation and motion signals, which may lead to ambiguous solutions. Several concepts of information integration are introduced in the following paragraphs.

Motion processing

Already in primary visual cortex many neurons are responsive to motion input. These cells are direction selective, meaning that they respond to a limited range of motion directions[15]. In order to signal motion information in a specific direction, the neuron needs to integrate visual contrast information over space and time. The first to model a neuron's mechanism for motion detection were Hassenstein and Reichardt[27] and the proposed motion sensor is often referred to as the Reichardt motion detector. There are several variations of this model, such as motion energy sensors[28] and elaborated Reichardt detectors[29], but all types of motion sensors rely on the integration of contrast over space and time. Simply put, a motion sensitive neuron will only produce a signal, if it detects a change in contrast at two or more spatially separated visual field locations of which at least one change in contrast is temporally delayed. From this it follows that motion sensitive neurons are not merely direction sensitive, but also exhibit a preference for motion velocity[30,31]. Reichardt motion sensors are generally considered as classical receptive field effects, meaning that the combined spatially separated visual field locations from which the sensor extracts its information constitute the motion sensor's receptive field. However, in early visual cortex receptive field sizes (including motion detectors) are still relatively small. This means that any moving object could cause a large chain of motion detectors to become activated,

especially if the motion trajectory covers a considerable portion of the visual field. Despite that motion signals transverse from one detector to the next, human observers do not perceive motion as fragmented snapshots hopping from one part of the visual field to the next. Rather, an additional integration over motion detectors themselves is likely to take place for motion to be perceived as fluent and coherent.

The most straightforward solution to integrate over motion signals is a pooling mechanism. Motion pooling is essentially a summation of motion signals over space and time[32–34]. Correspondence in activity between spatially separated motion detectors can be determined by adding motion signals across visual space, possibly through converging motion signals from V1 to MT[35]. Motion signals are additionally believed to be summated over time[36]. Psychophysical studies have shown that the visual system's sensitivity to motion direction and velocity is positively affected by the number of frames used to present a visual motion stimulus, indicating that motion detector activity is temporally summated[37,38]. Although it is generally believed that summation of motion signals increases sensitivity, temporal summation might also cause a motion smear, or motion blur. For similar reasons why moving objects might come out blurred on a photograph moving objects might cause a smear across cortical representations of the motion trajectory[39,40]. A motion smear would be akin to 'speed lines' that are often drawn in comics. Spatial motion integration might actually benefit from blurred cortical representations of motion trajectories to determine global motion directions. However, motion percepts increase in sharpness with increasing motion durations, suggesting that the motion smear might be actively suppressed. Possibly, motion-deblurring mechanisms play an important part in the formation of stable motion percepts[41,42].

How motion is integrated by the visual system over spatially extended visual field locations, might be exposed by investigation of directional motion biases. Using functional MRI (which will be explained in more detail below), several studies have reported biased motion responses at particular visual field locations for specific motion directions[43–45.] Raemaekers et al. (2009)[43] showed that a random dot kinematogram (Figure 1) consistently resulted in enhanced neural activity for representations in human early visual cortex subjected to radial motion (i.e. centrifugal and centripetal motion). Additionally, directional motion biases disappeared when the motion stimulus was partially occluded along the motion

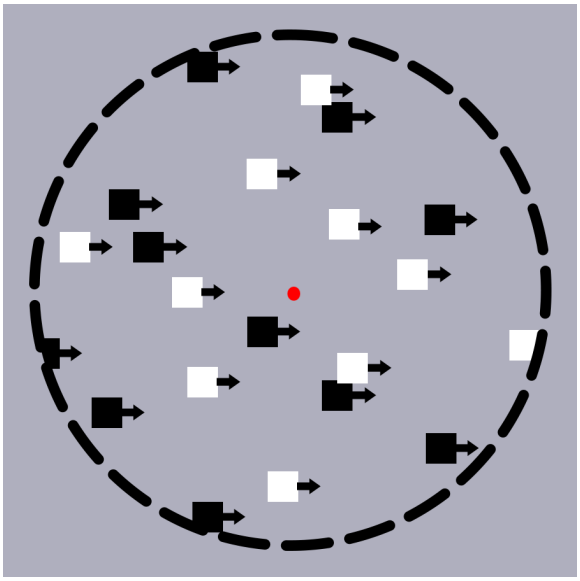

Figure 1. Random dot kinematogram. *Example of a moving random dot stimulus, which often consists of high spatial contrast signals, such as black and white dots (as in this example) or Gabor patches. Each dot can have its own motion vector (arrows). The current example shows all dots moving in the same rightward direction. The stimulus is presented within a large aperture denoted by the dashed line (not visible in experiments), resulting in a patch of motion information at a constant location within the visual field. In the current example with only rightward motion, dots appear at the left side of the stimulus, which is called the motion trailing edge. At the opposite side (i.e. leading edge) dots disappear from the stimulus area. In the middle of the stimulus a fixation dot is often presented.*

trajectory. The latter result may indicate that directional motion biases emerge as a result of motion integration over extended visual field locations. Furthermore, the biased motion responses may be related to an a priori preference of the visual system for radial motion. During self-locomotion in a forward direction, the entire visual field moves on the retina in centrifugal directions. The opposite is true when we move backwards: every object translates on the retina in a centripetal direction. It would make sense if the visual system exhibits a built-in bias for centrifugal and centripetal motion directions. Psychophysical studies have indeed confirmed sensitivity biases during direction discrimination tasks to centrifugal[46,47] and/or centripetal motion directions[48,49]. The visual field locations of directional motion biases could provide additional insight into visual motion processing. The biased cortical motion responses were found for locations where novel dots enter the visual field. Plausibly, neurons in visual cortex respond differently to novel input compared to visual input that has already been signaled by other neurons. Could it be that the visual system predicts upcoming input during visual motion integration?

Predictive coding

The brain needs to reconstruct the most likely causes of external signals reaching sensory nerves of any modality. However, any sensory stimulation can theoretically be evoked by

an almost infinite number of causes. It is unlikely that the brain computes all possibilities and weighs one against the other to find the best fitting solution. Instead, the brain would converge on a specific solution that has the highest probability of being true. This view of neural computations is widely accepted and is regarded as the main reason for illusions and other perceptual phenomena such as the aperture problem[50] and McGurk effect[51]. For the brain to find the optimal solution, several studies have suggested that predictions are estimated, directing neural processes towards likely scenarios. Prediction estimation would virtually occur at any level of processing, including predictions of individual (motion) signal detectors. The encoding of neural signals through predictions is generally referred to as 'predictive coding'. Although the term predictive coding was coined several decades ago, it was popularized by the study of Rao & Ballard[52]. Rao & Ballard described a simple mechanism of predictive coding for visual cortical neurons (Figure 2). The mechanism aims to inhibit neural responses to input that can be predicted by means of several feedforward and feedback connections. Predictive coding entails the existence of neurons that estimate predictions of lower-level neuronal input, the 'predictive estimator'. The response of a single neuron that receives a particular input is inhibited by a feedback prediction signal from the predictive estimator of that neuron. Neurons would therefore only signal the difference between input and prediction, which is called the prediction error. The prediction error is fed forward to the predictive estimator and used to update the old predictive state to the new one and therefore determines the inhibition which is fed back to the signaling neuron. This leads to a mechanism, where detector neurons (e.g. motion detectors) would ideally only signal events that were not predicted. No output would occur when a neuron's input matches the predicted state. Such a mechanism would imply that a moving object that enters the visual field is unlikely to be predicted for motion sensitive neurons that represent that portion of the visual field, resulting in a large prediction error and, hence, a large neural response. The further the object moves across visual space, the more accurate predictions will be for motion detectors along the object's trajectory. Note that predictions in this sense are not deterministic, but rather reflect a probability distribution similarly as described by Bayesian statistics[53].

There are several benefits to neuronal predictive computations. Firstly, they allow for discriminating between novel and previously detected input as neuronal firing changes in direct relation to the prediction error. Prediction errors to motion input would provide

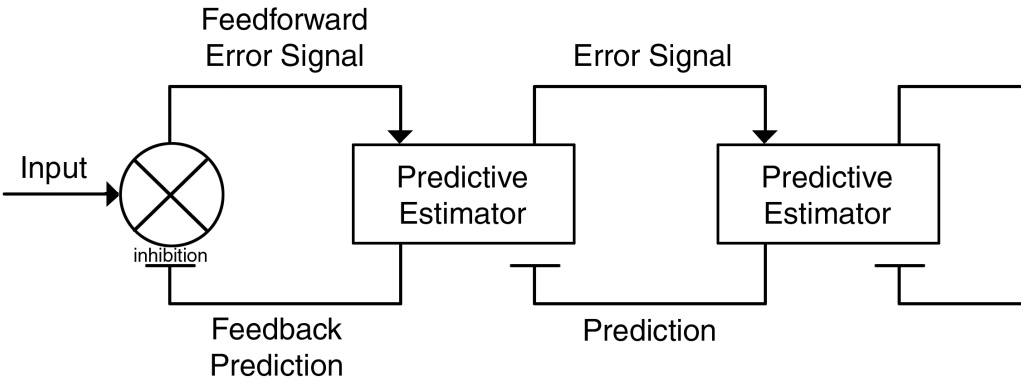

Figure 2. Hierarchical model predictive coding. *The schematic depicts the flow of feedforward and feedback connections in a predictive coding model. On the left of the figure, a detector neuron receives input from lower-level cells and a feedback inhibition signal from the 'predictive estimator'. The inhibition equals the estimated prediction. The detector neurons therefore only signals the prediction error, which is fed forward to the predictive estimator to update the current predictive state. Predictive estimators consist of neurons representing the predictive state of which the output can also be adjusted by higher-level predictions.*

detailed information on motion trajectories and would do so for each individual motion stimulus. Changes in prediction error may be both necessary and sufficient for the visual system to determine correspondence among motion signals. Secondly, predictive coding satisfies the 'free-energy principle'[54]. Here, the free-energy principle simply states that neural processes are construed in such a way that the required energy resources are minimized. This condition is met in predictive coding, since neuronal input that can be predicted is inhibited. In addition, it is worth noting that the free-energy principle is not a goal per se, but rather a means to an end: to process sensory input in the most energy efficient manner. Thus, predictive coding could offer an explanation why human observers perceive motion as fluent, rather than as fragmented snapshots. By anticipating the motion trajectory, the visual system is supplied with adequate tools to stitch space, time and external cause together.

Functional MRI and the BOLD response

The current thesis exploits high-field functional Magnetic Resonance Imaging (fMRI) as a method for measuring brain activity. The first fMRI studies were conducted in the early 1990's and since then its usage and contribution to the field of neuroscience has grown

considerably. One important reason for fMRI's popularity, is that it allows for non-invasive measurements of brain activity in humans with high spatial resolution. To understand the workings of functional MRI, the main concepts of MRI are introduced first.

Magnetic resonance imaging relies on a particular characteristic of an atom's nucleus: its spin. Normally, a nucleus' spin-axis is randomly oriented and not specifically aligned to neighboring nuclei. When placed in a strong magnetic field, the spin-axis of the nucleus aligns to the direction of the magnetic field (B0). This applies to many nuclei, and as a result the tissue becomes slightly magnetized. If additional energy in the form of a radio frequency pulse is applied to the tissue, the net magnetic vector of the tissue is deflected. Absorption of the radio frequency pulse depends on the resonance frequency of the atom of interest (e.g. hydrogen) which is fully dependent on the strength of the surrounding magnetic field. In most cases the nucleus of the hydrogen atom is used due its abundance in water and fat and thus in human tissue. When the radio frequency pulse is no longer applied, the nucleus' spin-axis returns to its initial state in alignment with B0, while releasing energy as electromagnetic waves, which are recorded by a receiver coil. The time it takes the nucleus to align itself again to the B0-field is called T1-relaxation. The T1-relaxation time varies, depending amongst others on the type of tissue in which the hydrogen atom resides. Small differences in relaxation time are used to differentiate between different types of tissue. The radio frequency pulse produces an additional magnetic field along the transverse plane of B0, which is called the B1-field, causing nuclei to spiral along the transverse plane. The transverse magnetization that is measured depends on the alignment of the spins, which drops rapidly after excitation due to magnetic field inhomogeneities and spin-spin interactions. The decay in net transverse magnetization due to spin-spin interactions is called the T2-relaxation time. The combined effect of T2 with other factors influencing decay of transverse magnetization is known as T2*, and it is exactly this T2* that lies at the heart of fMRI[55].

When any brain area becomes active, the blood flow is locally increased to supply the necessary resources. Besides glucose, red blood cells are carried along that contain hemoglobin, which is able to bind oxygen. Hemoglobin that carries oxygen (i.e. oxyhemoglobin) is diamagnetic, meaning it does not react to a magnetic field, whereas hemoglobin that does not carry oxygen (i.e. de-oxyhemoglobin) is para-magnetic and is

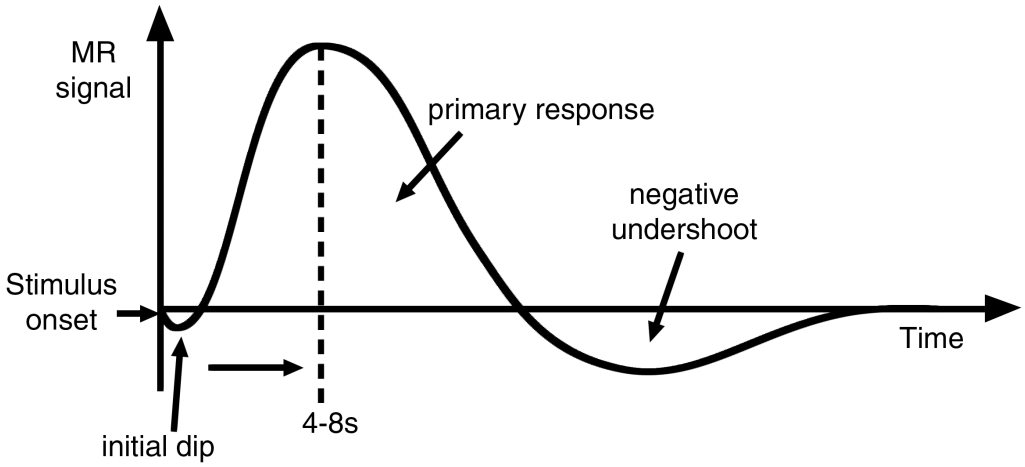

Figure 3. fMRI BOLD response. *The figure depicts a Blood-Oxygen-Level Dependent (BOLD) response. Immediately following the onset of a stimulus, the BOLD response may show an initial dip. The response subsequently peaks at around 4-8 seconds (primary response). After stimulation, the BOLD signal shows a negative undershoot before returning to baseline.*

sensitive to the magnetic field. De-oxyhemoglobin locally disturbs the magnetic field and causes a local drop in MRI signal. These differences in magnetic properties of oxy- versus de-oxyhemoglobin have an effect on T2*-relaxation. When a brain area becomes active, the ratio between oxyhemoglobin and de-oxyhemoglobin increases, resulting in a more homogeneous magnetic field around the capillary bed, resulting in longer T2* relaxation and a higher MR-signal. This results in a characteristic Blood-Oxygen-Level Dependent (BOLD) response. (Figure 3). The BOLD signal consists of an initial dip, caused by the relative decrease in oxyhemoglobin following neural activity; a large positive BOLD signal that peaks around 4-8 seconds; and an undershoot before the signal returns to baseline. fMRI does not measure brain activity directly, but measures dynamics of blood flow and vessels to changes in oxygen demand and is therefore an indirect measure of neural activity. In the current thesis, experiments are conducted at a static B0 field strength of 7 Tesla (7T). The signal-to-noise ratio (SNR) of the BOLD response generally benefits from higher B0 field strengths. There are several reasons why the SNR goes up with higher field strength. For one, the difference in susceptibility between oxygenated and de-oxygenated hemoglobin increases, meaning the impact of de-oxyhemoglobin on the MRI signal is higher. Secondly, large draining veins, which contaminate fMRI at lower field strengths due to apparent activity within vessels that transport hemoglobin away from active regions, become less visible and thus less contaminating. The higher SNR

translates to higher resolution images, faster scanning or increased sensitivity to brain activity.

Outline of this thesis

The current thesis investigates mechanisms for neural integration of visual motion signals, which are necessary for the construction of stable and fluent motion percepts. In general, the experiments make use of the presence or absence of directional motion biases under varying motion conditions. The presence of biased motion responses appears to be closely related to the visual system's ability to integrate motion signals, thereby allowing for the investigation of underlying integration methods[43]. In **Chapter 2**, we investigate whether visual motion is integrated spatially or spatiotemporally. If a chain of motion detectors is disrupted at fixed points in space or time, will the visual system still be able to integrate visual motion input? In **Chapter 3**, experiments are conducted to reveal the contribution of predictive coding mechanisms to visual motion integration. Does the novelty of moving dots determine the amplitude of the BOLD signal or can effects be explained by visuo-spatial attention? In **Chapter 4**, several plausible consequences of motion prediction in early visual cortex are investigated. The spatial extent of prediction effects on the BOLD amplitude is assessed, as well as effects of motion duration and velocity. If the visual system predicts the trajectories of moving dots, then prediction effects are expected along the full trajectory of dots and should be appropriately adjusted for differences in duration and velocity. In **Chapter 5**, experiments are conducted to determine whether motion input is also anticipated for a single moving bar stimulus. Furthermore, we investigate if a disruption of low-level stimulus features influences predictive activation patterns in early visual cortex, while motion stimuli remain predictable at a high-level. In **Chapter 6**, a summery is presented and the results are discussed as well as implications for the field of neuroscience.

References

1. Hartline, H. K. The response of single optic nerve fibers of the vertebrate eye to illumination of the retina. Am J Physiol 121, 400–415 (1938).
2. Balasubramanian, V. & Sterling, P. Receptive fields and functional architecture in the retina. J. Physiol. 587, 2753–67 (2009).
3. Lister, W. T. & Holmes, G. Disturbances of Vision from Cerebral Lesions, with Special Reference to the Cortical Representation of the Macula. Proc. R. Soc. Med. 9, 57–96 (1916).
4. Fishman, R. S. Gordon Holmes , the cortical retina , and the wounds of war. The seventh Charles B. Snyder Lecture. Doc. Ophthalmol. 93, 9–28 (1997).
5. Glickstein, M. & Whitteridge, D. Tatsuji Inouye and the mapping of the visual fields on the human cerebral cortex. Trends in Neurosciences 10, 350–353 (1987).
6. Hubel, D. h & Wiesel, T. N. Receptive fields of single neurones in the cat's striate cortex. J. Physiol. 148, 574–591 (1959).
7. Hubel, D. H. & Wiesel, T. H. Receptive Fields, Binocular Interaction and Functional Architecture in the Cat's Visual Cortex. J. Physiol. 160, 106–154 (1962).
8. Gilbert, C. D. Horizontal integration in the neocortex. Trends Neurosci. 8, 160–165 (1985).
9. Talbot, S. A. & Marshall, W. H. Physiological studies on neural mechanisms of visual localization and discrimination. Amer. J. Ophtalmol. 24, 1225–1264 (1941).
10. Hubel, D. h & Wiesel, T. N. Receptive Fields and Functional Architecture in Two Nonstriate Visual Areas (18 and 19) of the Cat. J. Neurophysiol. 28, 229–289 (1965).
11. Rees, G., Kreiman, G. & Koch, C. Neural correlates of consciousness in humans. Nat. Rev. Neurosci. 3, 261–70 (2002).
12. Van Essen, D. C., Anderson, charles H., Felleman, D. J. & Essen Van, D. C. Informative processing in the primate visual system: an integrated systems perspective. Science (80-.). 255, 419–423 (1992).
13. Zeki, S. M. Functional organization of a visual area in the posterior bank of the superior temporal sulcus of the rhesus monkey. J. Physiol. 236, 549–573 (1974).
14. Allman, J., Miezin, F. & Mcguinness, E. Stimulus Specific Responses from beyond the Classical Receptive Field: Neurophysiological Mechanisms for Local-Global Comparisons in Visual Neurons. Annu. Rev. Neurosci. 8, 407–430 (1985).
15. Albright, T. D. Cortical processing of visual motion. Rev. oculumoter Res. 5, 177–201 (1983).
16. Malach, R., Levy, I. & Hasson, U. The topography of high-order human object areas. Trends in Cognitive Sciences 6, 176–184 (2002).
17. Sergent, J., Ohta, S. & MacDonald, B. Functional neuroanatomy of face and object processing. A positron emission tomography study. Brain 115 Pt 1, 15–36 (1992).
18. Downing, P. E., Jiang, Y., Shuman, M. & Kanwisher, N. A cortical area selective for visual processing of the human body. Science 293, 2470–2473 (2001).
19. Gattass, R., Gross, C. G. & Sandell, J. H. Visual topography of V2 in the macaque. J. Comp. Neurol. 201, 519–539 (1981).
20. Gattass, R., Sousa, A. P. & Rosa, M. G. Visual topography of V1 in the Cebus monkey. J. Comp. Neurol. 259, 529–548 (1987).
21. Burkhalter, A., Felleman, D. J., Newsome, W. T. & Van Essen, D. C. Anatomical and physiological asymmetries related to visual areas V3 and VP in macaque extrastriate cortex. Vision Res. 26, 63–80 (1986).
22. Felleman, D. J. & Van Essen, D. C. Receptive field properties of neurons in area V3 of macaque monkey extrastriate cortex. J. Neurophysiol. 57, 889–920 (1987).
23. Van Essen, D. C., Newsome, W. T., Maunsell, J. H. & Bixby, J. L. The projections from striate cortex (V1) to areas V2 and V3 in the macaque monkey: asymmetries, areal boundaries, and patchy connections. J. Comp. Neurol. 244, 451–480 (1986).
24. Hegdé, J. & Van Essen, D. C. Selectivity for complex shapes in primate visual area V2. J. Neurosci. 20, RC61 (2000).
25. Bolz, J. & Gilbert, C. D. Generation of end-inhibition in the visual cortex via interlaminar connections. Nature 320, 362–365 (1986).
26. Tootell, R. B. et al. The retinotopy of visual spatial attention. Neuron 21, 1409–22 (1998).
27. Reichardt, W. Autocorrelation, a principle for the evaluation of sensory information by the central nervous system. Sens. Commun. 303–317 (1961).
28. Adelson, E. H. & Bergen, J. R. Spatiotemporal energy models for the perception of motion. J. Opt. Soc. Am. A. 2, 284–99 (1985).
29. Van Santen, J. P. H. Van & Sperling, G. Elaborated Reichardt detectors. J. Opt. Soc. Am. A. 2, 300–21 (1985).

30. Orban, G. A., De Wolf, J. & Maes, H. Factors influencing velocity coding in the human visual system. Vision Res. 24, 33–39 (1984).
31. Heeger, D. J. Optical flow using spatiotemporal filters. Int. J. Comput. Vis. 1, 279–302 (1988).
32. Fredericksen, R. E., Verstraten, F. A. & van de Grind, W. A. Spatial summation and its interaction with the temporal integration mechanism in human motion perception. Vision Res. 34, 3171–88 (1994).
33. Burr, D. C. & Santoro, L. Temporal integration of optic flow, measured by contrast and coherence thresholds. Vision Res. 41, 1891–9 (2001).
34. Webb, B. S., Ledgeway, T. & McGraw, P. V. Cortical pooling algorithms for judging global motion direction. Proc. Natl. Acad. Sci. U. S. A. 104, 3532–7 (2007).
35. Barlow, H. & Tripathy, S. P. Correspondence noise and signal pooling in the detection of coherent visual motion. J. Neurosci. 17, 7954–66 (1997).
36. Barlow, H. B. Temporal and spatial summation in human vision at different background intensities. J. Physiol. 141, 337–350 (1958).
37. McKee, S. P. & Welch, L. Sequential recruitment in the discrimination of velocity. J. Opt. Soc. Am. A. 2, 243–51 (1985).
38. Snowden, R. J. & Braddick, O. J. The combination of motion signals over time. Vision Res. 29, 1621–1630 (1989).
39. Burr, D. Motion smear. Nature 284, 164–165 (1980).
40. Geisler, W. S. Motion streaks provide a spatial code for motion direction. Nature 400, 65–9 (1999).
41. Anderson, C. H. & Van Essen, D. C. Shifter circuits: a computational strategy for dynamic aspects of visual processing. Proc. Natl. Acad. Sci. U. S. A. 84, 6297–6301 (1987).
42. Burr, D. C. & Morgan, M. J. Motion deblurring in human vision. Proc. Biol. Sci. 264, 431–436 (1997).
43. Raemaekers, M., Lankheet, M. J. M., Moorman, S., Kourtzi, Z. & van Wezel, R. J. A. Directional anisotropy of motion responses in retinotopic cortex. Hum. Brain Mapp. 30, 3970–80 (2009).
44. Clifford, C. W. G., Mannion, D. J. & McDonald, J. S. Radial biases in the processing of motion and motion-defined contours by human visual cortex. J. Neurophysiol. 102, 2974–81 (2009).
45. Beckett, A., Peirce, J. W., Sanchez-Panchuelo, R.-M. M., Francis, S. & Schluppeck, D. Contribution of large scale biases in decoding of direction-of-motion from high-resolution fMRI data in human early visual cortex. Neuroimage 63, 1623–32 (2012).
46. Ball, K. & Sekuler, R. Human vision favors centrifugal motion. Perception 9, 317–25 (1980).
47. Albright, T. D. Centrifugal directional bias in the middle temporal visual area (MT) of the macaque. Vis. Neurosci. 2, 177–188 (1989).
48. Van de Grind, W. a et al. Inhomogeneity and anisotropies for motion detection in the monocular visual field of human observers. Vision Res. 33, 1089–107 (1993).
49. Raymond, J. E. Directional anisotropy of motion sensitivity across the visual field. Vision Res. 34, 1029–37 (1994).
50. Nakayama, K. & Silverman, G. H. The aperture problem--I. Perception of nonrigidity and motion direction in translating sinusoidal lines. Vision Res. 28, 739–746 (1988).
51. McGurk, H. & MacDonald, J. Hearing lips and seeing voices. Lett. to Nat. 264, 746–748 (1976).
52. Rao, R. P. & Ballard, D. H. Predictive coding in the visual cortex: a functional interpretation of some extra-classical receptive-field effects. Nat. Neurosci. 2, 79–87 (1999).
53. Lee, T. S. & Mumford, D. Hierarchical Bayesian inference in the visual cortex. J. Opt. Soc. Am. A 20, 1434 (2003).
54. Friston, K. The free-energy principle: a unified brain theory? Nat. Rev. Neurosci. 11, 127–38 (2010).
55. Ogawa, S., Lee, T. M., Kay, A. R. & Tank, D. W. Brain magnetic resonance imaging with contrast dependent on blood oxygenation. Proc. Natl. Acad. Sci. U. S. A. 87, 9868–9872 (1990).

Chapter 2

Integration of motion responses underlying directional motion anisotropy in human early visual cortical areas

Wouter Schellekens
Richard J.A. Van Wezel
Natalia Petridou
Nick F. Ramsey
Mathijs Raemaekers

PloS one 8.6 (2013): e67468

Abstract

Recent imaging studies have reported directional motion biases in human visual cortex when perceiving moving random dot patterns. It has been hypothesized that these biases occur as a result of the integration of motion detector activation along the path of motion in visual cortex. In this study we investigate the nature of such motion integration with functional MRI (fMRI) using different motion stimuli. Three types of moving random dot stimuli were presented, showing either coherent motion, motion with spatial decorrelations or motion with temporal decorrelations. The results from the coherent motion stimulus reproduced the centripetal and centrifugal directional motion biases in V1, V2 and V3 as previously reported. The temporally decorrelated motion stimulus resulted in both centripetal and centrifugal biases similar to coherent motion. In contrast, the spatially decorrelated motion stimulus resulted in small directional motion biases that were only present in parts of visual cortex coding for higher eccentricities of the visual field. In combination with previous results, these findings indicate that biased motion responses in early visual cortical areas most likely depend on the spatial integration of a simultaneously activated motion detector chain.

Introduction

Recently, several imaging studies have provided evidence for anisotropies in cortical responses to motion[1–4]. However, the cause of motion anisotropy, or directional motion bias, is not well understood. Raemaekers et al.[4] reported strong centripetal and centrifugal directional motion biases in BOLD responses compared to tangential motion directions in V1, V2, and V3. Importantly, the latter study reported that the directional motion biases disappeared, when motion was occluded by bars orthogonal to the path of motion, whereas the biases remained present when these occluding bars were positioned parallel to the path of motion. This finding is an important indicator that the directional motion biases, as reported by Raemaekers et al.[4], are related to the integration of motion responses across several motion detectors in visual cortex, instead of being the result of local inhomogeneities in the density of motion detectors tuned for a particular motion direction (a local-field inhomogeneity would produce directional motion biases regardless of the position of occluders). This indicates that directional motion biases emerge on a relatively large scale in retinotopic cortex[1,5]. In addition, it suggests that directional motion biases are caused by an integration of motion information along the path of motion similarly as described in human psychophysical studies on motion recruitment[6–10]. An integration of motion information along the path of motion, implies a mechanism where aligned motion detectors influence neuronal activity of neighboring detectors when signaling a particular motion direction, thereby producing directional motion biases. Similar mechanisms have also been previously described in macaque physiological studies on visual neurons in extra-striate cortex, where multiple radially aligned neurons were necessary for the emergence of motion biases[11,12].

The integration of aligned motion detector information can have two distinguishable characteristics that are tested in the current experiment. One option is that integration is only spatial[13–15], meaning that directional biases are dependent on the length of a chain of activated motion detectors. In that case, the length of a motion stimulus parallel to the path of motion determines the extent of the motion integration. A simplified schematic of spatial integration over just two motion detectors is presented in Figure 1A. Alternatively, when the length of the motion stimulus is increased, not only the length of the activated detector chain increases, but also the duration that the individual dots are on the screen. It could, thus, be argued that interrupting the motion stimulus nullifies directional motion

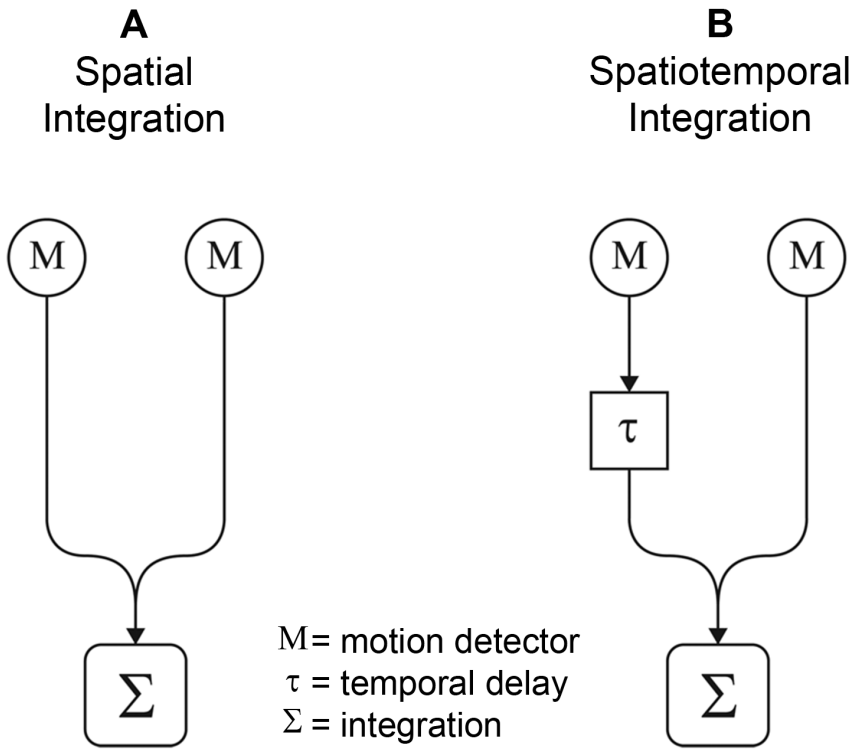

Figure 1. Simplified schematic of motion integration. *Spatial integration (A) only includes spatial information from activated motion detectors, whereas spatiotemporal integration (B) also includes the temporal component of motion detector activity. This figure only displays integration over 2 motion detectors, aligned with the path of motion. The actual motion integration may well extend beyond 2 motion detectors.*

biases by interrupting the trajectories of the individual dots instead of interrupting an activated motion detector chain. A mechanism that keeps track of motion signals from individual dots along a motion trajectory would require a spatiotemporal instead of a spatial integration across aligned motion detectors[16,17]. Therefore, if motion anisotropies are dependent on spatiotemporal information instead of only spatial information, then the duration of individual dots on screen is important for the emergence of directional motion biases. Spatiotemporal integration of motion responses would incorporate a temporal difference (delay) in activation of multiple spatially aligned motion detectors (Figure 1B). The following experiments are conducted to establish the nature of the integration of motion responses underlying directional biases in retinotopic cortex. We hypothesize that directional motion anisotropies emerge as a result of either spatial or spatiotemporal integration of activity of motion detectors. To discriminate these types of integration in

early visual cortical areas, the spatiotemporal correlation of moving dots was disrupted (decorrelated) at fixed points in space (spatial decorrelation) and time (temporal decorrelation). By shortening the spatial extent of coherent motion along the path of motion through spatial decorrelations, motion information integration is limited to the area between spatial decorrelations. This would not discriminate between spatial and spatiotemporal integration of motion. However, if the duration of coherent motion is shortened, while the spatial extent of coherent motion covers more extensive portions of the visual field (temporal decorrelation), spatiotemporal integration will be affected, whereas spatial integration of motion information will not.

Methods

Subjects

Eleven subjects (mean age = 24 years, 6 female) were recruited from Utrecht University. All subjects gave written informed consent for participation. The protocol was approved by the local ethics committee of the University Medical Center Utrecht, in accordance with the Declaration of Helsinki (2008).

Scanning Protocol

Scanning was performed on a 7 Tesla Philips Achieva scanner (Philips Healthcare, Best, Netherlands) with a 16-channel receive headcoil (Nova Medical, MA, USA). Functional MRI (fMRI) measurements were obtained using an EPI-sequence with the following parameters: SENSE factor=2.2, TR=1500 ms, TE = 25 ms, flip angle = 80°, coronal orientation, FOV (AP, FH, LR) = 52 x 169 x 169 mm^3. The acquired matrix had the following dimensions: 26 x 96 x 96, voxel size: 2 x 1.75 x 1.75 mm^3. The functional images were acquired from the posterior 52 mm of the brain, covering the occipital lobe, and were angulated along the z-axis to obtain an orthogonal orientation relative to the calcarine sulcus. Additionally, a T1-weighted image of the whole brain (0.49 x 0.49 x 0.50 mm^3, FOV = 512 x 380 x 512) and a proton density image of equal dimensions were acquired at the end of the experimental sessions.

Stimuli

For stimulus presentation a desktop PC, a projector and a rear projection screen were used. The stimuli were programmed using C++ software (Stroustrup, 1983, Bell

Laboratories, USA). The presentation of the stimuli was triggered by the scanner. All stimuli were projected in a circular aperture with a diameter of 15° visual angle on a grey background. In the center of each stimulus a red fixation dot (with a radius of 0.08° visual angle) was presented within a circular aperture (with a radius of 0.4° visual angle), which was the same color as the background. The mean luminance of the whole stimulus was 42.2 cd/m^2 and did not vary during any of the stimulus presentations. The participants were instructed to focus on the fixation dot at all times and attention to the fixation dot was controlled (see below). In total, five different stimuli were presented: two retinotopic mapping stimuli (polar angle and eccentricity mapping) and three motion stimuli (coherent motion, motion with spatial decorrelations, and motion with temporal decorrelations).

Retinotopic mapping stimuli

Retinotopic maps were acquired using a polar angle mapping stimulus and an eccentricity mapping stimulus. The polar angle mapping stimulus was a rotating wedge with a length of 7.5° visual angle. The width of the wedge was 45° circular angle. The wedge made 4 full rotations: twice clockwise and twice counterclockwise. A total of 192 images was acquired during the polar angle mapping. The eccentricity mapping stimulus was an expanding and contracting ring with a width of 1.5° visual angle, which was 1/5th of the maximum eccentricity (7.5° visual angle). Similar to the polar angle mapping, the eccentricity mapping completed 4 cycles: twice as an expanding ring and twice as a contracting ring. During the eccentricity mapping, 180 images were acquired. Both mapping stimuli consisted of a black and white checkerboard pattern, which switched contrast every 125 ms.

Coherent motion stimulus

The first stimulus was a moving random dot pattern that showed motion at full coherence (Figure 2A). The dot pattern was presented within a circular aperture with a radius of 7.5° visual angle. The entire pattern consisted of approximately 2400 square dots with a width and height of 0.38° visual angle, which were randomly distributed within the circular aperture. Most dots partially overlapped other dots. The dots were 50% black and 50% white and moved at a constant speed of 3.4°/s. In addition, the stimulus was partially occluded by 9 thin bars (0.075° visual angle), placed orthogonally to the path of motion. The occluding bars were never wide enough to block-out an individual moving

dot completely. When a dot reached the stimulus borders, it was randomly redistributed at the other extremity of the stimulus. A block of moving dots lasted for 15 seconds (10 functional images), which was alternated with a 15 seconds rest block showing static dots. During a motion block, the dot pattern moved in 1 of 4 directions: rightwards, downwards, leftwards or upwards. The thin occluding bars were repositioned every time the direction of motion altered, so that their position was orthogonal to the path of motion. In total, one session consisted of 4 cycles, in which all 4 motion directions were presented. During a session 320 images were acquired (Movie S1)[1].

Spatial decorrelation stimulus

The second moving random dot stimulus had the same main characteristics as the coherent motion stimulus described above. However, this stimulus included spatial decorrelations (Figure 2B). The path of a moving dot was disrupted after each occluding bar, located at spatially fixed points within the stimulus. When a dot approached an occluding bar, it gradually disappeared. The dot was randomly repositioned along the length of the bar, where it gradually reappeared. The disruption resulted in ten strips of motion between the nine thin occluding bars and the edges of the stimulus aperture (Movie S2). Therefore, the spatial decorrelations confined the path length of coherent motion to the motion path length in between occluders and stimulus apertures.

Temporal decorrelation stimulus

The third stimulus was a moving random dot pattern, in which the motion stimulus was temporally decorrelated (Figure 2C). All properties of the moving dot pattern were the same as the coherent motion stimulus, except that the dots were randomly and simultaneously redistributed across the entire stimulus every 500 ms (the same duration it took a dot to travel between bars during the spatial decorrelation stimulus). During the stationary period, the dot pattern was also redistributed across the stimulus every 500 ms to control for BOLD signal changes solely caused by the sudden change in contrast of redistributed dots (Movie S3). The path of motion of an individual dot lacked continuity due to disruptions of the stimulus at fixed points in time, while motion remained fully coherent between the dot rescrambling. Thus, the spatial range of coherent motion stretched out over the entire length of the stimulus, while the temporal motion coherence was disrupted every 500 ms.

1 Movies can be viewed at http://journals.plos.org/plosone/article?id=10.1371/journal.pone.0067468

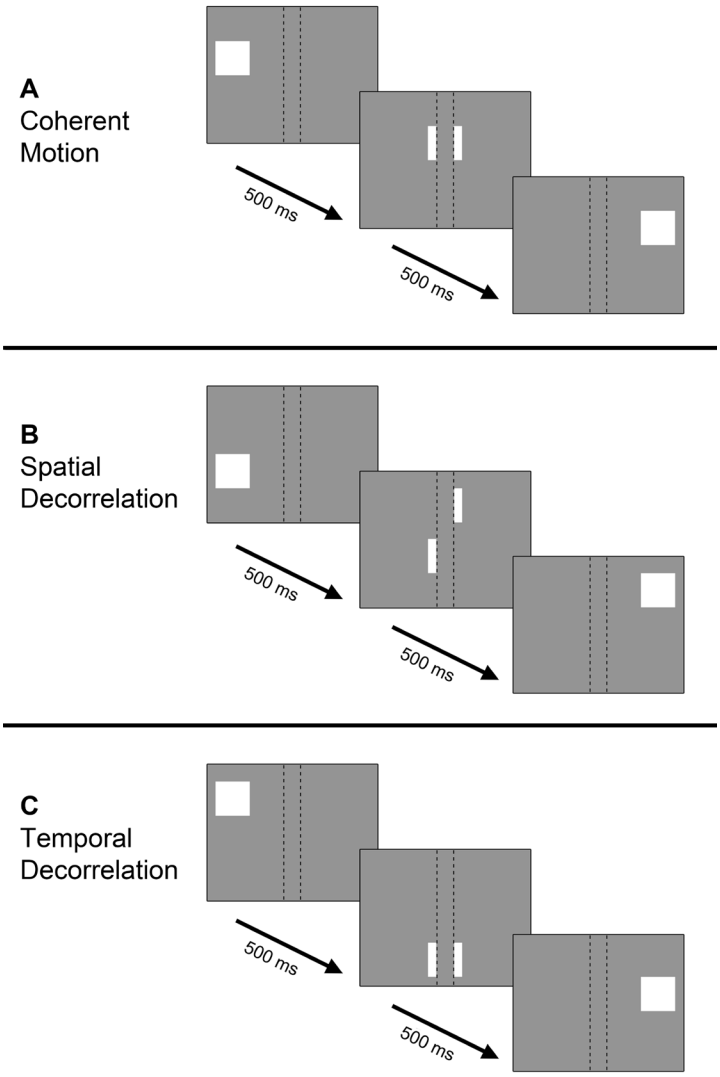

Figure 2. Simplified schematic of motion stimuli. *The behavior of a single dot in timeframes of 500 ms is shown. The occluding bars are denoted by dashed lines, which were not visible during the actual experiments. Coherent motion (A): the dot moves in a straight line. Spatial decorrelation (B): dot moves in a straight line until an occluder, where it is randomly repositioned alongside the other end of the occluder. Temporal decorrelation (C): dot moves in a straight line and is randomly repositioned within the stimulus every 500 ms.*

Attention task

During all experiments, an attention task was presented to ascertain that subjects kept their eyes and spatial attention fixed at the center of the stimulus regardless of the motion direction. During the motion stimuli, a white cross was projected every 1000 ms on top of the red fixation dot. During approximately 25% of all 480 cross-projections an

attention cue was presented, where the white cross was accompanied by a white arrow pointing in one of four directions: left, right, up or down. The participants were instructed to respond with a button press, using a button box with four buttons, that corresponded to the direction of the presented arrow. The inter-trial interval and arrow-direction were randomized.

Statistical Analysis

All functional images were spatially preprocessed using SPM8 (http://www.fil.ion.ucl.ac.uk/spm/). The preprocessing entailed the realignment of all scans to the mean scan, slice time correction and coregistration to the anatomical image. The T1 image was corrected for field inhomogeneities by dividing the T1 image by the proton density image as described by Van de Moortele et al.[18]. Afterwards the corrected T1 image was loaded into the Computerized Anatomical Reconstruction and Editing Toolkit (CARET[19]). The image was resampled to 1 mm isotropic and manually placed into Talairach orientation[20]. By determining gray/white matter intensities, the middle layer of gray matter was estimated and used to reconstruct a surface per hemisphere. Subsequently, the surface reconstruction was inflated and several cuts were applied, among which were cuts along the calcarine fissure and medial wall to obtain a flat map of the corresponding hemisphere. All functional images were mapped onto the surfaces of the left and right hemispheres, using a metric Gaussian mapping algorithm, resulting in a timeserie for every node of the surface. Low frequency noise was removed using multiple regression and a design matrix containing the mean of each image and four cosine functions per experiment, which formed a high-pass filter with a cutoff at 4.2×10^{-3} Hz. For the retinotopic mapping experiments a phase-encoded regressor-matrix was used. The regressor-matrix contained a regressor for every scan during a stimulus cycle and represented the cyclic activation during the presentation of rings (8,000 ms activation every 60,000 ms) and wedges (8,000 ms activation every 64,500 ms) and was convolved with a hemodynamic response function[21]. A correlation coefficient was calculated for every regressor in the regressor-matrix (i.e. every image in a cycle) for every node of the reconstructed surface. The peak correlation of a node determined the eccentricity or polar angle of a node's receptive field. The eccentricity was interpolated over 5 steps: 1.42° visual angle per eccentricity, which covered the maximum width of the stimulus ring. The polar angle coefficients were interpolated over 8 steps, including 4 cardinal and 4 oblique segments.

The visual areas were segmented by drawing borders on the flat representation of the (non-interpolated) polar angle and eccentricity results and contained the striate and extra-striate areas V1, V2, and V3 (Figure 3).

For the analysis of the motion stimuli, only 4 of all 8 polar angle steps were used, 45° circular angle each, that covered the horizontal (left and right) and vertical (top and bottom) meridians, corresponding to the four directions that were used during the motion stimuli. The procedure resulted in 60 segments (4 polar angles x 5 eccentricities x 3 visual areas). The average amount of nodes per segment was m=115.8 with a standard deviation of sigma=55.3 (Table 1). For each segment the percentage of BOLD signal increase was calculated for each relative motion direction (i.e. centripetal, centrifugal and tangential motion direction). The amplitude of the signal increase was estimated using a linear regression, resulting in a beta-value (beta-value) for each segment and motion direction. To test for significant effects, a univariate GLM (general linear model) repeated measures design was adopted for each motion experiment with the following layers: relative motion direction (centrifugal, centripetal, tangential) x visual area (V1, V2, V3) x eccentricity (the 5 eccentricity segments). Using Mauchly's test of sphericity[22] the variables (beta-values) in the univariate repeated measures design were tested for violations of the sphericity assumption. When a variable did not pass the sphericity test, the degrees of freedom were adjusted using Greenhouse-Geisser's epsilon[23].

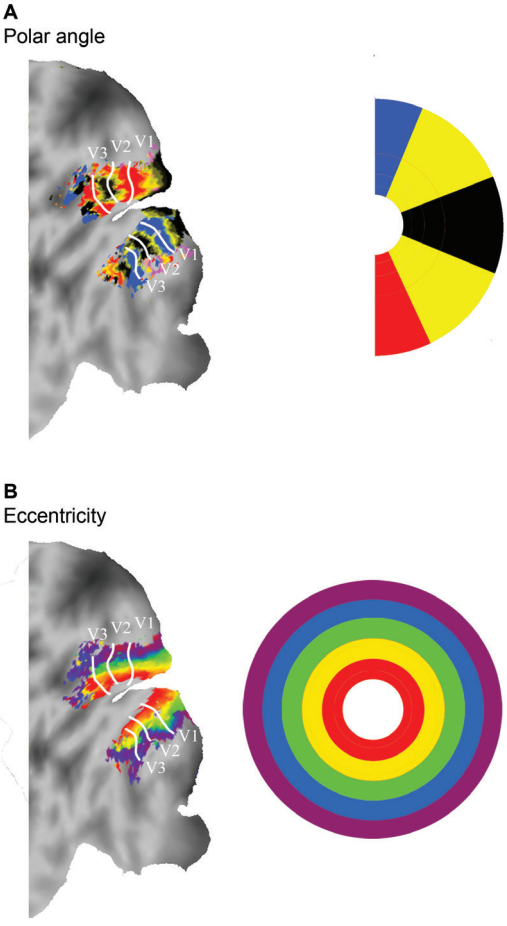

Figure 3. Retinotopic mapping. *Results from the polar angle (A) and eccentricity mapping stimuli (B) on a flattened cortical surface representation of the left hemisphere of one subject (JK). The color bars denote the 4 different polar angles (half of the hemifield) and all 5 eccentricities. The separate visual areas are marked by the white lines.*

To compare the BOLD amplitude of directional biases between stimuli, we calculated the amplitude of the centripetal bias (beta-difference between the centripetal and tangential motion directions) and the centrifugal bias (beta-difference between the centrifugal and tangential motion directions) for each eccentricity. This was done to control for differences in amplitude of motion responses relative to baseline and, therefore, for the different baseline conditions of the motion stimuli. The differences between stimuli in amplitudes of the biases were then tested for significance for each eccentricity using separate T-tests. A MANOVA test (Wilks' lambda) was used to test for differences in the performance on the attention task between motion experiments.

Results

Coherent motion stimulus

The relative motion direction (i.e. centripetal, centrifugal and tangential motion direction) had a significant effect on the BOLD amplitude during the presentation of coherent motion ($F_{(2,20)}$=12.9, p<0.001), indicating the presence of directional motion biases (Figure 4A). However, there was no significant interaction between relative motion direction and visual area ($F_{(4,40)}$=2.4, p=0.069). Figure 5A shows the differences in BOLD amplitude among the visual areas and also shows the presence of biased responses in all three visual areas. There was a strong interaction between eccentricity and motion direction ($F_{(3,32)}$=32.3, p<0.001). The interaction between eccentricity and motion direction is also visible in Figure 4A; a centrifugal bias was mainly observed in the inner eccentricity

	Eccentricities				
	0.40°-1.82°	1.82°-3.24°	3.24°-4.66°	4.66°-6.08°	6.08°-7.50°
Upper visual field	220.3	82.5	62.2	52.8	206.9
Left visual field	177.1	114.6	74.6	62.1	169.8
Lower visual field	149.9	82.6	69.8	52.5	145.1
Right visual field	182.1	108.0	83.2	60.9	158.5

Table 1. Mean number of surface vertices per mapping segment. *Mean number of surface vertices per polar angle visual field representation, 45° circular angle each, per eccentricity.*

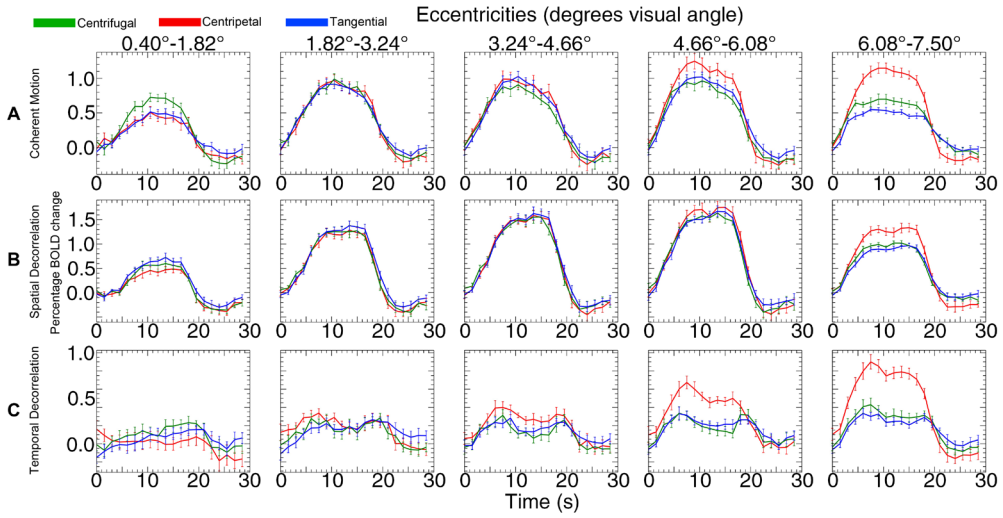

Figure 4. Signal change motion experiments. *Percentage of BOLD signal change (mean V1, V2, V3) is plotted over time (s) for all three motion experiments (n=11). Separate eccentricities are plotted in separate graphs from left to right. The separate lines denote the different motion directions. The error bars denote the standard error of the mean across subjects.*

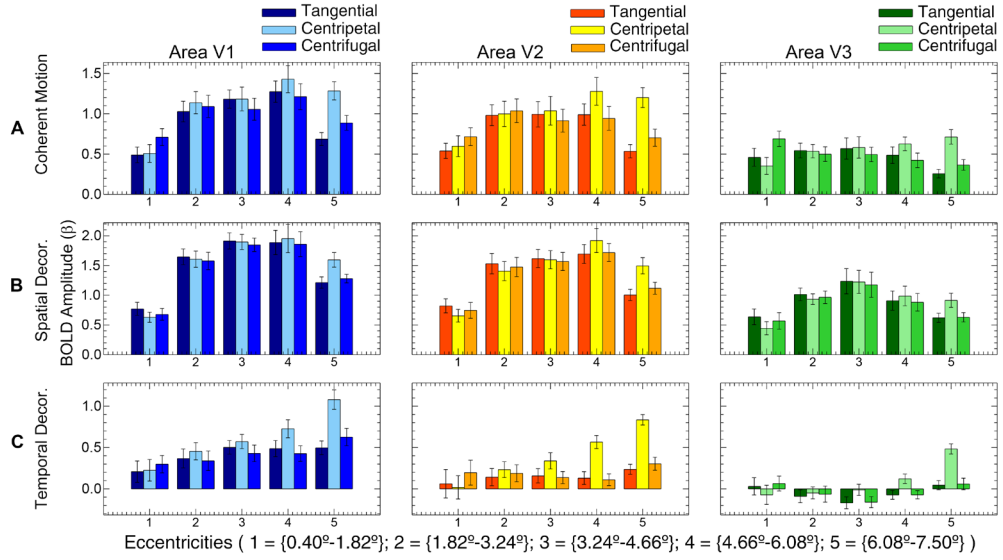

Figure 5. Amplitude motion experiments. *The estimated BOLD amplitude (beta) is plotted over the separate eccentricities (n=11). The results from the separate visual areas are plotted from left to right. The colored bars denote the different motion directions. Error bars denote the standard error of the mean across subjects.*

(0.4°-1.82°), while a centripetal bias was observed in the outer eccentricities (4.66°-7.5°). These results show that we were able to replicate the directional motion biases as reported by Raemaekers et al.[4].

Spatial decorrelation stimulus

The relative motion direction had a significant effect on BOLD amplitude in the spatial decorrelation motion stimulus ($F_{(2,18)}$=3.6, p=0.048). There was no significant interaction between motion direction and visual area ($F_{(4,36)}$=1.0, p=0.400). However, there was a strong interaction between motion direction and eccentricity ($F_{(8,72)}$=14.7, p<0.001), which can be attributed to the small centripetal bias at the border of the stimulus (6.08°-7.5° eccentricity). A centrifugal bias was not present at inner eccentricities (Figure 4B). In sum, we found a small centripetal bias in the far periphery of the stimulus, whereas we found no biased responses for any motion direction in the remaining parts of the stimulus.

Temporal decorrelation stimulus

The temporal decorrelation stimulus resulted in directional motion biases (Figure 4C); the effect of motion direction was significant on the BOLD amplitude ($F_{(2,20)}$=21.2, p<0.001). The interaction effect between motion direction and visual area was also significant ($F_{(4,40)}$=3.2, p=0.022), as was the interaction between motion direction and eccentricity ($F_{(4,38)}$=22.9, p<0.001). This latter interaction is also displayed in Figures 4C and 5C, for a large centripetal bias was measured in the outer eccentricities (3.24°-7.50°) and a small centrifugal bias was present in the inner eccentricity (0.40°-1.82°). These results show that the temporal decorrelation of moving dots did not remove the anisotropy in directional motion responses.

Comparison between motion stimuli

The differences in BOLD amplitude between centripetal and tangential (centripetal bias) and centrifugal and tangential (centrifugal bias) motion directions were compared between stimuli to investigate the effects of the stimulus type on the presence of motion biases using a normalized measure. In the innermost eccentricity (0.40°-1.82°), coherent motion showed a centrifugal bias, which was significantly larger compared to motion with spatial decorrelations ($T_{(20}$)=3.606, P=0.002), but not compared to motion with temporal decorrelations ($T_{(20)}$=1.597, P=0.126). The centrifugal bias difference between motion

with temporal and spatial decorrelations, however, was not significant in eccentricity '0.40°-1.82°' ($T_{(20)}$=1.873, P=0.076).

Centripetal biases were measured in the periphery of the motion stimuli. In eccentricity '4.66°-6.08°', the centripetal bias was not significantly larger for coherent motion compared to motion with spatial decorrelations ($T_{(20)}$=1.152, P=0.263). A large centripetal bias was also measured for motion with temporal decorrelations in eccentricity '4.66°-6.08°', which did not differ from coherent motion ($T_{(20)}$=1.577, P=0.130). However, the centripetal bias in eccentricity '4.66°-6.08°' during motion with temporal decorrelations was significantly larger compared to motion with spatial decorrelations ($T_{(20)}$=3.288, P=0.004). Although all motion stimuli displayed a centripetal bias in the outermost eccentricity (6.08° - 7.50°), the centripetal bias was significantly larger for coherent motion compared to motion with spatial decorrelations ($T_{(20)}$=2.465, P=0.023), while the centripetal bias did not differ between coherent motion and motion with temporal decorrelations ($T_{(20)}$=0.438, P=0.666). Finally, the centripetal bias in eccentricity '6.08° - 7.50°' was significantly larger for motion with temporal decorrelations compared to motion with spatial decorrelations ($T_{(20)}$=2.183, P=0.041). These results show that motion with temporal decorrelations resulted in similar motion biases compared to coherent motion. However, motion with spatial decorrelations only showed centripetal biases in the periphery of the stimulus, which were smaller than the centripetal biases of the other motion stimuli in the same region.

Note that the percentage of BOLD signal change relative to the stationary-dot condition differed substantially between stimuli (Figure 4). On average the signal increase during motion with temporal decorrelations was smaller than the other motion experiments. Possibly the rescrambling of the dot positions during the reference condition of the temporal decorrelation experiment may have elevated the baseline activation. In addition, the baseline elevation appeared to differ per visual area (Figure 5), while motion biases remained significantly present. There was no dot rescrambling during the reference condition of the other two stimuli.

Attention task

Performance data of the attention task was collected from the 3 motion experiments (11 subjects each). Of the 33 sets of psychophysical data 8 sets were excluded due

to technical problems with the button box. The remaining 25 sets of attention task data resulted in 71.9% correct button presses (i.e. after a cue the corresponding button was pressed before the next cue was presented). The percentages of missed and incorrect button presses during the attention task were 27.0% and 1.1% respectively. There was no difference in performance on the attention task between experiments ($F_{(6,40)}$=0.752, P=0.611).

Discussion

General discussion

In this study we presented three motion stimuli to investigate two possible types of motion integration that could underlie directional motion anisotropies in retinotopic areas V1, V2 and V3. As in Raemaekers et al.4, we found directional motion anisotropies for centrifugal and centripetal motion directions during the presentation of coherent motion. The current results only slightly differ with respect to the centripetal bias in lower eccentricities, that was absent during our motion experiments. This may be caused by the current study's larger stimulus area; no motion was presented in the highest eccentricity in the study of Raemaekers et al.4. In contrast to coherent motion, motion with spatial decorrelations showed a centripetal bias only in the outermost eccentricity of the stimulus and no centrifugal bias, whereas motion with temporal decorrelations resulted in motion biases similar to coherent motion.

If directional motion biases depend on an integration of spatial information of aligned motion detectors along the path of motion, then a disruption of motion coherence at fixed points in space will diminish motion biases, while a disruption of motion coherence at fixed points in time will not. On the other hand, if a temporal delay between aligned motion detectors is included in the integration of motion responses, then motion with either temporal or spatial decorrelations will result in a disappearance of directional motion biases. The spatial decorrelation stimulus showed that disrupting the path of moving dots at fixed points in visual space results in a disappearance of motion biases, except for a small centripetal bias in the periphery of the stimulus. However, when motion is disrupted at fixed points in time, directional motion biases will emerge similarly compared to coherent motion.

Although both hypothesized types of motion integration predict a complete disappearance of motion biases during motion with spatial decorrelations, a small centripetal bias in the periphery of the stimulus is observed during motion with spatial decorrelations. A putative explanation for the presence of this peripheral bias may be that a decorrelation at a fixed point in space does not always fully disrupt the activity of a motion detector chain at that point in the visual field. On-off detectors, which motion detectors are thought to pool from, are known to have overlapping receptive fields[24,25], and receptive field size increases with eccentricity[26,27]. Motion detectors that pool from cells with overlapping receptive fields can detect spatiotemporal motion coherence across a spatial decorrelation, which would result in a failure to effectively disrupt the motion detector chain. The larger the receptive fields, the more likely it becomes that motion detectors remain unaffected by small spatial decorrelations. This could cause a differential effect for the fovea and the periphery as is observed in the current study. This explanation is supported by the fact that directional biases were completely absent in a previous study[4], when large occluding bars were used instead of decorrelations to interrupt the motion detector chain. Large occluding bars will disrupt the motion detector chain, even for large overlapping receptive fields. Alternatively, the decrease or disappearance of motion biases during motion with spatial decorrelations and orthogonally placed occluders, could be related to the presence of orthogonally oriented (second-order) motion contours[2,28]. Motion-defined boundaries are clearly present at the spatial decorrelation locations and are orthogonally oriented relative to the direction of motion, which could possibly nullify any radial motion bias. However, such a scenario cannot explain, why specifically centrifugal or centripetal motion directions are affected, while second-order motion contours would affect centrifugal and centripetal motion directions to a similar extent. The current results, thus, indicate that it is not the traveled distance of individual dots that causes the motion biases, but rather the spatial length of an activated motion detector chain. Directional motion biases most likely result from a spatial instead of spatiotemporal integration of motion detector activity.

The dependence of directional motion biases on the spatial extent of an activated motion detector chain may be related to motion recruitment[6,9,10]. The psychophysical study of Van Doorn et al.[6] showed that motion detection mainly depends on the length of the path of motion and that the number of estimated activated motion units increases with a power of 1.6th of the motion path length. Thus, motion sensitive units are progressively recruited

in the direction of motion. In light of current results, motion biases may be a product of motion detector recruitment, which is aborted when a motion detector chain is interrupted. In addition, it has been suggested that the summation of detector information in motion recruitment is linear[8,29]. The centripetal bias during motion with spatial decorrelations can be the result of a linear spatial integration, given an ineffective disruption of the motion detector chain in the periphery of the stimulus.

The current results indicate that directional motion biases are most likely related to contextual or extra-classical receptive field effects instead of local inhomogeneities in detectors tuned for a particular motion direction. However, the mechanisms behind these extra-classical receptive field effects are still unknown. One possibility is that top-down influences from areas such as MT or MST play a role, as these areas are known to contain mechanisms for global motion perception of translating objects[30–32]. Theoretical frameworks of global motion perception have included the integration of local spatial as well as temporal motion information[17,33,34]. Additionally, recent studies on global motion perception suggest the presence of an adaptive pooling mechanism, allowing the visual system to switch between motion integration mechanisms, depending on the availability of particular motion information[35,36]. However, upstream areas related to global motion perception (e.g. MT and MST), have large receptive field sizes[37,38] and are not believed to be specifically sensitive to differences in spatial and temporal discontinuities, and subsequently provide differential feedback. Alternatively, top-down processes and feedback loops are present within early visual areas as well[39,40]. For example, extraclassical receptive field effects could be mediated through long-range horizontal connections. Long-range horizontal connections are known to cover large areas of striate and extra-striate cortex and have also been reported to facilitate contour and orientation detection[41,42]. In addition, it has been suggested that motion and orientation biases share a mutual underlying mechanism[2,43,44]. Clifford et al.[2] suggest that directional motion biases arise as a result of blurred temporal integration, resulting in motion streaks. Depending on the orientation of a motion streak, motion biases might emerge, which directly links motion biases to orientation biases. However, motion streaks cannot explain why the current experiment is able to discriminate between centripetal and centrifugal motion biases, since for both motion directions the motion streak would be roughly the same. As the presence or absence of directional biases is dependent on local features of the

motion stimulus, we believe anisotropies in long-range horizontal connections or other forms of local connectivity are at least necessary for the emergence of the directional motion biases.

There are a couple of factors that could have confounded the observed findings. Firstly, there is the possibility that the motion stimuli induced different eye movements for different motion directions. Eye movements are known to potentially influence low-level activity within the (extra-) striate cortex[45]. Secondly, covert spatial attention is also known to locally enhance visual responses[46,47] and motion could induce an attentional drift in the direction of motion or opposite to the direction of motion. However, in a previous study we found that directional motion biases are not related to differences in the fixation position nor the direction of microsaccades during different motion directions, while using similar stimuli as the current study[4]. Furthermore, subjects performed an attention task to keep their eyes and spatial attention fixed on the center of the stimulus. Performance on this task was well above chance (72% correct) and did not differ between the motion experiments. Another possible confounding factor is the usage of a different baseline condition for the temporal decorrelation stimulus with respect to the other motion stimuli. As is reported in the results section, the BOLD-response to motion with temporal decorrelations were considerably more noisy than the BOLD-responses of the other motion stimuli. Furthermore, the transient responses to the repetitive redistribution of dots every 500 ms, might have altered neuronal responses by means of adaption to contrast or changes to motion-after effects. However, we did find the same pattern of directional motion biases for motion with temporal decorrelations and coherent motion. One would expect that, if repetitive transient responses had an effect on directional motion biases, the pattern of motion anisotropy would differ from coherent motion. In addition, the redistribution of dots will briefly activate motion sensitive neurons with direction preferences other than the direction of the stimulus motion. This could possibly lead to a brief bistable percept or other effects, such as reverse-phi like phenomena[48,49]. However, the redistribution of dots was random and, thus, would equally stimulate motion detectors with different direction preferences. Furthermore, dot redistribution with equal contrast change was also present during baseline condition, which could lead to the exact same effects. It is, therefore, unlikely that the redistribution of the dots has confounded the observed BOLD signal changes.

Future research should address the nature of these directional biases in light of functional and evolutionary benefits. It would be interesting to investigate, as to whether the absence or presence of directional motion biases can be related to certain perceptual qualities, e.g. the saliency of coherent motion presented on a certain background[50,51]. The role of the different visual areas on directional motion biases should also be of future interest. For coherent motion there was no interaction between motion direction and visual areas, while during motion with temporal decorrelations there was a significant interaction. This finding might represent important clues on the different role of striate and extra-striate areas on motion biases in terms of feedforward- and feedback loops. Further attention should also be devoted to the presence of biased responses near the edges of a motion stimulus. Biases seem more pronounced near the edges of the stimulus in combination with a particular motion direction. This may indicate a relationship with the novelty of visual input. Neuronal output that is influenced by the novelty of visual input might be related to models on predictive coding[52,53].

Conclusions

The current study provides evidence that directional motion biases are related to a (linear) spatial integration as opposed to spatiotemporal integration of motion information parallel to the path of motion. Motion biases occur when multiple aligned motion detectors parallel to the path of motion are simultaneously activated. When the length of the path of coherent motion is shortened, motion biases decrease or even disappear.

References

1. Beckett, A., Peirce, J. W., Sanchez-Panchuelo, R.-M. M., Francis, S. & Schluppeck, D. Contribution of large scale biases in decoding of direction-of-motion from high-resolution fMRI data in human early visual cortex. Neuroimage 63, 1623–32 (2012).
2. Clifford, C. W. G., Mannion, D. J. & McDonald, J. S. Radial biases in the processing of motion and motion-defined contours by human visual cortex. J. Neurophysiol. 102, 2974–81 (2009).
3. Giaschi, D., Zwicker, A., Young, S. A. & Bjornson, B. The role of cortical area V5/MT+ in speed-tuned directional anisotropies in global motion perception. Vision Res. 47, 887–98 (2007).
4. Raemaekers, M., Lankheet, M. J. M., Moorman, S., Kourtzi, Z. & van Wezel, R. J. A. Directional anisotropy of motion responses in retinotopic cortex. Hum. Brain Mapp. 30, 3970–80 (2009).
5. Schluppeck, D. & Engel, S. A. Oblique effect in human MT+ follows pattern rather than component motion. J. Vis. 3, 282 (2003).
6. Doorn Van, A. J., Koenderink, J. J. & Van Doorn, A. J. Spatiotemporal integration in the detection of coherent motion. Vision Res. 24, 47–53 (1984).
7. Festa, E. K. & Welch, L. Recruitment mechanisms in speed and fine-direction discrimination tasks. Vision Res. 37, 3129–43 (1997).
8. Fredericksen, R. E., Verstraten, F. A. & van de Grind, W. A. Spatial summation and its interaction with the temporal integration mechanism in human motion perception. Vision Res. 34, 3171–88 (1994).
9. Koenderink, J. J., van Doorn, A. J. & van de Grind, W. A. Spatial and temporal parameters of motion detection in the peripheral visual field. J. Opt. Soc. Am. A. 2, 252–9 (1985).
10. Snowden, R. J. & Braddick, O. J. The combination of motion signals over time. Vision Res. 29, 1621–1630 (1989).
11. Motter, B. C., Steinmetz, M. a, Duffy, C. J. & Mountcastle, V. B. Functional properties of parietal visual neurons: mechanisms of directionality along a single axis. J. Neurosci. 7, 154–76 (1987).
12. Steinmetz, M. A., Motter, B. C., Duffy, C. J. & Mountcastle, V. B. Functional Properties of Parietal Visual Neurons: Radial Organization of Directions Within the Visual Field. J. Neurosci. 7, 177–191 (1987).
13. Berzhanskaya, J., Grossberg, S. & Mingolla, E. Laminar cortical dynamics of visual form and motion interaction during coherent motion perception. Spat. Vis. 20, 337–395 (2007).
14. Grossberg, S., Mingolla, E. & Viswanathan, L. Neural dynamics of motion integration and segmentation within and across apertures. Vision Res. 41, 2521–53 (2001).
15. Ringbauer, S., Tschechne, S. & Neumann, H. Mechanisms of Adaptive Spatial Integration in a Neural Model of Cortical Motion Processing. Adapt. Nat. Comput. Algorithms 110–119 (2011).
16. Cavanagh, P., Holcombe, A. O. & Chou, W. Mobile computation : Spatiotemporal integration of the properties of objects in motion. J. Vis. 8, 1–23 (2008).
17. Watamaniuk, S. N. J. & Sekuler, R. Temporal and Spatial Integration in Dynamic Random-Dot Stimuli. Vision Res. 32, 2341–2347 (1992).
18. Van de Moortele, P.-F. et al. T1 weighted brain images at 7 Tesla unbiased for proton density, T2* contrast and RF coil receive B1 sensitivity with simultaneous vessel visualization. Neuroimage 46, 432–446 (2009).
19. Van Essen, D. C. et al. An integrated software suite for surface-based analyses of cerebral cortex. J. Am. Med. Inform. Assoc. 8, 443–59 (2001).
20. Talairach, J. & Tournoux, P. Co-planar stereotaxic atlas of the human brain 3-dimensional proportional system: an approach to cerebral imaging. (Thieme Medical Pub, 1988).
21. Friston, K. J., Frith, C. D., Turner, R. & Frackowiak, R. S. Characterizing evoked hemodynamics with fMRI. Neuroimage 2, 157–165 (1995).
22. Mauchly, J. W. Significance test for sphericity of a normal n-variate distribution. Ann. Math. Stat. 11, 204–209 (1940).
23. Greenhouse, S. W. & Geisser, S. On methods in the analysis of profile data. Psychometrika 24, 95–112 (1959).
24. Balasubramanian, V. & Sterling, P. Receptive fields and functional architecture in the retina. J. Physiol. 587, 2753–67 (2009).
25. Borghuis, B. G., Ratliff, C. P., Smith, R. G., Sterling, P. & Balasubramanian, V. Design of a neuronal array. J. Neurosci. 28, 3178–89 (2008).
26. Harvey, B. M. & Dumoulin, S. O. The relationship between cortical magnification factor and population receptive field size in human visual cortex: constancies in cortical architecture. J. Neurosci. 31, 13604–12 (2011).
27. Smith, A. T., Singh, K. D., Williams, A. L. & Greenlee, M. W. Estimating receptive field size from fMRI data in human striate and extrastriate visual cortex. Cereb. Cortex 11, 1182–90 (2001).

28. Baker, C. L. J. Central neural mechanisms for detecting second-order motion. Curr. Opin. Neurobiol. 9, 461–466 (1999).
29. Baker, D. H. & Meese, T. S. Contrast integration over area is extensive : A three-stage model of spatial summation. J. Vis. 11, 1–16 (2011).
30. Bartels, A., Zeki, S. & Logothetis, N. K. Natural vision reveals regional specialization to local motion and to contrast-invariant, global flow in the human brain. Cereb. Cortex 18, 705–17 (2008).
31. Braddick, O. J. et al. Brain areas sensitive to coherent visual motion. Perception 30, 61–72 (2001).
32. Smith, A. T., Wall, M. B., Williams, A. L. & Singh, K. D. Sensitivity to optic flow in human cortical areas MT and MST. Eur. J. Neurosci. 23, 561–9 (2006).
33. Burr, D. C. & Santoro, L. Temporal integration of optic flow, measured by contrast and coherence thresholds. Vision Res. 41, 1891–9 (2001).
34. Webb, B. S., Ledgeway, T. & McGraw, P. V. Cortical pooling algorithms for judging global motion direction. Proc. Natl. Acad. Sci. U. S. A. 104, 3532–7 (2007).
35. Amano, K., Edwards, M., Badcock, D. R. & Nishida, S. Adaptive pooling of visual motion signals by the human visual system revealed with a novel multi-element stimulus. J. Vis. 9, 1–25 (2009).
36. Webb, B. S., Ledgeway, T. & Rocchi, F. Neural computations governing spatiotemporal pooling of visual motion signals in humans. J. Neurosci. 31, 4917–25 (2011).
37. Albright, T. D. Direction and orientation selectivity of neurons in visual area MT of the macaque. J. Neurophysiol. 52, 1106–1130 (1984).
38. Dumoulin, S. O. & Wandell, B. a. Population receptive field estimates in human visual cortex. Neuroimage 39, 647–60 (2008).
39. Blasdel, G. G., Lund, J. S. & Fitzpatrick, D. Intrinsic Connections of Macaque of Striate cortex: Axonal Projections of Cells Outside Lamina 4C. J. Neurosci. 5, 3350–3369 (1985).
40. Lamme, A. F., Supèr, H. & Spekreijse, H. Feedforward, horizontal, and feedback processing in the visual cortex. Curr. Opin. Neurobiol. 8, 529–535 (1998).
41. Gilbert, C. D. & Wiesel, T. N. Clustered intrinsic connections in cat visual cortex. J. Neurosci. 3, 1116–1133 (1983).
42. Somers, D. C. et al. A Local Circuit Approach to Understanding Integration of Long-range Inputs in Primary Visual Cortex. Cereb. Cortex 8, 204–217 (1998).
43. Apthorp, D. et al. Direct evidence for encoding of motion streaks in human visual cortex. Proc. R. Soc. B Biol. Sci. 280, (2013).
44. Sun, P. et al. Demonstration of Tuning to Stimulus Orientation in the Human Visual Cortex: A High-Resolution fMRI Study with a Novel Continuous and Periodic Stimulation Paradigm. Cereb. Cortex (2012). doi:10.1093/cercor/bhs149
45. Corbetta, M. et al. A common network of functional areas for attention and eye movements. Neuron 21, 761–73 (1998).
46. Jack, A. I., Shulman, G. L., Snyder, A. Z., McAvoy, M. & Corbetta, M. Separate modulations of human V1 associated with spatial attention and task structure. Neuron 51, 135–47 (2006).
47. Tootell, R. B. et al. The retinotopy of visual spatial attention. Neuron 21, 1409–22 (1998).
48. Anstis, S. M. & Rogers, B. J. Illusory reversal of visual depth and movement during changes of contrast. Vision Res. 15, 957–61 (1975).
49. Bours, R. J. E., Kroes, M. C. W. & Lankheet, M. J. Sensitivity for reverse-phi motion. Vision Res. 49, 1–9 (2009).
50. Kastner, S., Nothdurft, H. C. & Pigarev, I. N. Neuronal correlates of pop-out in cat striate cortex. Vision Res. 37, 371–6 (1997).
51. Nothdurft, H. C. Feature analysis and the role of similarity in preattentive vision. Percept. Psychophys. 52, 355–375 (1992).
52. Rao, R. P. & Ballard, D. H. Predictive coding in the visual cortex: a functional interpretation of some extra-classical receptive-field effects. Nat. Neurosci. 2, 79–87 (1999).
53. Spratling, M. W. Predictive coding as a model of response properties in cortical area V1. J. Neurosci. 30, 3531–43 (2010).

Chapter 3

Predictive coding for motion stimuli in human early visual cortex

Wouter Schellekens
Richard J.A. Van Wezel
Natalia Petridou
Nick F. Ramsey
Mathijs Raemaekers

Brain Structure and Function (2014),1-12

Abstract

The current study investigates if early visual cortical areas, V1, V2 and V3, use predictive coding to process motion information. Previous studies have reported biased visual motion responses at locations where novel visual information was presented (i.e. the motion trailing edge), which is plausibly linked to the predictability of visual input. Using high-field functional Magnetic Resonance Imaging (fMRI), we measured brain activation during predictable versus unpreceded motion-induced contrast changes during several motion stimuli. We found that unpreceded moving dots appearing at the trailing edge gave rise to enhanced BOLD responses, whereas predictable moving dots at the leading edge resulted in suppressed BOLD responses. Furthermore, we excluded biases in directional sensitivity, shifts in cortical stimulus representation, visuo-spatial attention and classical receptive field effects as viable alternative explanations. The results clearly indicate the presence of predictive coding mechanisms in early visual cortex for visual motion processing, underlying the construction of stable percepts out of highly dynamic visual input.

Introduction

The world around us is constantly changing. Objects within our visual field are moving all the time either because of the objects' characteristics or because we are moving ourselves. Nonetheless, we are able to construct stable and coherent percepts from the ever-changing scenery. It is, however, still unclear how stable percepts are formed from such dynamic visual input. Particularly, neural responses to motion pose the following problem: how do neurons in the visual cortex determine, whether detected contrast changes are caused by stimuli moving from receptive fields of neighboring detectors into the neuron's own receptive field, rather than by an unpreceded contrast change?

One currently popular theory, predictive coding, offers an interesting solution to this problem by means of integrating prior information in the form of predictions[1,2]. The mismatch between the anticipated and observed input, the prediction error, is used to encode novel information present in the input and alter predictions to better process future sensory input[3]. Neural firing is thought to mainly represent the prediction error[4], which represents the predictability of any given input. Thus, predictive coding allows neural activity to be guided by prior information on, for instance, moving objects. In turn, this allows for discriminating between predictable contrast changes that have been detected by other neurons and unpreceded contrast changes.

Although predictive coding offers a viable solution to the aforementioned problem, it is unclear to what extent predictive coding is utilized in visual motion processing. Incoherent motion has been reported to generate enhanced responses compared to coherent motion[5], which possibly reflects the difference in prediction error. Other imaging studies may also have shown evidence for a motion related predictive coding mechanism in early visual cortex[6,7]. These studies reported visual field dependent directional motion biases relative to the fovea (radial versus tangential) during perception of moving random dot stimuli. However, these results can also be explained by a more general principle, where BOLD responses are relatively increased at the trailing compared to the leading edge of a motion stimulus. Such principle is plausibly linked to predictive coding, since randomly positioned dots cannot be predicted at the point of appearance within the stimulus, i.e. the trailing edge, as opposed to other parts of a motion stimulus.

In the current study we investigate whether there is evidence for predictive coding in early visual cortical areas using moving random dot stimuli and functional MRI (fMRI). We hypothesize that in V1, V2, and V3 larger BOLD signals will be measured at the trailing edge of a motion stimulus, where contrast changes are unpreceded and cannot be predicted, compared to the leading edge of the motion stimulus, where contrast changes can be predicted based on visual information detected earlier along the path of motion. Moreover, we hypothesize that the novelty of a motion stimulus offers a more general and simpler explanation for previously observed directional motion biases, than differences in sensitivity for radial versus tangential motion directions. Finally, a control experiment was conducted to exclude spatial attention and classical receptive field effects as alternative explanations to increased BOLD responses at the trailing edge.

Methods

Subjects

Twenty-five healthy volunteers were recruited from the Utrecht University. Sixteen subjects performed the main experiment and 9 subjects performed the control experiment. The protocol was approved by the local ethics committee of the University Medical Center Utrecht, in accordance with the Declaration of Helsinki (2013).

Scan protocol

Scanning was performed on a 7 Tesla Philips Achieva scanner (Philips Healthcare, Best, Netherlands) with a 32-channel receive headcoil (Nova Medical, MA, USA). Functional MRI (fMRI) measurements were obtained using an EPI-sequence with the following parameters: SENSE factor=2.2, TR=1500 ms, TE = 25 ms, flip angle = 80°, coronal orientation, FOV (AP, FH, LR) = 52 x 190 x 190 mm^3. The acquired matrix had the following dimensions: 26 x 96 x 96, voxel size: 2 x 1.979 x 1.979 mm^3. The functional images were acquired from the posterior 52 mm of the brain, covering the occipital lobe, and slices were angulated along the z-axis so that their orientation was orthogonal relative to the calcarine sulcus. Additionally, a T1-weighted image of the whole brain (1.00 x 0.98 x 0.98 mm^3, FOV = 252 x 200 x 190) and a proton density image of equal dimensions were acquired at the end of the functional sessions.

Stimuli

For stimulus presentation a desktop PC, a projector and a rear projection screen were used. The stimuli were programmed using C++ software (Stroustrup, 1983, Bell Laboratories, USA). The presentation of the stimuli was triggered by the scanner. All stimuli were projected on a gray background and the mean luminance was held constant at 42.2 cd/m^2. During the presentation of all stimuli, a red fixation dot with a radius of 0.08° visual angle was projected on the center of the screen.

Polar angle mapping

To obtain the boundaries of the separate visual areas V1, V2, and V3, a polar angle mapping stimulus was used. The polar angle mapping stimulus was a rotating wedge of 48° circular angle, with a maximum eccentricity of 15° visual angle along the horizontal axis. The wedge consisted of a checkerboard pattern that switched contrast every 125 ms (8 Hz). The wedge made 6 full rotations: 3 times clockwise and 3 times counterclockwise. A total of 220 volumes was acquired during the polar angle mapping.

Main experiment

Prior to the motion experiments, a custom-designed motion area mapping stimulus was presented. The purpose of this stimulus was to obtain the retinotopic representations of 5 areas in each hemifield (10 in total), where motion was to be presented during the main motion experiments (Figure 1). Our target motion areas were two 4.0° x 4.0° areas that were centered at 7.0° eccentricity along the left and right horizontal meridian. The other 8 motion areas were located adjacent to the target areas: directly to the right, left, top and bottom. The adjacent areas were all squares with the exact same dimensions as the target area (Figure 1). All areas were mapped one at a time with a contrast switching checkerboard pattern (8 Hz), which was repeated 4 times. In total, 240 volumes were acquired during the motion area mapping experiment.

The motion stimuli of the main experiment consisted of moving random dot patterns that were designed to test the effect of predictable motion input at a motion stimuli's leading edge versus unpredictable motion input at a motion stimuli's trailing edge on the amplitude of the BOLD signal. This was achieved by varying the locations of trailing and leading edges of motion stimuli across the previously mapped motion areas, while we measured the BOLD responses in the target motion areas. Only BOLD responses from

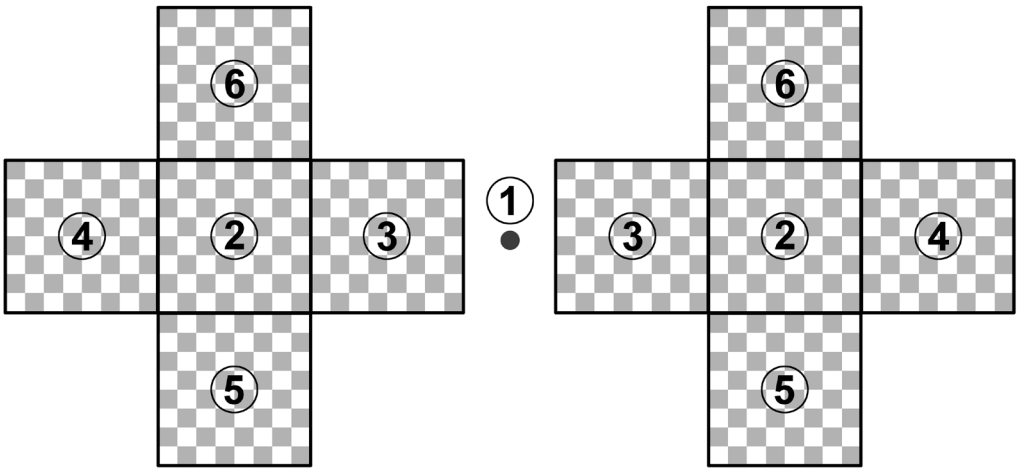

1 Fixation dot
2 Target motion area
3 Central motion area
4 Peripheral motion area
5 Lower motion area
6 Upper motion area

Figure 1. Main experiment motion areas. *Schematic representation of the motion areas. Participants were instructed to maintain focus at the dot at central fixation (1) at all times. Each motion area was 4°x4° visual angle. BOLD responses were obtained only from the target motion area (2) that was centered on the horizontal meridian at 7° visual angle.*

the target motion areas were used, so that the influence of trailing and leading edges of the motion stimuli was always measured in the exact same retinotopic area. Two motion stimuli were used, one with radial motion and one with tangential motion. Due to time limits that subjects were allowed to be in the scanner, each subject was only presented one of the two motion stimuli, meaning that each motion stimulus was presented to 8 subjects.

For the radial motion experiment, dots were projected within the 6 previously mapped motion areas on the horizontal meridian (3 per hemifield), namely the peripheral, target, and central motion areas (Figure 1). Per motion area, approximately 250 black and white dots were projected (width & height: 0.4° visual angle), moving at a speed of 4.5°/s. We used 3 categories of stimulus conditions, which varied the distance of leading and trailing edges relative to the target motion area. Category 1: moving dots were presented over the target motion area and 1 adjacent motion area (Figure 2A, 2B). In these conditions, either the leading or trailing edge bordered the target motion area, depending on motion areas and direction. Category 2: moving dots were presented over the target motion area only (Figure 2C). During this condition, both the leading and trailing edge bordered

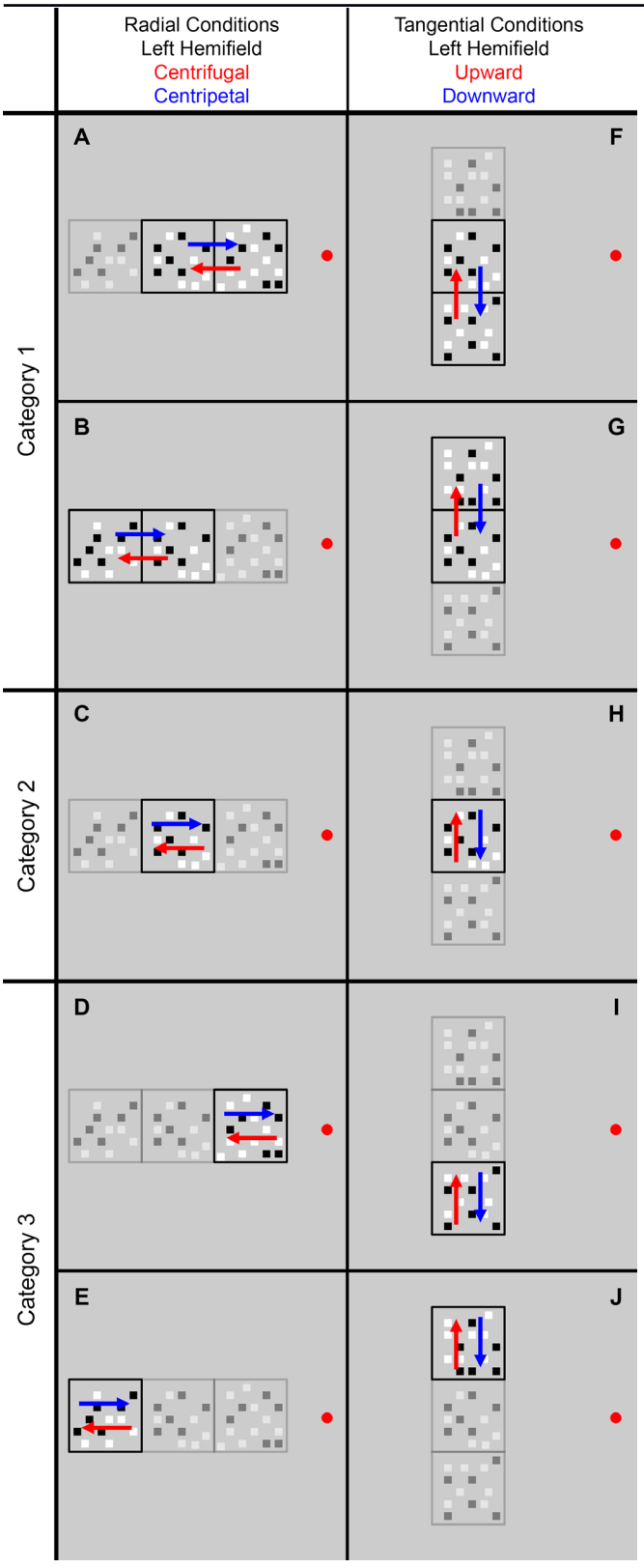

Figure 2. Main experiment stimulus locations. *The positions of the motion stimuli presented in the left hemifield are depicted for radial motion (A – E) and tangential motion (F – J). Motion was presented in the following motion areas: (A) target and central, (B) target and peripheral, (C) target, (D) central, (E) peripheral, (F) target and lower, (G) target and upper, (H) target, (I) lower and (J) upper. The colored arrows denote the different motion directions. At the areas, which are shown having lesser opacity in this schematic, stationary dots were shown during the MRI-experiments. Presentation in the right hemifield (not depicted) was an exact mirror image of this schematic. Stimuli were presented simultaneously in both hemifields.*

the target motion area, regardless of motion direction. Category 3: moving dots were only presented over 1 motion area adjacent to the target motion area (Figure 2D, 2E). Therefore, either the leading or trailing edge bordered the target motion area, while motion was not directly present over the target motion area. The motion direction was either centrifugal or centripetal, and every condition was presented in both hemifields simultaneously. Static dots were presented in the remaining location(s) to keep visual stimulation similar among all conditions. Every motion period lasted for 15s and was alternated with a 15s rest period, when all dots were static. All conditions were repeated 3 times and a total of 600 volumes was acquired.

The tangential motion stimulus was similar to the radial motion stimulus, except that dots were now positioned over the target, upper, and lower areas (Figure 1). The motion direction also changed to upward or downward. However, the same stimulus categories applied: motion over the target motion area and 1 adjacent motion area (Figure 2F, 2G); motion over the target motion area only (Figure 2H); motion over 1 motion area adjacent to the target motion area only (Figure 2I, 2J).

Control experiment

The control experiment was conducted on 9 participants to investigate confounding factors as classical receptive field (RF) effects and visuo-spatial attention. A classical receptive field representing the trailing edge will detect novel dots directly in its center, rather than in the periphery. As a result, the sequence of an RF's surround and center stimulation may differ greatly at the trailing edge compared to all other parts of a motion stimulus. Possibly, this could lead to relatively enhanced (transient) responses near the trailing edge. Therefore, in contrast to the main experiment, BOLD responses were not obtained from 1 motion area, but from 20 equally spaced locations across the entire width of the screen. This stimulus allowed us to investigate the spatial range of signal enhancements near the trailing edge. The area from which BOLD responses were obtained, the main area, was centered in each hemifield on the horizontal meridian at 8° visual angle, with a width and height of 14° x 4° visual angle (Figure 3). The cortical representations of the main area's 20 locations were assessed using another custom-designed mapping stimulus, which was a checkerboard pattern (width x height: 3° x 4°; switching contrast: 8 Hz), that moved along the 20 locations in 30s, and was repeated 8 times (220 volumes

in total). After the mapping experiment, approximately 800 square dots (width & height: 0.4°) were randomly projected across the main area. The dots moved (velocity: 4.5 °/s) in either a centrifugal or centripetal motion direction for 15s, alternated with a 15s stationary period.

Additionally, 4 rectangular areas (2 in each hemifield) of equal dimensions and similar dot distribution, the distractor areas, were positioned above and below the main area (Figure 3). If new appearing dots draw spatial attention, causing elevated BOLD-responses, the presentation of 3 times more novel dots would reduce the signal at all trailing edges in equal proportions. This would not happen, if elevated BOLD-responses are the result of novel dots *per se*. To minimize direct influence of the distractor areas on the main area, there remained a blank space of 2.2° visual angle between motion areas. There were 2 conditions regarding the distractor areas: dots either moved in the opposite direction of the main area dots with equal velocity, or the distractor area dots remained stationary, while motion was shown over the main area. The full set-up resulted in 4 conditions (2 motion directions x 2 distractor area conditions), which was repeated 8 times (640 volumes).

Attention task

During all motion experiments (i.e. main and control experiments), a white cross was projected every 1000 ms. During approximately 25% of all cross-projections, an additional small triangle was presented, that transformed one of the bars of the white cross in an arrow pointing in one of four directions: left, right, up or down. The participants were instructed to respond with a button press that corresponded to the direction of the presented arrow, using a button box with four buttons. A correct response was counted, if participants pressed the correct corresponding button before the next attention cue was presented. If a non-corresponding button was pressed, the response was incorrect. When participants failed to press a button before the next attention cue, it counted as a missed response. The inter-trial interval and arrow-direction were randomized.

Image analysis

All functional images were spatially preprocessed using SPM8 (http://www.fil.ion.ucl.ac.uk/spm/). The preprocessing entailed the realignment of all functional images

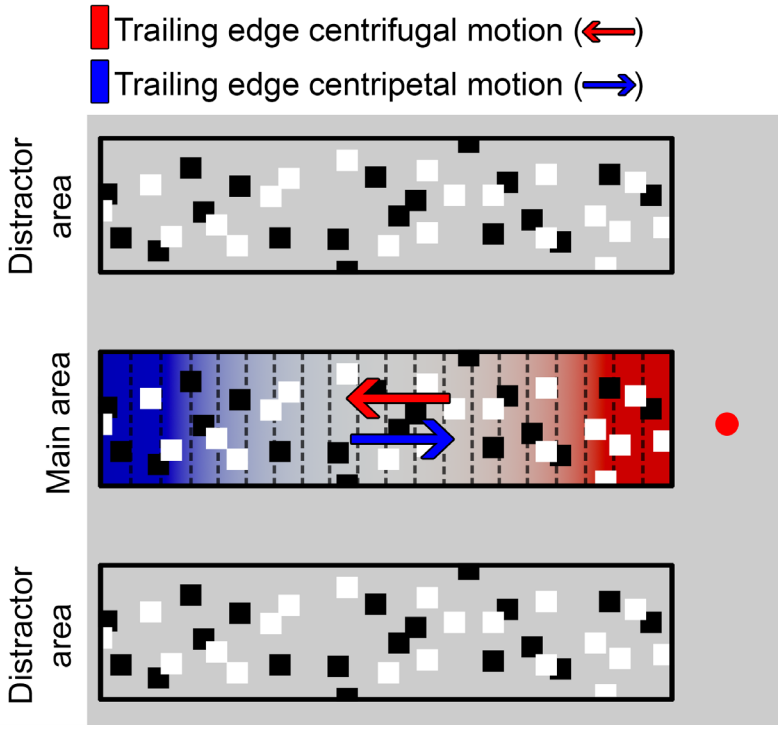

Figure 3. Control experiment stimulus. *The figure shows the motion stimuli presented in the left hemifield during the control experiment. BOLD responses were obtained from the rectangular area along the horizontal meridian (main area) at 20 equally spaced locations, denoted by dashed lines. Dots in this area moved either in centrifugal or centripetal directions (arrows). The location of the trailing edge depended on the motion direction, which is denoted by colors within the main area. The colors of the trailing edge locations are in correspondence with the colored arrows of the motion directions. Above and below, 2 additional stimuli were presented in each hemifield (4 in total): the distractor areas. Dots in the distractor areas either moved in the opposite direction of the dots in the main area, or remained stationary. Presentation in the right hemifield (not depicted) was an exact mirror image of this schematic. Stimuli were presented simultaneously in both hemifields.*

to the mean image, slice time correction and coregistration to the anatomical image (T1). The T1 image was corrected for field inhomogeneities by dividing the T1 image by the proton density image[8]. Surface reconstructions for each hemisphere were created with the Computerized Anatomical Reconstruction and Editing Toolkit (CARET,[9]). The reconstructed surfaces contained on average 1.6 nodes/mm^2. All functional images were mapped onto the surfaces of the left and right hemispheres, using a metric Gaussian mapping algorithm, resulting in a time series for every node of the surface. Low frequency noise was removed using multiple regression and a design matrix containing the mean of each image and six cosine functions per experiment, which formed a high-pass filter

with a cutoff at 3.3 x 10^{-2} Hz.

For the polar angle mapping stimulus, we used a phase-encoded regressor-matrix to obtain the polar angles for the nodes on the reconstructed cortical surface. The regressor-matrix contained a regressor for every scan during a stimulus cycle and represented the cyclic activation of the rotating wedge (6400 ms activation during every 48000 ms cycle), which was convolved with a hemodynamic response function[10]. A correlation coefficient was calculated for every regressor in the regressor-matrix (i.e. every image in a cycle) for every node of the reconstructed surface. The peak correlation of a node determined the polar angle of a node's receptive field. The polar angle results were used to draw ROIs on the reconstructed surfaces of each hemisphere, and included the early visual cortical areas V1, V2, and V3.

Main experiment

The motion area mapping stimulus was analyzed with a multiple linear regression analysis, using a design matrix that contained 5 factors, one for each motion area. The analysis resulted in 5 T-statistics per node on the surface. Only nodes on the surface that responded to the target motion area ($t \geq 4.51$), and that were situated within V1, V2, or V3, were included. The T-statistics of the remaining 4 motion areas were used to exclude nodes that represented part of the target area, but whose activation could also be influenced by stimulation from adjacent squares. Nodes were excluded if the T-value for the factor corresponding to one of the adjacent areas exceeded 2.71. This procedure resulted in on average 104 included nodes (SD=27) on the reconstructed surfaces of both hemispheres per subject. Thus, these nodes responded to the target motion area and not to any of the other motion areas.

For the radial and tangential motion experiments, we estimated the BOLD amplitude at the target motion area surface nodes, using a linear regression with a design matrix that contained factors for all stimulus conditions. To test for significant differences in the BOLD amplitude between stimulus conditions within the 3 categories, 3 GLM repeated measures designs were adopted. All GLMs included the 3 visual areas as independent measures and the radial/tangential groups as a between-subjects factor. The first GLM tested for differences in BOLD amplitude between leading or trailing edge bordering the target motion area. This GLM contained leading/trailing edge as within-subjects factor.

The second GLM was designed to test for difference in the BOLD amplitude between radial and tangential motion directions (i.e. centrifugal/centripetal vs. upward/downward motion directions), when motion was presented solely over the target motion area. This GLM contained opposite motion directions (i.e. centrifugal/centripetal and upward/downward) as within-subjects factor. The third GLM again tested for differences between leading or trailing edges bordering the target motion area, while motion was presented outside the target motion area, and contained leading/trailing edge as within-subjects factor.

Control experiment

For the main area mapping stimulus, we used a phase-encoded regressor-matrix to establish cortical representations of all 20 locations on the reconstructed cortical surface. The regressor-matrix contained 20 regressors, 1 for each location, and represented the cyclic activation of each node (7300 ms activation during every 30000 ms), which was convolved with a hemodynamic response function 10. A correlation coefficient was calculated for every regressor in the regressor-matrix, and the peak correlation determined to which of the 20 locations a node was most responsive. Additionally, T-statistics were calculated for every peak correlation, and only those nodes were included that showed a T-value of $T \geq 4.51$, and that were situated in V1, V2, or V3.

We estimated the BOLD amplitude at all 20 locations using a linear regression with a design matrix that contained factors that represented the BOLD activation for all 4 motion conditions of the control experiment. To test for significant effects of the motion direction, we performed a paired sample T-test per location of the main area (centrifugal vs centripetal). To test for significant effects between distractor areas with moving and stationary dots on the main area representations, a multivariate repeated measures design was used. The 3 visual areas were included as independent measures and distractor square condition as within-subject factor.

Results

We presented various visual motion stimuli in 25 healthy subjects, while measuring brain activation with fMRI. The main experiment (n=16) was designed to test the effect of predictable contrast changes at a motion stimuli's leading edge versus unpredictable

contrast changes at a motion stimuli's trailing edge on the amplitude of the BOLD signal. We did this by showing moving dots in 5 predefined motion areas in each hemifield, while we measured the BOLD response in the target motion area only. Using 3 categories of motion stimuli, we varied the distance of leading and trailing edges relative to the target motion area. This setup allowed us to assess the effect of leading and trailing motion edges in the exact same retinotopic area (i.e. target motion area) for the different stimulus configurations.

To measure the effect of distance towards the motion stimuli's leading and trailing edges on the BOLD signal, motion was presented in 2 adjacent motion areas (Figure 2: Category 1). The motion direction determined whether the leading or trailing edge bordered the target motion area. We found that the motion direction had a large effect on the BOLD amplitude ($F_{(3,12)}$=15.967, p<.001), while motion was present over the target motion area; a short distance between the leading edge and target motion area resulted in lower BOLD amplitudes, compared to a short distance between motion target area and the trailing edge (Figure 4A). In addition, there was no significant difference between radial and tangential motion directions ($F_{(3,12)}$=1.000, p=.426). Thus, these results indicate that BOLD amplitudes to a moving random dot pattern depend on the distance of the motion stimulus' leading or trailing edge to the target motion area. When the trailing edge was near the target motion area, amplitudes of the BOLD signal were higher, than when the leading edge was near the target motion area (Figure 5). These results are true for both radial and tangential motion directions, showing the possible presence of predictive coding effects in early visual areas.

To assess whether activity in the target motion area could have been biased by local anisotropies towards particular motion directions, we measured BOLD amplitudes when the stimuli's leading and trailing edges were both bordering the target motion area (Figure 2: Category 2). Therefore, changing the motion direction had no effect on distances towards leading and trailing edges relative to target motion area. Subsequently, we found no effect of motion directions for radial ($F_{(3,5)}$=0.053, p=.982) and tangential ($F_{(3,5)}$=2.396, p=.184) directions (Figure 4B), nor did we find a general difference between radial and tangential directions ($F_{(3,12)}$=.782, p=.526). These results exclude the possibility that local anisotropies for different motion directions can explain our findings.

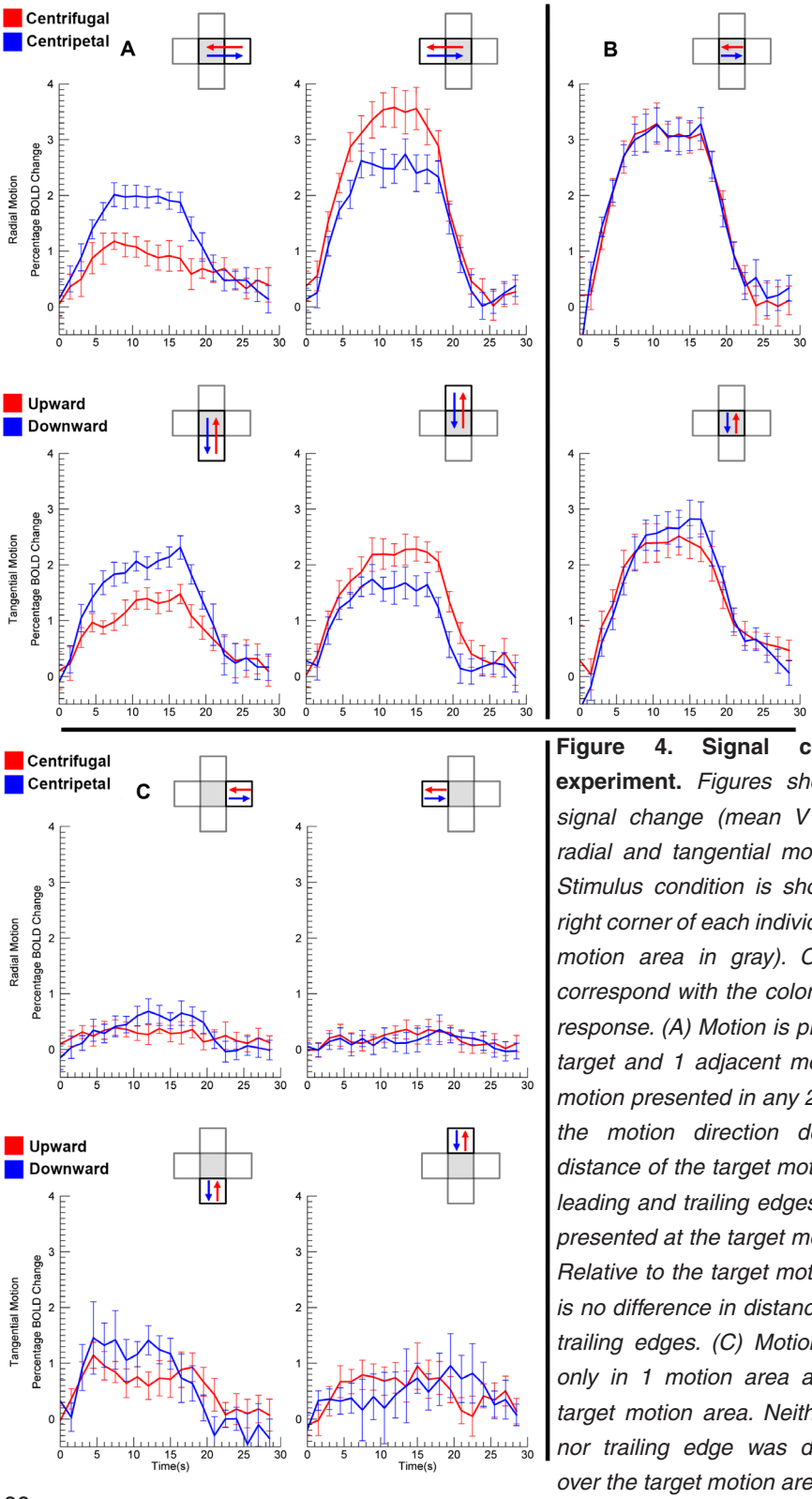

Figure 4. Signal change main experiment. *Figures show the BOLD signal change (mean V1, V2, V3) for radial and tangential motion directions. Stimulus condition is shown in the top right corner of each individual plot (target motion area in gray). Colored arrows correspond with the colors of the BOLD response. (A) Motion is presented at the target and 1 adjacent motion area. For motion presented in any 2 motion areas, the motion direction determined the distance of the target motion area to the leading and trailing edges. (B) Motion is presented at the target motion area only. Relative to the target motion area, there is no difference in distance to leading or trailing edges. (C) Motion is presented only in 1 motion area adjacent to the target motion area. Neither the leading nor trailing edge was directly present over the target motion area.*

In addition, to check if effects of leading and trailing motion edges were caused by motion induced shifts in the cortical location of the stimulus representation, as has been suggested by previous research[11], we measured activation for the target motion area, while motion was only presented in an adjacent area (Figure 2: Category 3). Putative effects of a motion induced flexible retinotopy should be evident under this stimulus configuration. To the contrary, we found no significant effect of motion direction on the BOLD amplitude in the target motion area representation ($F_{(3,12)}$=2.546, p=.105). Therefore, it is unlikely that motion induced shifts in the location of the stimulus representation can account for differences between leading and trailing motion edges. (Figure 4C).

The control stimulus was designed to measure the maximum extent of biased BOLD responses near the trailing edge, to assess the possible contribution of extraclassical receptive field effects. We found that the biases were not merely restricted to the edge representations. Para-foveally, biases stretched from 1° to approximately 3° visual angle, and peripherally, biases were measured from approximately 14° to 10° visual angle (Figure 6). Biased responses were also clearly visible on the level of individual subjects (Figure 7). The range in which enlarged BOLD responses were present, is well beyond the sizes of classical (population) receptive fields to be found in early visual cortex, indicating that extraclassical receptive effects must have contributed to observed effects[12].

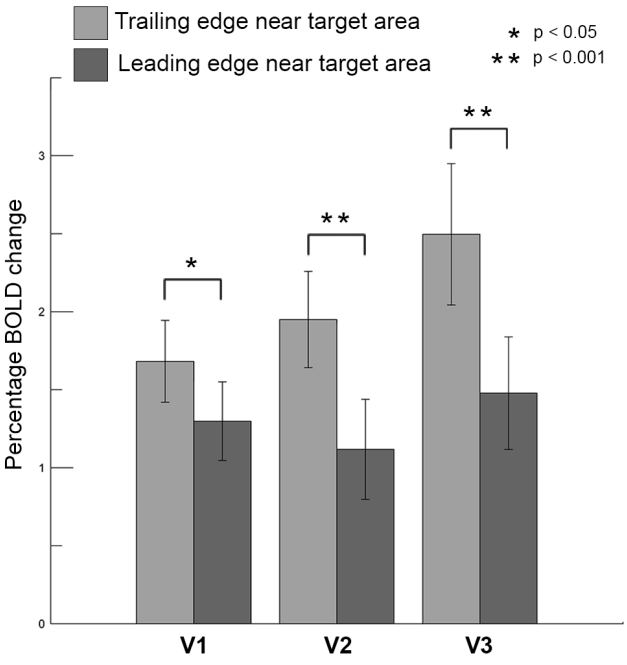

Figure 5. BOLD amplitudes trailing and leading edges. *The estimated peak signal change is shown for Category A stimuli during the main experiment (both radial & tangential). Stimulus conditions that presented the trailing motion edge bordering the target motion area are shown by the light gray bars, while stimulus conditions that presented the leading motion edge bordering the target motion area are shown by the dark gray bars. From left to right the amplitude at separate visual areas is shown. Error bars denote standard error of the mean across subjects and the asterisks indicate significant levels.*

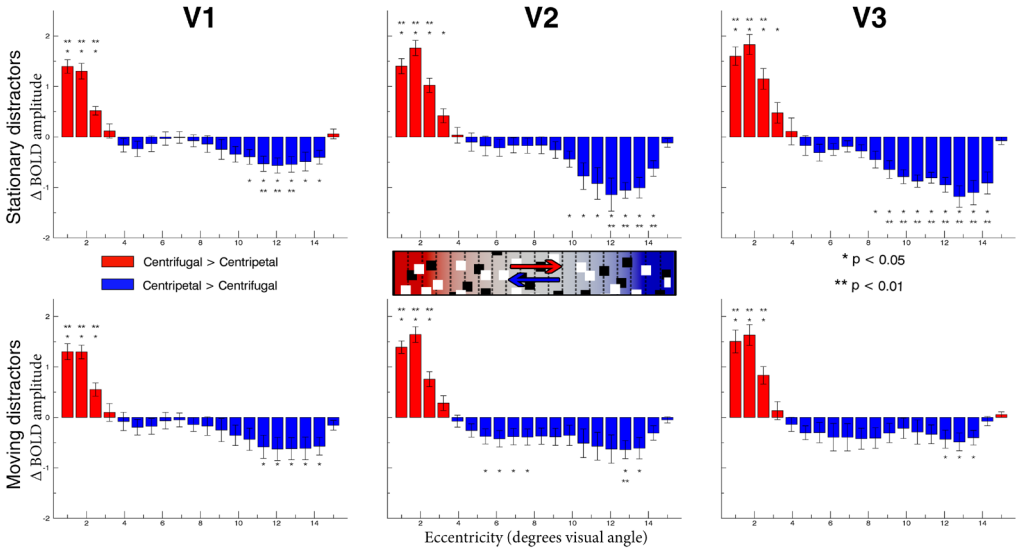

Figure 6. Difference BOLD amplitude control experiment. *Difference in estimated amplitudes of the BOLD signal during the control experiment between centrifugal and centripetal motion direction are shown for each location of the main area. Red bars signify locations where centrifugal motion resulted in larger signal changes compared to centripetal motion, and vice versa for the blue bars. Therefore, the amplitude of the bars approximate the effect size of the biased responses. The stimulus schematic of the control experiment is shown in the center of the figure. The colored locations within the center schematic (gradient) depict the trailing edge locations of each motion direction and correspond to the edge representations of the bar plots. Graphs from left to right show responses from separate visual areas. The upper graphs show responses when distractor area dots were stationary. The lower graphs show responses, when distractor area dots were moving. Error bars denote standard error of the mean across subjects.*

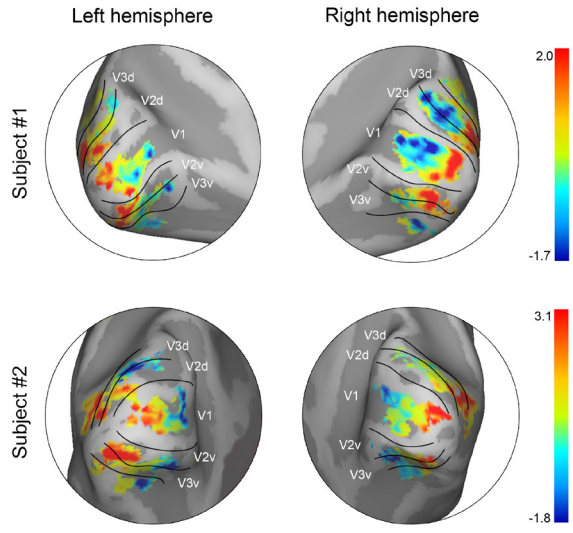

Figure 7. Individual results control experiment. *The difference between centrifugal and centripetal motion is shown on inflated surface reconstructions of 2 subjects (rows) during the control experiment with stationary. distractors. The surface reconstructions show medial-posterior view of the occipital lobes. The foveal representation resides at the occipital pole. Cortical locations where centrifugal motion resulted in larger BOLD signal changes are depicted by positive numbers, while cortical locations where centripetal motion resulted in larger BOLD signal changes are depicted by negative numbers.*

Lastly, the BOLD activity difference between leading and trailing edge can be explained by (covert) visuo-spatial attention shifts towards novel dots at the trailing edge. To estimate the possible contribution of attention shifts, distractor dot patterns were presented during the control stimulus (Figure 3). The distractor dot patterns either moved in opposite direction of the main area dot pattern, or did not move at all. Moving distractor dot patterns presented subjects with a threefold increase in leading and trailing edges, compared to the stationary distractor condition. If spatial attention shifts are the cause of elevated BOLD responses near the trailing edge, this threefold increase would reduce the effect with roughly 66% due to a division of attentional resources. However, whether distractor dots were moving or remained stationary had no effect on the BOLD signal ($F_{(3,6)}$=1.830, p=.242). Moreover, during all experiments subjects were engaged in a demanding attention task at central fixation on which they had good but not perfect performance (86% correct detections), making it exceedingly unlikely that effects of visuo-spatial attention can account for the observed effects.

Thus, the current results show that BOLD responses are relatively enlarged for unpreceded contrast changes at a motion stimulus' trailing edge compared to predictable contrast changes at the leading edge. Furthermore, we have been able to demonstrate that these effects are neither caused by differences in sensitivity to any presented motion direction (radial or tangential), nor by motion induced shifts of cortical representations of the stimuli, nor by (covert) shifts in visuo-spatial attention to leading or trailing motion edges. Furthermore, we were able to show that enhanced activity for novel dots near the trailing edge most likely represent an extraclassical receptive field effect.

Discussion

In the current study, we hypothesize that neural activity in early visual cortex during perception of moving random stimuli depends on novelty, and therefore predictability, of visual input. Based on predictive coding, we expect increased BOLD signals for unpreceded contrast changes relative to contrast changes that have previously been detected by other neurons. In visual areas V1, V2, and V3, we indeed measured larger BOLD amplitudes near the trailing edge of a motion stimulus, where new dots enter the visual field, as opposed to smaller BOLD responses near the leading edge, where dots have traveled the maximum distance of the stimulus area. Furthermore, we excluded

several alternative explanations for the observed findings, which indicates that some form of predictive coding for moving stimuli is present in early visual cortex.

We observed that cortical responses to motion decrease, when the trailing edge of a motion stimulus is distant from a retinotopic area, compared to the trailing edge being near that same retinotopic area. This phenomenon can also explain the directional motion biases we observed in two previous studies[6,7]. These directional biases were observed for a large circular moving random dot stimulus (15° diameter) with an aperture at central fixation. Enhanced activation was found for centrifugal motion at low eccentricities, and for centripetal motion at high eccentricities. Probably, the centripetal bias at high eccentricity may be the result of novel dots entering the stimulus area at the trailing edge near the stimulus' outer rim, whereas the centrifugal bias at low eccentricity may be the result of a second trailing edge caused by the fixation aperture. Moreover, we have found that there exists no fundamental difference between radial and tangential motion directions. This contradicts the idea that directional motion biases share a common cause with the radial orientation bias[13,14]. In addition, it has been suggested that orientation selective cells in visual cortex are activated by motion streaks[15,16]. Possibly, motion streaks cause different activation levels along a motion trajectory. However, under current experimental paradigms motion streaks would be roughly equal along the full motion trajectory. Hence, differences in motion streaks do not offer a plausible explanation for enhanced BOLD signals at the trailing edge, nor the gradual decrease in activity towards the leading edge, nor do different orientations of motion streaks exert a differential effect on BOLD responses to a moving random dot pattern. Instead, it is the novelty of moving visual input that explains different activation levels. Similar findings have been reported with different types of stimuli[17,18], confirming that the amplitude of the BOLD response to motion stimuli depends on stimulus novelty or predictability.

The novelty of dots could additionally influence current observations in more than one way. At the trailing edge of a motion stimulus, moving dots enter the visual field from behind the stimulus aperture. This might cause moving dots to visually appear in the middle of a neuron's receptive field. Subsequently, this might cause a differential effect with respect to neurons signaling information at the leading edge, where moving dots drift into a neuron's receptive field[19,20]. Thus, the results could be due to classical

receptive field effects, instead of stimulus predictability. However in the main experiment, we excluded the voxels that responded to motion areas directly adjacent to the target motion area. This automatically excludes voxels that were responsive to the edges of the target motion area, where new dots entered the visual field. As the size of the target motion area (4° x 4° visual angle at 7° eccentricity) by far exceeds receptive field sizes in V1, V2 and V3[12], there is a substantial number of voxels that responds solely to the stimulus' inner part. Although it is possible that some voxels included neurons that still responded to the edge of the target motion area, it is unlikely that they could have caused the large observed effects, as their relative contribution to the signal would simply be too small. Furthermore, when motion was presented outside, but directly adjacent to the target motion area, no significant differences in BOLD signal were detected. If only those voxels that represented the edge of the stimulus were causing the effect, the effect should also be pronounced during this condition. Finally, the control experiment showed that elevated BOLD responses were present beyond the range of classical receptive fields that represented the control stimulus' trailing edge. Hence, it is unlikely that the current results can be explained by differentiating classical receptive field effects for dots appearing in the center of receptive fields and dots drifting into receptive fields.

The difference in BOLD signal between predictable and unpreceded moving dots appears to be caused by extraclassical receptive field effects of local neuronal populations. This may also include (covert) visuo-spatial attention, which could shift to the stimulus part where novel dots appear. However, there are several reasons why spatial attention is an unsatisfactory explanation. First, the effect was observed during stimulus presentation in two hemifields simultaneously. Although it has been shown that spatial attention can be divided over multiple visual field locations[21], this certainly adds a restraint on its possible contribution. Secondly, the current study included an attention task at the location of the fixation dot. Performance on the attention task indicated that participants were able to maintain spatial attention directed at the center of the screen. Finally, the control experiment showed that the presentation of 4 additional motion stimuli had no effect on elevated BOLD responses near the trailing edge. If visuo-spatial attention were to cause elevated BOLD responses, dividing one's attention over 4 additional stimuli should have diminished the anticipated effect.

Predictive coding offers a plausible explanation for the observed effects, stating that unpreceded motion contrast changes at the trailing edge would yield larger prediction errors compared to predictable contrast changes near the leading edge. However, underlying mechanisms for predictive coding are still under debate. Currently, most predictive coding models incorporate predictive states, i.e. predictions for observational or otherwise lower-level input[22,23]. Predictive states have among others been proposed as a construct of Bayesian inference[24] or a competition of many possible predictions[25]. Additionally, extra-striate areas may accommodate predictive states for the primary visual cortex[1]. Although we have found that motion novelty effects were largest in V3 (Figure 4), the temporal limitations of fMRI BOLD do not allow us to infer that extra-striate areas hold predictions for area V1. However, predictive coding in early visual cortex would arguably be more efficient without actual predictions, for they might be computationally taxing for the visual system. If predictions are estimated for all neuronal input, predictive states virtually act as a buffer. Especially in early visual cortex, where receptive field sizes are small, it might be more expensive than beneficial to buffer the entire cortical visual field representation. Computational load further increases, as some models include an additional layer of prediction errors[4,26].

Alternatively to predictive states, predictive coding may utilize simple heuristic mechanisms that have predictive outcomes. We propose a simplistic heuristic for motion processing, where detector activity in early visual cortex is suppressed from trailing to leading edge of the motion stimulus by means of corticocortical connections[27,28]. Automatic suppression along the motion direction would be computationally less demanding, since it would not need actual predictions and would also support preservation of energy resources[29]. Predictive coding without actual predictions has been previously suggested, where detector input is auto-correlated with input from neighboring detectors[30]. Such auto-correlation does not need actual predictions to be estimated. Similarly, a heuristic suppression mechanism for motion processing would affect neighboring motion and/or contrast detectors. A simple suppression mechanism is also supported by current results, when moving dots were presented outside the area of measurement, but moved towards the area of measurement. During this condition, a predictive mechanism based on predictive states would detect an unpreceded contrast change of opposite polarity, due to the fact that motion suddenly seizes to exist. However, this condition did not result

in enhanced BOLD activity, which indicates that the mechanism underlying the observed effects is not based on predictive states. Our previous findings also support evidence for a suppression mechanism, showing motion biases when dots were randomly repositioned every 500 ms[7]. Under such circumstances, predictions would match detector input to a lesser extent. However, we observed that random repositioning of dots did not attenuate motion biases, indicating that the effects observed during the current study are not based on matching input with predictions. Nonetheless, future studies are needed to resolve the actual processes of predictive coding for moving stimuli in early visual cortex.

Based on current results, no direct inferences can be made on the psychophysical correlates of the suppression effect on visual motion perception. However, recent studies have reported differences in detection thresholds of Gabor patterns that depended on the patterns' position and phase relative to a motion stimulus[31,32]. Both studies reveal lower detection thresholds for Gabor patterns that are located near the leading edge of a motion stimulus. In one study[32], the authors argue that the discrepancy in Gabor pattern detection threshold is caused by flexible retinotopy[11]. However, we have been able to demonstrate that there are no novelty effects for motion stimuli presented directly adjacent to the area from where BOLD responses were obtained. This implies that flexible retinotopy, where motion induces shifts in cortical representation of the stimuli, cannot explain the observed findings. Alternatively, motion deblurring (or motion streak suppression) has been suggested to specifically target the motion trailing edge[33,34]. If motion deblurring is underlying the current findings then the enhanced BOLD activity near the trailing edge may in fact reflect increased inhibitory synaptic activity[35]. However, contribution of inhibitory processes to positive BOLD signal change is thought to be limited[36,37], which makes a relative inhibition increase near the trailing edge seem at odds with current results. Instead, less excitatory activity offers a more straightforward interpretation of the reported signal decrease from trailing to leading edge, which is plausibly caused by a motion induced predictive suppression mechanism. This may in turn have the previously reported psychophysical result of lower detection thresholds near a motion stimulus' leading edge due to a relative increase in available resources. Still, it is possible that the BOLD signal is comprised of additional mechanisms that specifically target motion trailing and leading edges (e.g. motion streak suppression).

To obtain further information on the currently observed motion-induced suppression, future studies should address motion displacement through motion velocity and motion duration. Arguably, these variables have large effects on the extent and range of the suppression. In addition, more data is needed to assess whether motion-induced suppression effects are related to certain perceptual qualities, such as motion direction discrimination[38,39] or motion saliency[40]. Finally, it would be interesting to see if predictive coding not only affects motion responses across visual space, but also in the spatiotemporal domain[41].

In conclusion, we found evidence for a predictive coding mechanism for motion processing in early visual cortex. The current results show that the near presence of a leading or trailing edge greatly determines the BOLD amplitude during observation of motion stimuli. Moreover, BOLD responses in early visual cortex directly reflect the predictability of motion information. The observed mechanism offers a more general and simpler explanation for motion biases, than differences in sensitivity for particular motion directions. These results could, thus, underlie the formation of stable percepts from an ever-changing scenery.

References

1. Rao, R. P. & Ballard, D. H. Predictive coding in the visual cortex: a functional interpretation of some extra-classical receptive-field effects. Nat. Neurosci. 2, 79–87 (1999).
2. Friston, K. A theory of cortical responses. Philos. Trans. R. Soc. Lond. B. Biol. Sci. 360, 815–36 (2005).
3. Wacongne, C., Changeux, J.-P. & Dehaene, S. A neuronal model of predictive coding accounting for the mismatch negativity. J. Neurosci. 32, 3665–78 (2012).
4. Egner, T., Monti, J. M. & Summerfield, C. Expectation and surprise determine neural population responses in the ventral visual stream. J. Neurosci. 30, 16601–8 (2010).
5. McKeefry, D. J., Watson, J. D., Frackowiak, R. S., Fong, K. & Zeki, S. The activity in human areas V1/V2, V3, and V5 during the perception of coherent and incoherent motion. Neuroimage 5, 1–12 (1997).
6. Raemaekers, M., Lankheet, M. J. M., Moorman, S., Kourtzi, Z. & van Wezel, R. J. A. Directional anisotropy of motion responses in retinotopic cortex. Hum. Brain Mapp. 30, 3970–80 (2009).
7. Schellekens, W., Van Wezel, R. J. A., Petridou, N., Ramsey, N. F. & Raemaekers, M. Integration of Motion Responses Underlying Directional Motion Anisotropy in Human Early Visual Cortical Areas. PLoS One 8, e67468 (2013).
8. Van de Moortele, P.-F. et al. T1 weighted brain images at 7 Tesla unbiased for proton density, T2* contrast and RF coil receive B1 sensitivity with simultaneous vessel visualization. Neuroimage 46, 432–446 (2009).
9. Van Essen, D. C. et al. An integrated software suite for surface-based analyses of cerebral cortex. J. Am. Med. Inform. Assoc. 8, 443–59 (2001).
10. Friston, K. J., Frith, C. D., Turner, R. & Frackowiak, R. S. Characterizing evoked hemodynamics with fMRI. Neuroimage 2, 157–165 (1995).
11. Whitney, D. et al. Flexible retinotopy: motion-dependent position coding in the visual cortex. Science 302, 878–81 (2003).
12. Dumoulin, S. O. & Wandell, B. a. Population receptive field estimates in human visual cortex. Neuroimage 39, 647–60 (2008).
13. Sasaki, Y. et al. The radial bias: a different slant on visual orientation sensitivity in human and nonhuman primates. Neuron 51, 661–70 (2006).
14. Clifford, C. W. G., Mannion, D. J. & McDonald, J. S. Radial biases in the processing of motion and motion-defined contours by human visual cortex. J. Neurophysiol. 102, 2974–81 (2009).
15. Geisler, W. S. Motion streaks provide a spatial code for motion direction. Nature 400, 65–9 (1999).
16. Apthorp, D., Wenderoth, P. & Alais, D. Motion streaks in fast motion rivalry cause orientation-selective suppression. J. Vis. 9(5), 1–14 (2009).
17. Alink, A., Schwiedrzik, C. M., Kohler, A., Singer, W. & Muckli, L. Stimulus predictability reduces responses in primary visual cortex. J. Neurosci. 30, 2960–6 (2010).
18. Maloney, R. T., Watson, T. L. & Clifford, C. W. G. Determinants of motion response anisotropies in human early visual cortex: The role of configuration and eccentricity. Neuroimage 100, 564–79 (2014).
19. Gieselmann, M. a & Thiele, a. Comparison of spatial integration and surround suppression characteristics in spiking activity and the local field potential in macaque V1. Eur. J. Neurosci. 28, 447–59 (2008).
20. Borg-Graham, L. J., Monier, C. & Frégnac, Y. Visual input evokes transient and strong shunting inhibition in visual cortical neurons. Nature 393, 369–73 (1998).
21. Adamo, M., Pun, C., Pratt, J. & Ferber, S. Your divided attention, please! The maintenance of multiple attentional control sets over distinct regions in space. Cognition 107, 295–303 (2008).
22. Mumford, D. On the computational architecture of the neocortex. Biol. Cybern. 66, 241–251 (1992).
23. Spratling, M. W. Predictive coding as a model of biased competition in visual attention. Vision Res. 48, 1391–408 (2008).
24. Lee, T. S. & Mumford, D. Hierarchical Bayesian inference in the visual cortex. J. Opt. Soc. Am. A 20, 1434 (2003).
25. Spratling, M. W. Predictive coding as a model of response properties in cortical area V1. J. Neurosci. 30, 3531–43 (2010).
26. Arnal, L. H., Wyart, V. & Giraud, A.-L. Transitions in neural oscillations reflect prediction errors generated in audiovisual speech. Nat. Neurosci. 14, 797–801 (2011).
27. Angelucci, A. et al. Circuits for local and global signal integration in primary visual cortex. J. Neurosci. 22, 8633–46 (2002).
28. Lamme, A. F., Supèr, H. & Spekreijse, H. Feedforward, horizontal, and feedback processing in the visual cortex. Curr. Opin. Neurobiol. 8, 529–535 (1998).

29. Friston, K. The free-energy principle: a unified brain theory? Nat. Rev. Neurosci. 11, 127–38 (2010).
30. Srinivasan, M. V., Laughlin, S. B. & Dubs, a. Predictive Coding: A Fresh View of Inhibition in the Retina. Proc. R. Soc. B Biol. Sci. 216, 427–459 (1982).
31. Roach, N. W., McGraw, P. V & Johnston, A. Visual motion induces a forward prediction of spatial pattern. Curr. Biol. 21, 740–5 (2011).
32. Arnold, D. H., Thompson, M. & Johnston, A. Motion and position coding. Vision Res. 47, 2403–10 (2007).
33. Arnold, D. H., Marinovic, W. & Whitney, D. Visual motion modulates pattern sensitivity ahead, behind, and beside motion. Vision Res. 98, 99–106 (2014).
34. Marinovic, W. & Arnold, D. H. An illusory distortion of moving form driven by motion deblurring. Vision Res. 88, 47–54 (2013).
35. Logothetis, N. K. What we can do and what we cannot do with fMRI. Nature 453, 869–78 (2008).
36. Waldvogel, D. et al. The relative metabolic demand of inhibition and excitation. Lett. to Nat. 406, 995–998 (2000).
37. Goense, J. B. M. & Logothetis, N. K. Neurophysiology of the BOLD fMRI signal in awake monkeys. Curr. Biol. 18, 631–40 (2008).
38. Lam, K. et al. Magnetic response of human extrastriate cortex in the detection of coherent and incoherent motion. Neuroscience 97, 1–10 (2000).
39. Webb, B. S., Ledgeway, T. & McGraw, P. V. Relating spatial and temporal orientation pooling to population decoding solutions in human vision. Vision Res. 50, 2274–83 (2010).
40. Kastner, S., Nothdurft, H. C. & Pigarev, I. N. Neuronal correlates of pop-out in cat striate cortex. Vision Res. 37, 371–6 (1997).
41. Maus, G. W., Fischer, J. & Whitney, D. Motion-Dependent Representation of Space in Area MT+. Neuron 78, 554–62 (2013).

Chapter 4

Predictions to motion stimuli in human early visual cortex: effects of motion displacement on motion predictability

Wouter Schellekens
Nick F. Ramsey
Mathijs Raemaekers

Abstract

Recently, we have found that fMRI BOLD responses to moving random dots are enhanced at the location of dot appearance, i.e. the motion trailing edge. Possibly, BOLD signals reflect predictability of motion input. Alternatively, the sudden appearance of novel dots itself may enhance neural firing, not because of predictability, but due to classical receptive field effects. In the current study, we investigate the nature of enhanced BOLD activity at a motion stimulus' trailing edge. We varied motion displacement parameters (duration & velocity), while measuring BOLD amplitudes as a function of distance from the trailing edge. We have found that for all stimulus configurations, BOLD signals decrease with increasing distance from the trailing edge. This finding indicates that neural activity directly reflects the predictability of moving dots, rather than their appearance within classical receptive fields. However, different motion displacement parameters exerted only marginal effects on predictability, suggesting that early visual cortex does not literally predict motion trajectories. Rather, the results reveal a heuristic mechanism of motion suppression from trailing to leading edge, plausibly mediated through short-range horizontal connections. Simple heuristic suppression allows the visual system to recognize novel input among many motion signals, while being most energy efficient.

Introduction

The human visual system is constantly exposed to visual motion information; objects within our visual field move, and the observer moves in his surroundings. Yet, one perceives the external world as stable and coherent. Imagine a new object moving into one's visual field. How does the visual system distinguish this novel motion information from the already present abundance of other motion signals? Recent studies suggest that the human brain treats novel or unpredictable input differently from previous detected or predictable input[1,2]. These studies report a relative increase in neural activity for novel stimuli. In line with these findings, we recently reported elevated BOLD responses during the presentation of moving random dot stimuli at the locations where novel dots entered the stimulus area: the trailing edge[3,4]. A possible mechanism behind these findings is that the human brain pro-actively predicts its input, rather than passively waiting for it. Predictive coding describes such a mechanism where predictions are estimated for all sensory input[5–7]. Could it be that early visual cortex makes predictions, while encoding motion information? In the current study, we investigate the notion that directional biases in activity in visual areas V1, V2, and V3 reflect predictions to a moving random dot stimulus.

Predictions are not the only explanation for elevated BOLD responses at trailing edges of moving random dot stimuli. The effects could, for instance, also be caused by response properties of neurons, representing the trailing edge. At the trailing edge, dots might appear in the middle of a neuron's receptive field (RF), which might cause strong transient responses[8,9]. On the other hand, moving dots more distant from the trailing edge gradually pass over neurons' RFs, which might not result in a strong transient. Consequently, if elevated BOLD responses are due to strong transient responses to novel moving dots alone, then the novelty effect should only be present close to the trailing edge (Figure 1A). This stands in contrast with a prediction based mechanism. Predictive coding suggests that every input is compared to its prediction, resulting in a prediction error. Neurons would only signal the prediction error, since that part contains new and possibly valuable information[10,11]. Thus, for randomly positioned moving dots, the prediction error would be largest at the trailing edge, but gradually decrease as neurons code for portions of the stimulus that are further away from the trailing edge[12]. As a result, the amplitude of the BOLD signal would be inversely correlated with the distance from

the trailing edge (Figure 1B).

Integration of prior visual input is essential to the formation of predictions. This process could be facilitated by the fact that visual cortical areas are retinotopically organized[13,14]; any adjacent locations in visual space are also represented by adjacent locations on the cortex. Predictions could, thus, be created through short-distance neuronal interactions, possibly through horizontal corticocortical connections[15,16.] However, such scenario has an interesting consequence, for the cortical representation of the visual field is not fully continuous. Left and right visual field maps are represented in right and left hemispheres respectively. Additionally, extrastriate visual areas V2 and V3 are divided in ventral and dorsal parts, representing upper and lower visual fields. These separations might prohibit horizontal connections to bridge the horizontal and vertical meridians. Thus, if novelty effects are caused by a prediction mechanism, novelty effects may recommence when moving stimuli cross horizontal or vertical meridians. Consequently, the location of cortical boundaries influences the signal amplitude (Figure 1C).

Varying displacement characteristics of moving dots could reveal additional support for either explanation of the novelty effect. The displacement of dots is characterized by motion direction, duration, and velocity. For all explanations of the novelty effect, the motion direction determines where the trailing edge resides and where neural activity is largest. However, the spatial extent of an RF-based novelty effect would be indifferent to motion duration and velocity; the effect is caused by dot appearances within RFs, not the manner of dot translation across visual space. A prediction-based mechanism, on the other hand, would be sensitive to the actual displacement of dots within motion stimuli. Longer motion durations allow the visual system to increase prediction accuracy, while the spatial extent of estimated motion predictions would scale with motion velocity. Therefore, different motion displacement parameters would affect the slope of the signal decrease for prediction-based mechanisms. When prediction accuracy increases, prediction errors and therefore the BOLD amplitude decreases. However, prediction errors are expected to remain large directly at the trailing edge, where novel randomly positioned dots keep appearing. Thus, an increase in prediction accuracy would result in a steeper signal decrease with increasing distance from trailing edge. The opposite would be true for a decrease in prediction accuracy.

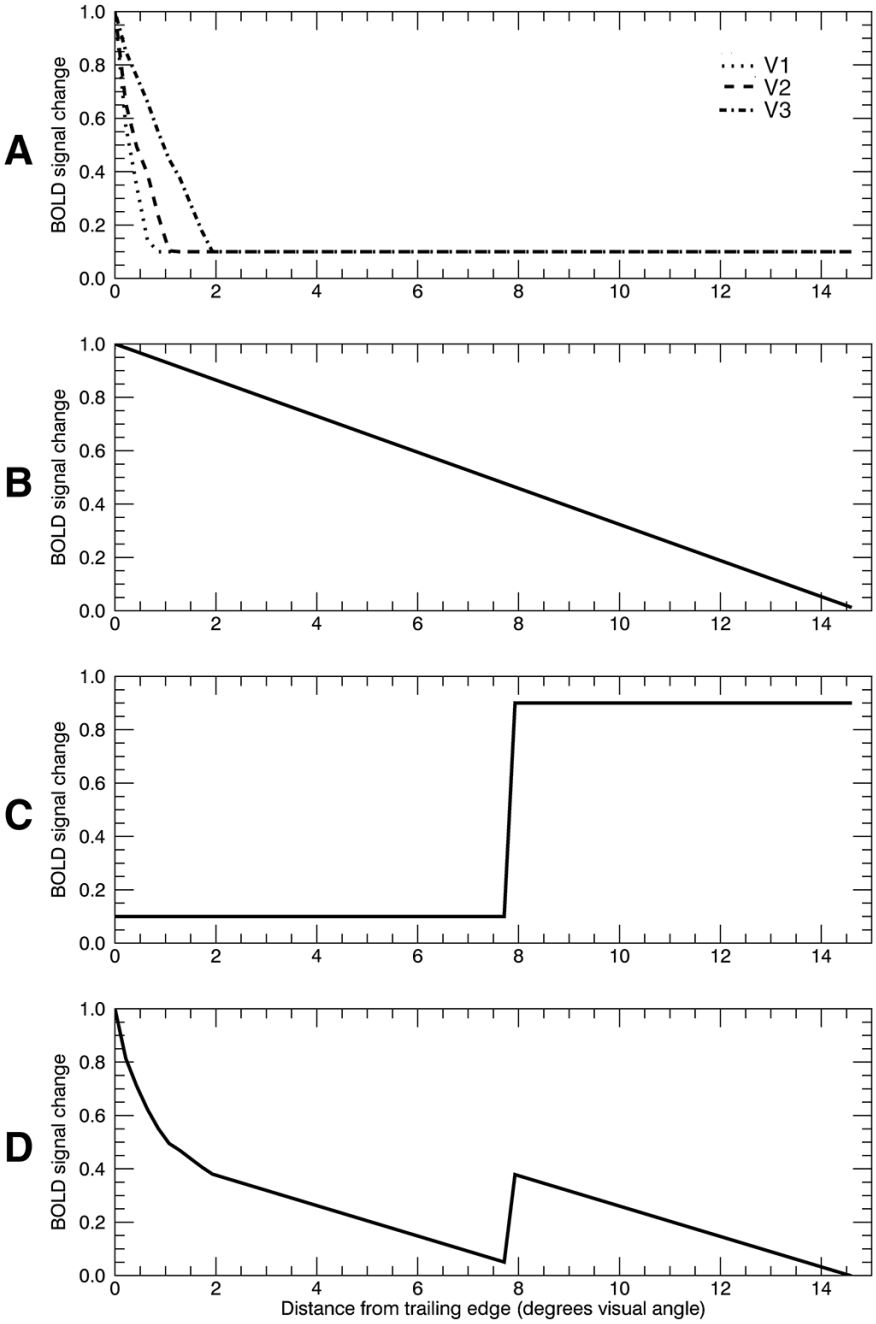

Figure 1. Components for enhancement of motion signals. *From top to bottom, hypothesized components that contribute to enlarged BOLD activity, while viewing the motion stimulus. The components depict the BOLD signal change as a function of distance from trailing edge, where novel motion information appears. The presented components are (A) classical RF effects at the trailing edge; (B) linear prediction; (C) cortical boundaries. Panel D shows a possible linear combination of all components.*

In the current study, we investigate previously reported novelty effects for a moving random dot stimulus. The novelty effect is caused strictly by response properties of neurons coding for the motion stimulus' trailing edge, by predictions of moving dots throughout the motion stimulus, or both. We hypothesize that the human visual system actually uses predictions to encode motion stimuli. Accordingly, we expect BOLD amplitudes to decrease as a function of distance from the trailing edge. However, motion crossing horizontal or vertical meridians, might reset the prediction error, due to restrictions on short-range neural interactions. Furthermore, we expect different motion displacement parameters to alter the slope of the BOLD signal decrease with increasing distance from the trailing edge.

Methods

Subjects

Twelve healthy volunteers (mean age = 23, female = 5) were recruited from the Utrecht University. All participants gave written informed consent before entering the study. The protocol was approved by the local ethics committee of the University Medical Center Utrecht, in accordance with the Declaration of Helsinki (2013).

Scan protocol

Scanning was performed on a 7 Tesla Philips Achieva scanner (Philips Healthcare, Best, Netherlands) with a 32-channel receive headcoil (Nova Medical, MA, USA). Functional MRI (fMRI) measurements were obtained using an EPI-sequence with the following parameters: SENSE factor=2.2, TR=1500 ms, TE = 25 ms, flip angle = 80°, coronal orientation, interleaved slice acquisition, FOV (AP, FH, LR) = 35.2 x 152 x 152 mm^3. The acquired matrix had the following dimensions: 22 x 96 x 96, voxel size: 1.6 x 1.583 x 1.583 mm^3. The functional images were acquired from the posterior 35 mm of the brain, covering the occipital lobe, and slices were angulated along the z-axis so that their orientation was orthogonal relative to the calcarine sulcus. Additionally, a T1-weighted image of the whole brain (1.00 x 0.98 x 0.98 mm^3, FOV = 190 x 256 x 256) and a proton density image of equal dimensions were acquired at the end of the functional sessions.

Stimuli and experimental design

Stimuli were presented with a projector on a rear projection screen placed in the MR-bore. Stimuli were programmed using C++ software (Stroustrup, 1983, Bell Laboratories, USA), and were triggered by the scanner. All stimuli were projected on a gray background and the mean luminance was held constant at 42.2 cd/m^2. During the presentation of all stimuli, a red fixation dot with a radius of 0.08° visual angle (VA) was projected on the center of the screen. Participants viewed 2 retinotopic mapping stimuli (i.e. polar angle and eccentricity mapping) and 8 moving random dot stimuli.

Retinotopic mapping

To establish the retinotopic representation of the stimulus area, where motion stimuli were to be presented, we showed participants polar angle and eccentricity mapping stimuli. The polar angle mapping stimulus was a rotating wedge (48° circular angle), containing a checkerboard pattern that reversed contrast every 125 ms (8 Hz). The polar angle stimulus made 4 full rotations (2 clockwise; 2 counterclockwise), each of which took 64.5s to complete. In total 192 functional images were acquired during polar angle mapping. Secondly, subjects perceived an eccentricity mapping stimulus, which was an expanding and contracting ring (2 cycles each) that also contained a checkerboard pattern (reversing contrast: 8 Hz). The ring had a width of 1.5° VA and covered a maximum eccentricity of 7.5° VA. One full cycle took 60s to complete, resulting in 180 acquired volumes in total.

Motion stimuli

Moving random dot patterns were presented to investigate mechanisms behind the novelty effect. For every location within the stimulus area, we calculated the distance to the trailing edge. Whether novelty effects are caused by classical RF properties or motion predictability, should become apparent in BOLD responses as a function of distance from the trailing edge. In addition, moving dot patterns had different motion durations and velocities to further investigate the underlying mechanisms.

All motion stimuli were presented within a circular area (radius 7.5° VA) that corresponded to the portion of the visual field that was retinotopically mapped. Approximately 2400 black and white square dots (width & height: 0.3° VA) were randomly distributed within this circular area. Additionally, a small circular aperture was presented around the fixation dot

(radius 0.4° VA). All dots moved in 1 of 4 motion directions: rightward, leftward, upward or downward. The motion direction determined the position of the trailing edge. Therefore, every location within the stimulus area entailed 4 distances to the trailing edge: one for each motion direction (Figure 2).

We used 4 motion durations; the dot pattern either moved for 1.25, 2.5, 7.5, or 15 seconds in one of the 4 directions. Stimuli were presented in a blocked design, where every period of motion was alternated with a 15s rest period with stationary dots. The velocity of moving dots was either 3°/s or 6°/s. Each combination of motion duration and velocity was repeated 8 times, except for the 1.25s motion duration, which was repeated 12 times, to compensate for possible low SNR as a result of its short duration. In total, 1016 functional images were acquired during the motion stimuli.

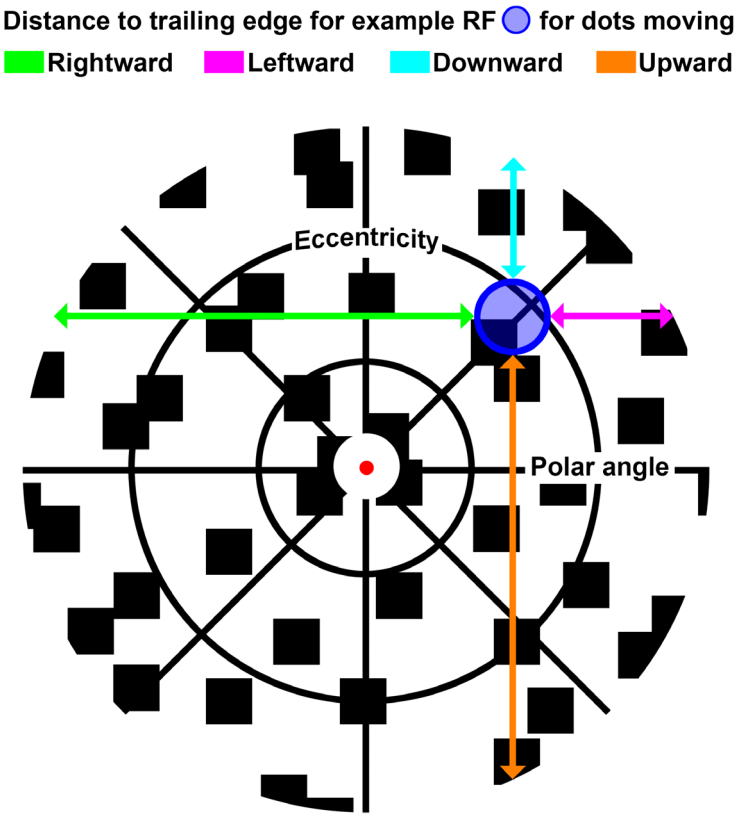

Figure 2. Condensing BOLD signals for distances from the trailing edge. *This schematic shows an example for the distances to the trailing edge for one particular RF (blue circle). The distances depend on the direction that the dots are moving, which is indicated by the colored arrows. This procedure was carried out for all visual field representations as obtained from the polar angle and eccentricity mapping.*

Attention task

To ascertain that participants fixated on the center of the screen, an attention task was presented on top of the fixation dot. Every 1000ms a white cross was briefly projected on top of the fixation dot. However for 25% of the cross projections, 3/4th of the cross was omitted, resulting in the projection of a white bar either on the left, right, top or bottom of the fixation dot (i.e. attention cue). Participants were instructed to respond to the attention cue with a button press, using a button box with 4 buttons (left, right, top and bottom buttons). For a correct response the corresponding button needed to be pressed. Any other button was an incorrect response. A missed response was reported, whenever the participant failed to press a button before the next attention cue was presented on screen.

Statistical Analysis

The T1 anatomical volume was corrected for macroscopic field inhomogeneities by dividing it with the proton density image[17]. Afterwards, the corrected T1 volume was loaded in CARET[18], and a surface was constructed per hemisphere, corresponding to gray matter layer 4. The functional volumes were preprocessed using SPM8 (i.e. slice time correction and realignment). Additionally, the functional images' timeseries were filtered using a high-pass filter with a cut-off at 5.2×10^{-3} Hz. The preprocessed functional images were mapped unto the reconstructed surfaces using a Gaussian mapping algorithm. This procedure resulted in a timeserie for each node on the reconstructed surface (on average 1.6 nodes per mm^2).

Retinotopic mapping

Both polar angle and eccentricity mapping stimuli were analyzed with a phase-encoded design matrix, where every factor in the design represented the cyclic activation of the mapping stimuli (8000ms every 64500 and 60000 ms respectively). A node's peak correlation with any of the design matrix factors determined its polar angle and eccentricity representation. Additionally, T-statistics were calculated for every node's peak correlation. The results of the polar angle mapping stimulus were used to draw ROIs on a flattened surface, encompassing the visual areas V1, V2, and V3. For analysis of the motion stimuli, only nodes were included that were situated in early visual cortical areas (i.e. V1, V2, V3), and represented the visual field position with a T-value of $T \geq 4.51$.

Motion stimuli

For each motion direction, duration and velocity, the amplitude of the BOLD response was estimated using a linear regression and a design matrix that contained factors for each condition. As cortical motion responses are known to show different activity at different eccentricities[3,19,20], the BOLD amplitude of each visual field segment was corrected for the mean BOLD activity of the eccentricity it represented. The correction was done by subtraction of the mean amplitude measured at a particular eccentricity. This correction allowed us to directly compare responses of visual field representations at different eccentricities. Subsequently, the corrected BOLD amplitudes were condensed over their distance to the trailing edge. The distance was calculated per visual field representation and motion direction, using the following formula for right- and leftward motion (D_{iRL}):

$$D_{iRL} = \sqrt{R^2 - (r_i \cos \varphi_i)^2} + x_{RL} r_i \sin \varphi_i \, , x_{RL} \in \{-1,1\}$$

For up- and downward motion (D_{iUD}):

$$D_{iUD} = \sqrt{R^2 - (r_i \sin \varphi_i)^2} + x_{UD} r_i \cos \varphi_i \, , x_{UD} \in \{-1,1\}$$

Where R is the stimulus radius, r_i is node's eccentricity and φ_i is a node's polar angle representation, and x_{RL} and x_{UD} are -1 or 1, representing either left- or rightward motion and up- or downward motion. Additionally, the fixation aperture causes a second trailing edge. Therefore, the distance to the trailing edge was corrected for visual field representations that were directly positioned between the fixation aperture and the leading edge.

Our primary objective was to establish to what extent certain predefined components contribute to the motion novelty effect. The contributing components were: classical receptive field effect (RF), linear prediction (LP), and cortical boundaries (CB). We used a multiple linear regression with a design matrix, containing factors for each component (Figure 1 A-C) on the BOLD amplitudes condensed over distance from trailing edge. The multiple linear regression resulted in a regression coefficient for each component. We tested if the regression coefficients differed significantly from 0 with a 2-tailed student's T-test. Thus, the T-test reveals for each component, whether its contribution to the multiple linear regression with the obtained BOLD amplitudes was significant. We also tested whether the regression coefficients of the CB-component differed between horizontal

and vertical motion directions in visual area V1. This could reveal if the anatomically continuous representation of dorsal and ventral visual field areas in the primary visual cortex influenced the CB-component, as would be expected.

Additionally, we expected motion displacement parameters to influence the slope, i.e. the regression coefficient of the LP component. Therefore, we used a multivariate repeated measures design to test for effects of motion duration and velocity on the LP linear regression coefficients. The design contained motion duration and velocity as within-subject factors and the visual areas as separate measures. By doing so, we were able to assess if motion duration and velocity affected the slope of BOLD amplitudes as a function of distance from trailing edge. Finally, a similar multivariate repeated measures design was used to test for differences among motion displacement parameters on the estimated BOLD amplitude, averaged across the full stimulus representation.

Results

Signal components

We showed moving random dot patterns with different motion durations and velocities to investigate underlying mechanisms of elevated BOLD responses at a motion stimulus' trailing edge. We selected 3 components, which likely contribute to the amplitude of the BOLD response, when viewing a moving random dot pattern: classical receptive field effects (RF), linear prediction (LP), and cortical boundaries (CB). Visual inspection of the BOLD amplitudes averaged across all conditions and corrected for eccentricity effects clearly showed variations in the amplitude with distance to the trailing edge (Figure 3). When testing the contributing factors we found that the RF component did not explain a significant amount of variance in the BOLD amplitudes condensed over distance from trailing edge ($T_{(11)}$=0.133, p=.897), while LP and CB components did ($T_{(11)}$=7.176, p<.001 and $T_{(11)}$=5.929, p<.001, respectively). Thus, variance in the BOLD signal in early visual cortex while viewing moving random dot stimuli is significantly explained by linear prediction and cortical boundary effects, but not by classical receptive field effects.

We found that classical RF effects did not contribute to changes in BOLD amplitude as a function of distance from trailing edge. However, BOLD amplitudes exhibited a peak near the trailing edge in addition to linear prediction effects (Figure 4). Nonetheless, this

peak was not located directly at the trailing edge, but was shifted approximately 0.5° VA inside the stimulus. Hence, this peak cannot be explained by strong transients to novel appearing dots directly at the trailing edge, as classical RF effects predict. Additionally, the BOLD amplitudes condensed over distance from trailing edge show strong mid-trajectory effects for most motion directions in V1, V2 and V3. However, upward and downward motion do not produce strong mid-trajectory effects in the primary visual cortex (Figure 4). Accordingly, the CB-component differed significantly between motion along the horizontal axis (i.e. right- and leftward motion) and vertical axis (i.e. up- and downward motion) in visual area V1 ($T_{(11)}$=2.379, p=0.037). Contrastingly, the CB-component did not differ significantly between motion along the horizontal and vertical axis in visual areas V2 ($T_{(11)}$=1.213, p=.251) and V3 ($T_{(11)}$=0.247, p=.810). These findings correlate with anatomical characteristics of early visual cortical areas: all areas are physically separated along representations of horizontal and vertical meridians, except for dorsal and ventral V1, which are fully connected along the calcurine sulcus. This indicates that the mid-trajectory effects (i.e. CB-component) are indeed related to short-range corticocortical connectivity effects.

Duration and velocity

We hypothesized that motion duration and motion velocity would affect linear prediction effects. Therefore, we tested whether LP regression coefficients differed among the 4 motion durations and 2 motion velocities. We found that motion duration significantly influenced the slope of linear prediction effects ($F_{(3,9)}$=18.366, p<.001). Shorter motion durations showed a steeper signal decrease with increasing distance from trailing edge compared to longer motion durations (Figure5). Additionally, shorter motion durations also resulted in higher absolute BOLD signal changes ($F_{(3,9)}$=9.351, p=.004).

For different motion velocities, we did not find a significant difference in the slope of the linear prediction component ($F_{(1,11)}$=2.848, p=.120). The slope of the signal decrease with distance from trailing edge was approximately equal between dots moving at 3°/s and 6°/s (Figure 5). Also, the absolute BOLD signal change differed between the 2 motion velocities ($F_{(1,11)}$=11.389, p=.006). Motion at 6°/s resulted in overall larger signal changes than motion at 3°/s. This had, however, no effect on the slope of the prediction component.

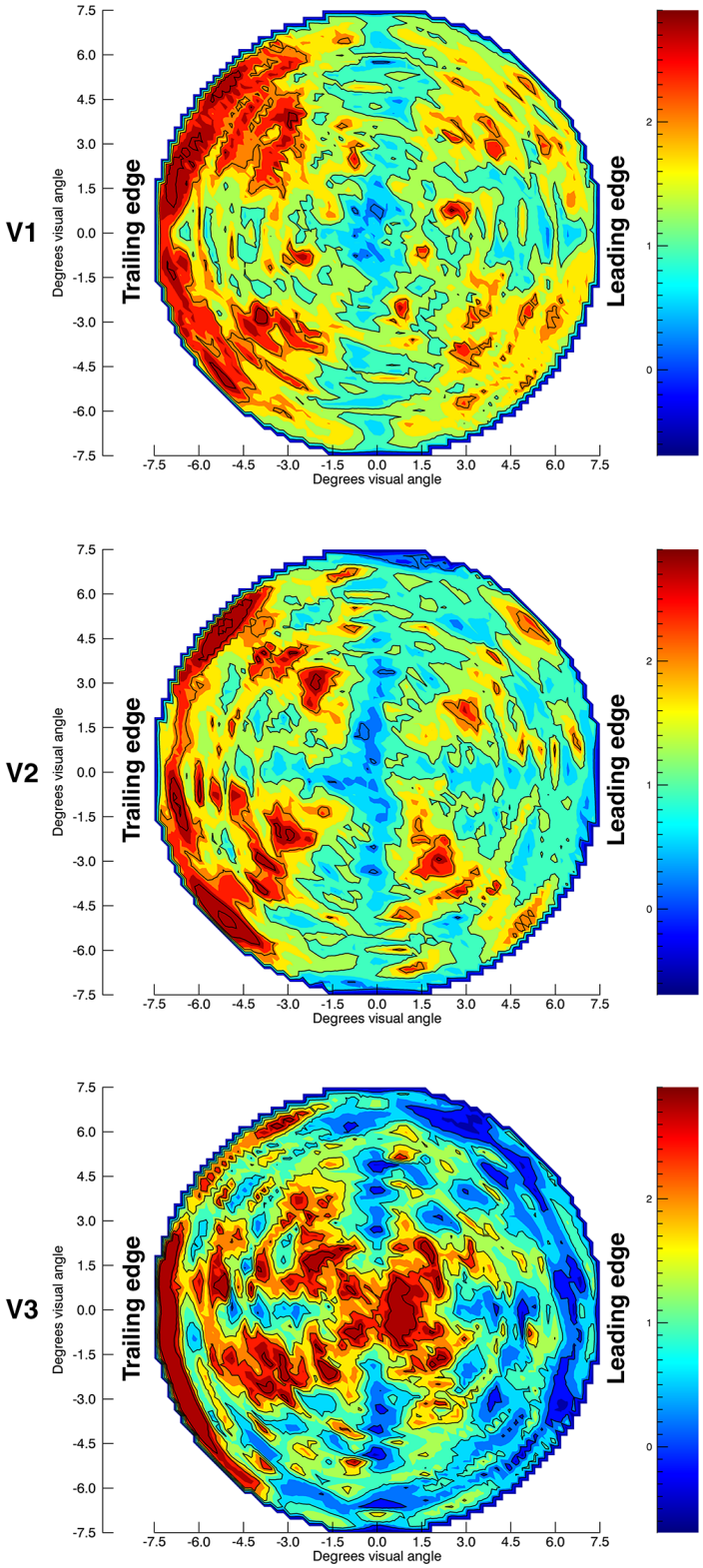

Figure 3. Contour results. *Normalized BOLD activity across the representation of the stimulus from the trailing to the leading edge. The figure was generated by averaging different motion directions after aligning leading and trailing edges. Results are shown for visual areas V1, V2 and V3 (rows) and are the mean of all stimulus conditions. The color-bar shows the estimated amplitudes of the BOLD responses, which were corrected for the mean activity per eccentricity.*

Thus, results from varying motion displacement parameters do not present us with a univocal outcome. We found that the slope of the prediction component differed for varying motion durations, but not for motion velocities. However, there were large differences in absolute levels of BOLD activity between all motion displacement conditions. Possibly, the slope of the prediction component scales with the absolute signal change, since both the slope of the prediction component as well as the estimated peak signal change

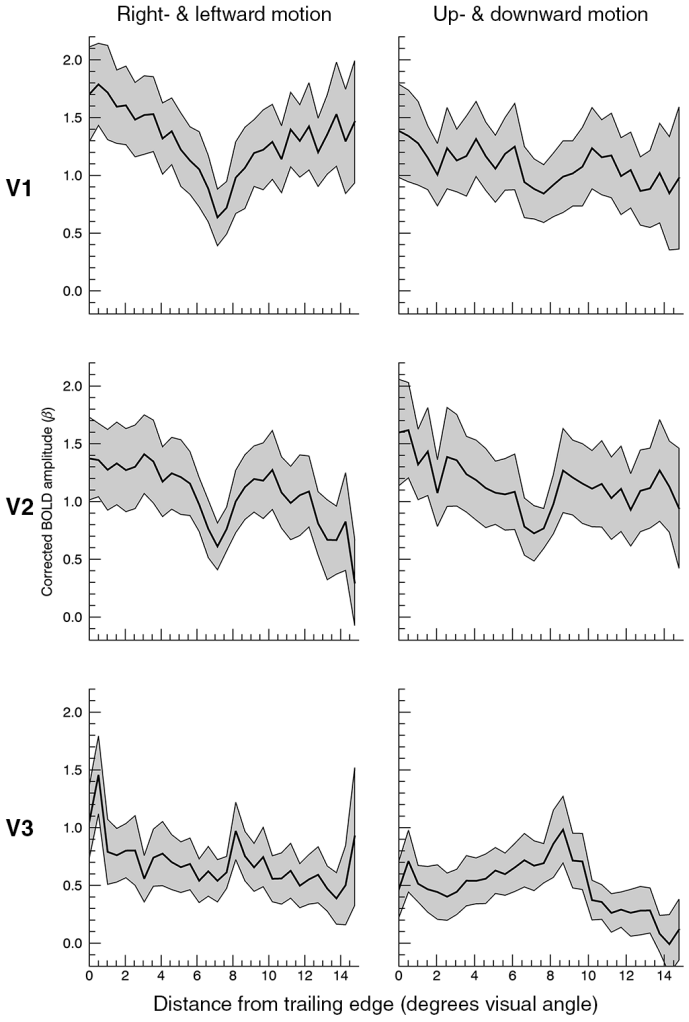

Figure 4. BOLD activity with distance from trailing edge for vertical and horizontal motion. *BOLD amplitudes are plotted for visual areas V1, V2, and V3 (rows) In the left column, mean results from right- and leftward motion are presented, where the results from leftward motion are rotated 180° to align trailing and leading edges. The right column presents the mean of up- and downward motion, where downward motion is rotated 180°. BOLD amplitudes were corrected for the mean activity per eccentricity. The plotted gray areas represent the standard error of the mean across subjects.*

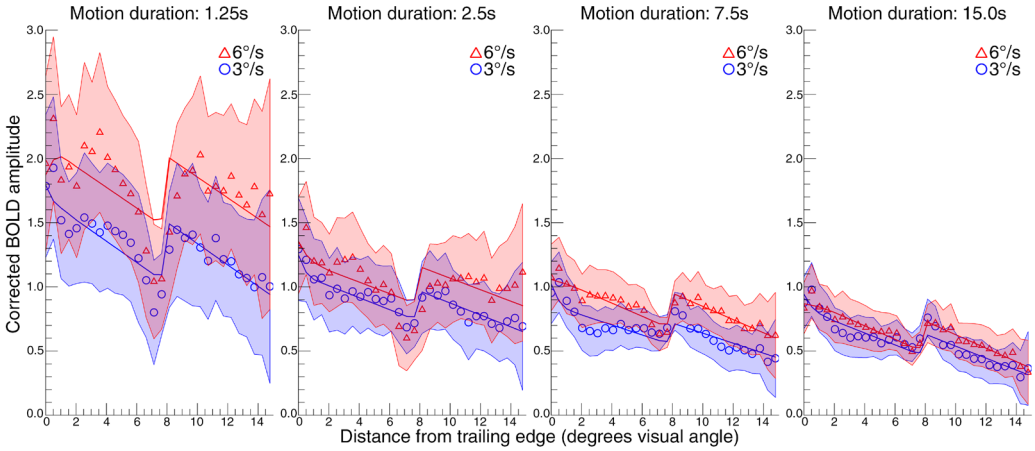

Figure 5. BOLD activity with distance from trailing edge for different durations & velocities. *BOLD amplitudes are the mean of V1, V2, and V3. The amplitudes are corrected for the mean activity per eccentricity. The separate graphs from left to right show different motion durations. Different velocities are shown in different colors and symbols. Additionally, the fits from the multiple linear regression are shown per motion duration and velocity (solid line). The plotted areas with lighter shade represent the standard error of the mean across subjects.*

decrease for longer motion durations. Detection of effects on the slope could, thus, have been confounded or obscured by a scaling by absolute levels of BOLD activity.

Attention task

Finally, during all stimulus configurations participants were instructed to remain fixated on the center of the screen, where an attention task was presented. On average, participants responded correctly to 77% of attention cues, incorrectly to 1% of attention cues, and no button was pressed for 22% of attention cues (missed response). These results show that participants were able to remain focused on the screen center, and that the attention task was difficult enough to keep participants engaged at the center.

Discussion

In this study, we conducted an in-depth investigation on previously reported motion novelty effects at the trailing edge of motion stimuli. We hypothesized that enlarged BOLD responses to novel moving dots are not mere enlarged transients caused by sudden dot appearances (i.e. classical receptive field effects), but rather reflect the predictability of visual input. The results show that BOLD signals in early visual cortex decrease for

motion information further away from the trailing edge, reflecting the predictability of motion input. Importantly, we did not find support for classical receptive field (RF) effects enhancing BOLD activity directly at the motion trailing edge. In fact, observed effects are likely caused by corticocortical, or horizontal, connections as the linear decrease in BOLD signal is interrupted at cortical boundaries. We also postulated that motion duration and velocity would affect motion predictability, altering the rate at which the signal decreases with distance from the trailing edge. Varying motion durations affected the slope of the linear signal decrease, but different motion velocities did not. However, effects of motion displacement parameters on the linear prediction could be a scaling effect secondary to large absolute differences in BOLD responses that were observed between conditions. The equivocal motion displacement effects may indicate that the visual system does not literally predict trajectories of moving dots. Alternatively, the visual system could mimic predictions by means of automatic suppression from trailing to leading edge, which also allows for the integration of prior motion information (i.e. heuristically).

We report that BOLD amplitudes during perception of a moving random dot pattern decrease as the distance between visual field representation and trailing edge increases. For large portions of the stimulus representation, this signal decrease was linear, in accordance with previous findings regarding effects of predictability on BOLD responses[12]. However, there are signs of other components that contributed to the BOLD signal. Near the trailing edge BOLD amplitudes exhibit a peak in addition to a linear prediction mechanism. Importantly, this additional signal peak was not found directly at the trailing edge (Figure 4), and could thus not be explained by an RF model. The signal peak may be caused by enlarged transient responses of motion detectors[21], rather than contrast detectors[8]. More specifically, motion detectors are not effectively stimulated directly at the trailing edge, as opposed to further inside the stimulus representation where enough evidence has been gathered for the presence of motion. Alternatively, non-linear effects of predictive processing of motion may be introduced directly at the trailing edge[22,23].

The second component that contributed to variations in the amplitude across the stimulus was the effect of cortical boundaries. We found a sharp signal decrease and sequential increase at the horizontal and vertical meridians when observing BOLD amplitudes

as a function from distance to the trailing edge (Figure 3). Such an activity pattern can be explained if motion information is integrated by corticocortical, or horizontal, connections[15,16,24]. Due to the physical separation of cortical visual areas along horizontal and vertical meridians[25], integration of prior motion information cannot be accomplished through horizontal connections. In further support of this interpretation, we found no boundary effect in V1 during vertical motion, which makes sense since the dorsal and ventral part of V1 form a single continuous anatomical representation, and motion integration would not be interrupted when dots cross the horizontal meridian.

Cortical responses to visual motion are largely explained by a linear prediction mechanism, which could mean that motion displacement (i.e. motion duration and velocity) would affect visual motion predictions. We anticipated that longer motion durations would increase prediction accuracy, which should then result in a steeper linear prediction slope. However, we found that longer motion durations resulted in a less steep prediction slope, which is opposite to the hypothesized effect. Moreover, effects of motion durations are predominantly found in absolute amplitude estimates of the BOLD responses, rather than the prediction slope. Larger amplitude estimates were found throughout the entire stimulus representation for shorter compared to longer motion durations. These large differences could perhaps be accounted for by adaptation mechanisms[26–28] and/or nonlinear characteristics of the fMRI BOLD signal[29–31]. In addition, the large variation in absolute amplitudes could induce a scaling of the linear prediction slope's size, and thereby explain current observed findings.

The second motion displacement parameter, motion velocity, did not influence the linear prediction slope. Dots moving at 3°/s and 6°/s produce linear prediction slopes of similar steepness. Interestingly, the estimated peak signal changes did exhibit large differences between the two velocities. Motion at 6°/s consistently results in higher percentage BOLD signal change than motion at 3°/s. Differences in the percentage BOLD signal change could have been caused by a difference in baseline activity for motion detectors sensitive to different speeds, as well as a difference in the amount of contrast change that the visual system was subjected to[32,33]. One could expect that the difference in amount of contrast change caused by various motion velocities would also affect the accuracy of motion predictions. Nonetheless, we have found no evidence for changes in the prediction

component caused by changes in motion velocity. Thus, we investigated the effects of 2 motion displacement parameters that were expected to influence mechanisms for motion predictions. Since neither parameter convincingly influenced the prediction slope, we did not obtain compelling evidence that human early visual cortex literally predicts trajectories of moving dots. The visual system does, however, produce a prediction-like pattern for all motion conditions, which suggests that the visual system mimics predictions, rather than actually representing anticipated states. Prediction patterns could be formed by automatic suppression from trailing to leading edge. Plausibly, this information is both sufficient and necessary to integrate motion information over space and time.

We conducted the motion experiments anticipating predictive coding mechanisms[6], but the results do not support the notion that motion trajectories are literally predicted. Instead, we propose a heuristic motion suppression mechanism that produces prediction-like responses, albeit one that is perhaps limited to a certain category of predictive coding. Most recent accounts of predictive coding assume the existence of predictions for all neuronal input[5,34]. Neuronal input may even be predicted through competition of many possible predictions[22,35]. However, one could question the necessity of actual predictions, considering that alternative, simpler, algorithms may produce similar outcomes. For instance, one of the first reported accounts of predictive coding[36], suggests that predictive aspects can be derived from auto-correlating neuronal activity with activity from neighboring neurons. Such auto-correlation does not require an actual prediction to be estimated. Inclusion of predictive qualities through heuristic algorithms that do not require real predictions should be interpreted as a conceptual as opposed to ontological account of neuronal input prediction. Current results could then be taken to suggest that predicting motion information by early visual cortex plausibly ensues through heuristic predictive coding mechanisms. Possibly, activated motion detectors, sensitive to a specific range of motion directions at a certain part of the visual field, could induce a hyperpolarization of other motion detectors along the anticipated motion trajectory. The visual system would still benefit greatly from heuristic predictive coding mechanisms, allowing for appropriate processing of previously detected input in an energy resources efficient manner[37].

There are a couple of factors that could have confounded current findings. First, there is the possibility of eye movements along any of the motion directions. However, in a previous study with similar stimuli, no correlation was found between locations of enhanced motion responses and the direction of micro saccades[4]. Furthermore, we found sharp signal decreases and sequential increases near the visual representations of the cardinal axes, which would have been spread out over the stimulus if participants had not been able to fixate properly. Second, the results could have been influenced by covert spatial attention, which is known to locally enhance responses in early visual cortex[38–40]. However, participants were engaged in a demanding attention task at central fixation on which they had good, but not perfect performance (77% correct responses). Thus, current results are best explained by predictive aspects of visual motion processing in early visual cortex.

The present study investigates previously reported novelty effects for motion stimuli. We found that the amplitudes of BOLD responses to moving random dot patterns decrease with distance from the trailing edge, resulting in relatively enhanced BOLD activity near the trailing edge. Additionally, we present evidence that linear prediction effects are mediated through horizontal connections. Despite the prediction-like responses to motion stimuli, motion displacement parameters only marginally influenced predictions made by the visual system. We therefore propose that predictive coding for motion stimuli follows a heuristic algorithm, rather than literally predicting the trajectories of motion contrast changes.

References

1. Wacongne, C., Changeux, J.-P. & Dehaene, S. A neuronal model of predictive coding accounting for the mismatch negativity. J. Neurosci. 32, 3665–78 (2012).
2. Alink, A., Schwiedrzik, C. M., Kohler, A., Singer, W. & Muckli, L. Stimulus predictability reduces responses in primary visual cortex. J. Neurosci. 30, 2960–6 (2010).
3. Schellekens, W., Van Wezel, R. J. A., Petridou, N., Ramsey, N. F. & Raemaekers, M. Integration of Motion Responses Underlying Directional Motion Anisotropy in Human Early Visual Cortical Areas. PLoS One 8, e67468 (2013).
4. Raemaekers, M., Lankheet, M. J. M., Moorman, S., Kourtzi, Z. & van Wezel, R. J. A Directional anisotropy of motion responses in retinotopic cortex. Hum. Brain Mapp. 30, 3970–80 (2009).
5. Rao, R. P. & Ballard, D. H. Predictive coding in the visual cortex: a functional interpretation of some extra-classical receptive-field effects. Nat. Neurosci. 2, 79–87 (1999).
6. Friston, K. A theory of cortical responses. Philos. Trans. R. Soc. Lond. B. Biol. Sci. 360, 815–36 (2005).
7. Lee, T. S. & Mumford, D. Hierarchical Bayesian inference in the visual cortex. J. Opt. Soc. Am. A 20, 1434 (2003).
8. Borg-Graham, L. J., Monier, C. & Frégnac, Y. Visual input evokes transient and strong shunting inhibition in visual cortical neurons. Nature 393, 369–73 (1998).
9. Gieselmann, M. a & Thiele, a. Comparison of spatial integration and surround suppression characteristics in spiking activity and the local field potential in macaque V1. Eur. J. Neurosci. 28, 447–59 (2008).
10. Den Ouden, H. E. M., Daunizeau, J., Roiser, J., Friston, K. J. & Stephan, K. E. Striatal prediction error modulates cortical coupling. J. Neurosci. 30, 3210–9 (2010).
11. Egner, T., Monti, J. M. & Summerfield, C. Expectation and surprise determine neural population responses in the ventral visual stream. J. Neurosci. 30, 16601–8 (2010).
12. Abler, B., Walter, H., Erk, S., Kammerer, H. & Spitzer, M. Prediction error as a linear function of reward probability is coded in human nucleus accumbens. Neuroimage 31, 790–5 (2006).
13. Hubel, D. H. & Wiesel, T. N. Receptive fields and functional architecture of monkey striate cortex. J. Physiol. 195, 215–243 (1968).
14. Wandell, B. A. & Winawer, J. Imaging retinotopic maps in the human brain. Vision Res. 51, 718–37 (2011).
15. Angelucci, A. et al. Circuits for local and global signal integration in primary visual cortex. J. Neurosci. 22, 8633–46 (2002).
16. Gilbert, C. D. & Wiesel, T. N. Columnar Specificity of Intrinsic Horizontal and Corticocortical Connections in Cat Visual Cortex. J. Neurosci. 9, 2432–2442 (1989).
17. Van de Moortele, P.-F. et al. T1 weighted brain images at 7 Tesla unbiased for proton density, T2* contrast and RF coil receive B1 sensitivity with simultaneous vessel visualization. Neuroimage 46, 432–446 (2009).
18. Van Essen, D. C. et al. An integrated software suite for surface-based analyses of cerebral cortex. J. Am. Med. Inform. Assoc. 8, 443–59 (2001).
19. Arnold, D. H., Thompson, M. & Johnston, A. Motion and position coding. Vision Res. 47, 2403–10 (2007).
20. Johnston, A. & Wright, M. J. Lower thresholds of motion for gratings as a function of eccentricity and contrast. Vision Res. 25, 179–185 (1985).
21. Borst, a & Egelhaaf, M. Principles of visual motion detection. Trends Neurosci. 12, 297–306 (1989).
22. Spratling, M. W. Predictive coding as a model of biased competition in visual attention. Vision Res. 48, 1391–408 (2008).
23. Bastos, A. M. et al. Canonical microcircuits for predictive coding. Neuron 76, 695–711 (2012).
24. Somers, D. C. et al. A Local Circuit Approach to Understanding Integration of Long-range Inputs in Primary Visual Cortex. Cereb. Cortex 8, 204–217 (1998).
25. Deyoe, E. A. et al. Mapping striate and extrastriate visual areas in human cerebral cortex. Proc. Natl. Acad. Sci. U. S. A. 93, 2382–2386 (1996).
26. Carandini, M. & Ferster, D. A Tonic Hyperpolarization Underlying Contrast Adaptation in Cat Visual Cortex. Science (80-.). 276, 949–952 (1997).
27. Krekelberg, B., Boynton, G. M. & van Wezel, R. J. a. Adaptation: from single cells to BOLD signals. Trends Neurosci. 29, 250–6 (2006).
28. Dhruv, N. T. & Carandini, M. Cascaded effects of spatial adaptation in the early visual system. Neuron 81, 529–35 (2014).
29. Boynton, G. M., Engel, S. a, Glover, G. H. & Heeger, D. J. Linear systems analysis of functional magnetic resonance imaging in human V1. J. Neurosci. 16, 4207–21 (1996).

30. Vazquez, a L. & Noll, D. C. Nonlinear aspects of the BOLD response in functional MRI. Neuroimage 7, 108–18 (1998).
31. Wager, T. D., Vazquez, A., Hernandez, L. & Noll, D. C. Accounting for nonlinear BOLD effects in fMRI: parameter estimates and a model for prediction in rapid event-related studies. Neuroimage 25, 206–18 (2005).
32. Price, N. S. C., Ono, S., Mustari, M. J. & Ibbotson, M. R. Comparing acceleration and speed tuning in macaque MT: physiology and modeling. J. Neurophysiol. 94, 3451–64 (2005).
33. Thiel, A., Greschner, M., Eurich, C. W., Ammermüller, J. & Kretzberg, J. Contribution of individual retinal ganglion cell responses to velocity and acceleration encoding. J. Neurophysiol. 98, 2285–96 (2007).
34. Arnal, L. H., Wyart, V. & Giraud, A.-L. Transitions in neural oscillations reflect prediction errors generated in audiovisual speech. Nat. Neurosci. 14, 797–801 (2011).
35. Spratling, M. W. Predictive coding as a model of response properties in cortical area V1. J. Neurosci. 30, 3531–43 (2010).
36. Srinivasan, M. V., Laughlin, S. B. & Dubs, a. Predictive Coding: A Fresh View of Inhibition in the Retina. Proc. R. Soc. B Biol. Sci. 216, 427–459 (1982).
37. Feldman, H. & Friston, K. J. Attention, uncertainty, and free-energy. Front. Hum. Neurosci. 4, 215 (2010).
38. Kastner, S., De Weerd, P., Desimone, R. & Ungerleider, L. G. Mechanisms of directed attention in the human extrastriate cortex as revealed by functional MRI. Science (80-.). 282, 108–111 (1998).
39. Corbetta, M. et al. A common network of functional areas for attention and eye movements. Neuron 21, 761–73 (1998).
40. Jack, A. I., Shulman, G. L., Snyder, A. Z., McAvoy, M. & Corbetta, M. Separate modulations of human V1 associated with spatial attention and task structure. Neuron 51, 135–47 (2006).

Chapter 5

Changes in fMRI BOLD dynamics reflect anticipation of a moving object in human early visual cortex

Wouter Schellekens
Nick F. Ramsey
Richard, J. A. van Wezel
Mathijs Raemaekers

Abstract

The human brain is thought to respond differently to novel versus predictable neural input. In human visual cortex, neural response amplitude to visual input might be determined by the degree of predictability. It has, for instance, been shown that fMRI BOLD responses to random dot kinematograms are relatively enhanced at the onsets of motion trajectories, where novel motion input cannot be predicted. However, it remains unclear whether the entire trajectory of a single moving object is anticipated. We investigated how fMRI BOLD responses in human early visual cortex reflect the anticipation of a single moving bar's trajectory. We found that BOLD signals decreased linearly from onset to offset of the stimulus trajectory. Moreover, decreased amplitudes of BOLD responses coincided with an increased initial dip as the stimulus moved along its trajectory. The same pattern of results was observed for a stepwise moving bar that progressed along the motion trajectory in discrete steps, creating an apparent motion trace. Importantly, motion anticipation effects were absent, when motion coherence of a similar stepwise moving bar was disrupted by contrast reversals at each step. These results show that human early visual cortex anticipates the trajectory of a coherently moving object by means of a preliminary suppression of neural activity along the path of motion. Plausibly, the suppression of predictable input underlies visual motion integration, assisting the formation of stable motion percepts.

Introduction

Over the last decades, it has been suggested that the human brain actively predicts input, rather than passively waiting for it. Mechanisms like 'predictive coding' pose that predictions are made for all sensory input, possibly using Bayesian statistics[1,2]. Several studies have shown signs of prediction-based mechanisms in the brain, with novel or unpredictable input resulting in relatively enhanced neural activity[3,4]. Additionally, elevated BOLD signals have been reported in early visual cortex at the trailing edge of moving random dot patterns, where novel dots enter the stimulus area[5–9]. The latter results suggest that the visual system may encode novelty of a moving stimulus through anticipation of its trajectory. However, motion novelty effects have specifically been demonstrated using random dot kinematograms, rather than single moving objects. If visual cortex genuinely anticipates motion trajectories, encoding of stimulus novelty is naturally expected for single object motion.

In this study, we address two essential questions regarding motion input prediction in the human brain. For one, what is the spatial extent of changes in BOLD activity along the trajectory of a single moving object? If effects are only found directly near motion trailing/leading edges or any particular visual field eccentricity, they could be due to classical receptive field effects[10,11], rather than predictive integration of motion input. Under visual input prediction, a gradual change in neural activity along the entire motion trajectory is expected. A second issue concerns the hierarchical level at which predictive processing of visual motion occurs[12]. If predictive motion integration is primarily a low-level bottom up process, then disrupting low, but not high-level motion features along the motion trajectory, would diminish or even decimate effects of motion anticipation, while top-down or feedback processes would remain relatively unaffected. Modifying the coherence of a moving stimulus could thereby reveal details on the level of processing at which the visual system anticipates an object's movement.

In the current study, we investigate whether fMRI BOLD signals in human early visual cortex, induced by single object motion, reflect anticipation of motion trajectories. We hypothesize that BOLD amplitudes in early visual cortical areas (V1, V2 and V3) during the presentation of a single moving object depend on stimulus novelty. Elevated BOLD signals are expected for novel motion input at cortical representations, where

the moving object enters the visual field. As the object moves across the visual field, increased prediction accuracy should result in a gradual decrease in BOLD amplitude along cortical representations of the motion trajectory. Furthermore, we hypothesize that motion anticipation occurs at the earliest stages in visual processing, which should result in a disappearance of prediction effects, when low-level motion coherence is disrupted.

Material & Methods

Subjects

Twelve healthy volunteers (mean age = 24, female = 6) were recruited from the Utrecht University. All participants gave written informed consent before entering the study. The protocol was approved by the local ethics committee of the University Medical Center Utrecht, in accordance with the Declaration of Helsinki (2013).

Scan protocol

Scanning was performed on a 7 Tesla Philips Achieva scanner (Philips Healthcare, Best, Netherlands) with a 32-channel receive headcoil (Nova Medical, MA, USA). Functional MRI (fMRI) measurements were obtained using an EPI-sequence with the following parameters: SENSE factor=2.2, TR=1500 ms, TE = 25 ms, flip angle = 80°, coronal orientation, interleaved slice acquisition, FOV (AP, FH, LR) = 35.2 x 152 x 152 mm^3. The acquired matrix had the following dimensions: 22 x 96 x 96, voxel size: 1.6 x 1.583 x 1.583 mm^3. The functional images were acquired from the posterior 35 mm of the brain, covering the occipital lobe, and slices were angulated orthogonal to the calcarine sulcus. Additionally, a T1-weighted image of the whole brain (1.00 x 0.98 x 0.98 mm^3, FOV = 190 x 256 x 256) and a proton density image of equal dimensions were acquired at the end of the functional sessions.

Stimuli and experimental design

Stimuli were presented with a projector on a rear projection screen that was placed in the bore of the scanner. Stimuli were programmed using C++ software (Stroustrup, 1983, Bell Laboratories, USA), and their onset was triggered by the scanner. All stimuli were projected on a gray background and the mean luminance was held constant at 42.2 cd/m^2. During the presentation of all stimuli, a red fixation dot with a radius of 0.075° visual angle (VA) was projected on the center of the screen. Participants were instructed to

remain focused on the fixation dot during all experiments. The experiments consisted of a retinotopic mapping and 3 different moving bar stimuli.

Retinotopic mapping

The mapping stimulus was a moving bar-shaped checkerboard pattern (height: 15.° VA; width: 1.875° VA), that reversed contrast every 125 ms (8 Hz). This mapping stimulus assessed the visual field in Cartesian coordinates and covered the area in visual space, where the motion stimulus was to be presented (i.e. the 15° horizontal x 15° vertical VA area at central view). Coordinates on the horizontal axis were mapped with a vertically oriented bar (Figure 1A) that made 4 cycles: twice moving rightward and twice moving leftward. Coordinates along the vertical axis were assessed with a similar contrast reversing checkerboard bar, which was oriented horizontally and moved upwards and downwards for 2 cycles each (Figure 1B). The bidirectional mapping of the visual field, allowed for a nullification of the shape of the BOLD response13, possibly biasing cortical visual field representations. The mapping of both horizontal and vertical coordinates was performed in a single run, resulting in 400 functional images.

Motion stimuli

We presented 3 different stimulus conditions to investigate the effect of stimulus novelty of single moving objects on BOLD activity in early visual cortex. During all stimulus conditions, a bar (length: 15° VA; width: 1.1° VA) moved with a speed of 3.3°/s across the mapped visual field. The bar moved in one of four directions: right, left, up, or down. When the motion direction was right- or leftward, the bar was vertically oriented, whereas its orientation was horizontal for up- and downward motion directions (Figure 2A).

Each cycle of the moving bar (i.e. presentation from start to end location) was alternated with a 12 second rest period, allowing the BOLD responses to return to baseline. During the rest period, only the gray background, fixation dot and attention task were visible. Each motion direction was repeated 5 times, resulting in 20 trials, and 240 functional images per stimulus condition, and 720 functional images in total. There was a circular aperture (equal color as the background) around the fixation dot (0.3° VA), which allowed the fixation dot and attention task (see below) to be visible at all times. The stimulus conditions included (1) fluent motion, (2) coherent stepwise motion, or (3) incoherent

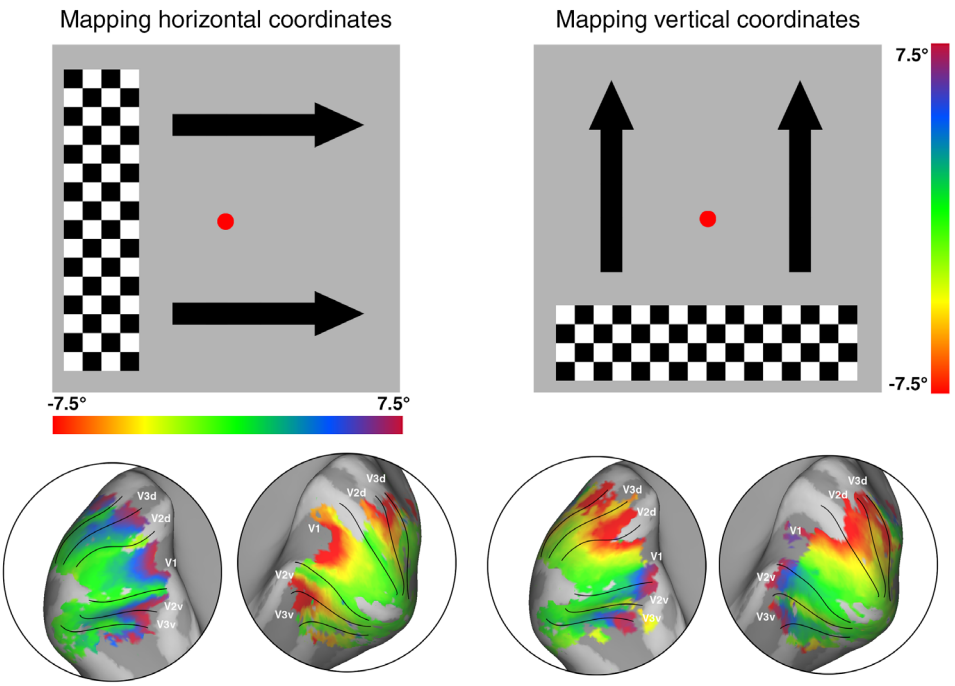

Figure 1. Retinotopic mapping Cartesian coordinates. *The figure displays a schematic of the mapping stimulus for horizontal (left) and vertical (right) coordinates. Results of 1 participant in both hemispheres are shown in the bottom row. Colors correspond to the color bar of the visual field maps.*

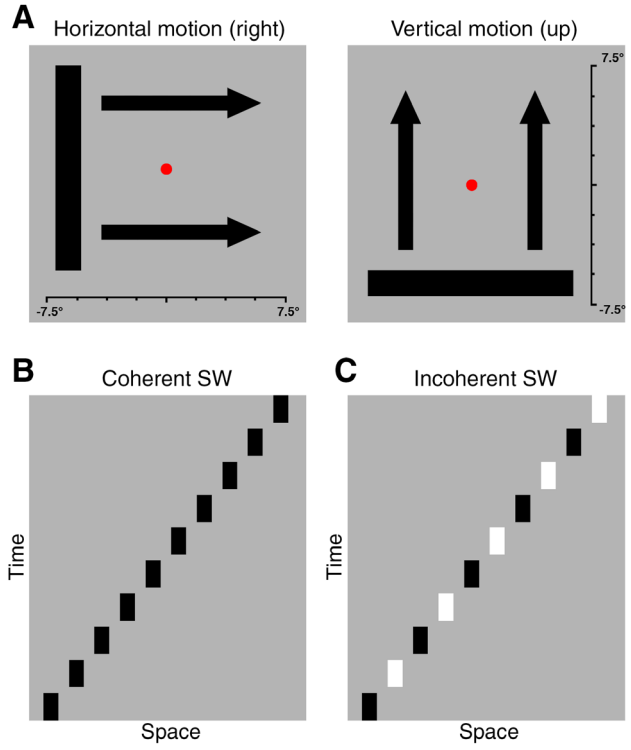

Figure 2. Stimulus design. *Figure displays a schematic of the different bar stimuli. (A) Fluent motion. A black bar moved along the horizontal (rightward and leftward motion) or vertical axis (upward and downward motion). The orientation of the bar was orthogonal to the motion direction. (B) Coherent stepwise motion. The experiment is presented as a space-time plot, showing the sequential presentation of a black bar at discrete locations across the stimulus area. (C) Incoherent stepwise motion. Bar stimulus was presented at discrete and sequential locations across the stimulus area. However, the bar contrast switched between black and white at every other location.*

stepwise motion, which were defined by variations in features of the moving bar.

(1) During fluent motion, a black bar moved fluently along the full motion trajectory (15° VA). The moving bar gradually appeared and disappeared at the edges of the mapped visual field. (2) During coherent stepwise motion, the bar was consecutively presented at 20 equally spaced locations (0.75° VA apart) across the mapped visual field for 300 ms per location (Figure 2B). The stimulus progression across the visual field in 20 discrete and consecutive steps creates an apparent motion trace. Since apparent motion contours are known to produce responses similar to fluent motion[14], similar response patterns are expected compared to the fluently moving bar. (3) During incoherent stepwise motion, the bar was again presented a bar at 20 equally spaced and consecutive locations for 300 ms per location. However, the bar switched between black and white contrast at every consecutive location (Figure 2C). This stimulus exhibited a form of motion incoherence (i.e. incoherence on the basis of contrast), while population receptive fields are visually stimulated in similar fashion compared to coherent stepwise motion.

Attention task

To ascertain that participants fixated on the center of the screen, an attention task was presented on top of the fixation dot. The attention task consisted of a white cross that was briefly presented (300ms) on top of the fixation dot every 1000ms. For 25% of the cross projections, 3/4th of the cross was omitted, resulting in the projection of a white bar either on the left, right, top or bottom of the fixation dot (i.e. attention cue). Participants were instructed to respond to the attention cue with a button press, using a button box with 4 buttons (left, right, top and bottom buttons). For a correct response, the corresponding button needed to be pressed. Any other button was an incorrect response. A missed response was reported, whenever the participant failed to press a button before the next attention cue was presented on screen.

Statistical Analysis

The T1-weighted anatomical image was divided by the proton density image to correct for macroscopic field inhomogeneities[15]. The corrected T1-weighted image was loaded in CARET[16] and a surface was constructed per hemisphere, corresponding to gray matter layer 4 (on average 1.6 nodes per mm^2). The functional volumes were preprocessed

(including slice time correction and realignment) using SPM8 (http://www.fil.ion.ucl.ac.uk/spm/). The preprocessed functional images were mapped to the reconstructed surfaces using a Gaussian mapping algorithm. This procedure resulted in a timeseries for each node on the reconstructed surface. Additionally, the timeseries were filtered using a high-pass filter with a cut-off at 7.1 x 10^{-3} Hz.

Retinotopic mapping

The mapping stimulus was analyzed with a phase-encoded design matrix. Every factor in the design matrix represented the cyclic BOLD activation of the moving checkerboard pattern, which lasted 7500 ms every 60000 ms for both the mapping of the horizontal and vertical axes of the stimulus area. For every node in the surface, Pearson correlation coefficients were calculated between the nodes timeseries and each factor in the design matrix. A node's peak correlations during the mapping of the horizontal and vertical axes determined the node's receptive field location in Cartesian coordinates. The mapping results were also used to draw ROIs on the surfaces, encompassing the visual areas V1, V2 and V3. For analysis of the motion stimuli, only nodes were included that were situated in early visual cortical areas (i.e. V1, V2, V3), and were significantly activated during the horizontal and vertical mapping stimuli ($T \geq 4.51$).

Motion Experiments

All 3 motion experiments were analyzed identically. The trajectory of the moving bar (fluent and stepwise) was divided in 10 equally spaced steps. Responses were averaged across the cortical surface area of the bar for each of the 10 steps. This procedure resulted in 10 locations in each fieldmap for which BOLD responses were analyzed, as the bar made a sweep across the visual field. Note that this procedure is the same for opposite motion directions (e.g. rightward and leftward), but that fieldmap locations are flipped 90° for the other 2 opposite motion directions (upward and downward). Additionally, the onset of the BOLD signal was corrected for the lag of the stimulus, since the moving bar was positioned at any of the 10 fieldmap locations at different points in time.

The amplitude of the BOLD response was estimated using a linear regression and a design matrix that contained factors representing BOLD activation during the different motion directions. Subsequently, BOLD amplitudes were to be compared among the 10

visual field locations along the bar's trajectory. To compensate for eccentricity dependent variations in contrast and motion sensitivity[6,17], BOLD amplitudes were subtracted from those induced by a bar with opposite motion direction. In the case of absence of anticipation effects, the difference in activity for opposing motion directions should be roughly 0 for each fieldmap position along the bar's trajectory. However, if the bar's movement is anticipated, then the difference in activity for opposing motion directions should decrease along the trajectory, becoming negative halfway the motion trajectory. We determined the slope of this activity decrease (separate for right-leftward and up-downward) by fitting a first order polynomial using a simple linear regression. A student's T-test was used to determine whether the slope differed significantly from 0. Additionally, paired samples T-tests were used to test if the slopes differed for horizontal (i.e. right-leftward) and vertical (i.e. up-downward) motion, or differed between stimulus conditions. A multivariate repeated measures test was used on the average correct responses of the attention task to asses differences in attention task performance between motion experiments.

Results

Fluent motion

We investigated if human early visual cortex anticipates the motion trajectory of a single moving bar stimulus. There were 3 stimulus conditions, i.e. fluent, coherent stepwise and incoherent stepwise motion, where the change in BOLD signal was measured at the fieldmap locations in V1, V2 and V3 along the trajectory of a moving bar. For the fluently moving bar we found a decrease in signal along the bar's trajectory ($T_{(11)}$= -5.560, p<.001), corresponding to relatively enhanced BOLD activity at the beginning of the motion trajectory (Figure 3A). This effect did not differ between horizontal and vertical motion directions ($T_{(11)}$=.554, p=.591). Furthermore, there was no difference between opposing motion directions near the middle of the trajectory, where the novelty for oppositely moving bars was equal. Thus, the fluently moving bar resulted in enhanced BOLD activity at the beginning of its trajectory, which decreased as the bar moved towards the end of its trajectory. We found this effect to be consistent for all motion directions and in all 3 visual areas, although the effect was most pronounced in visual area V2 (Figure 4).

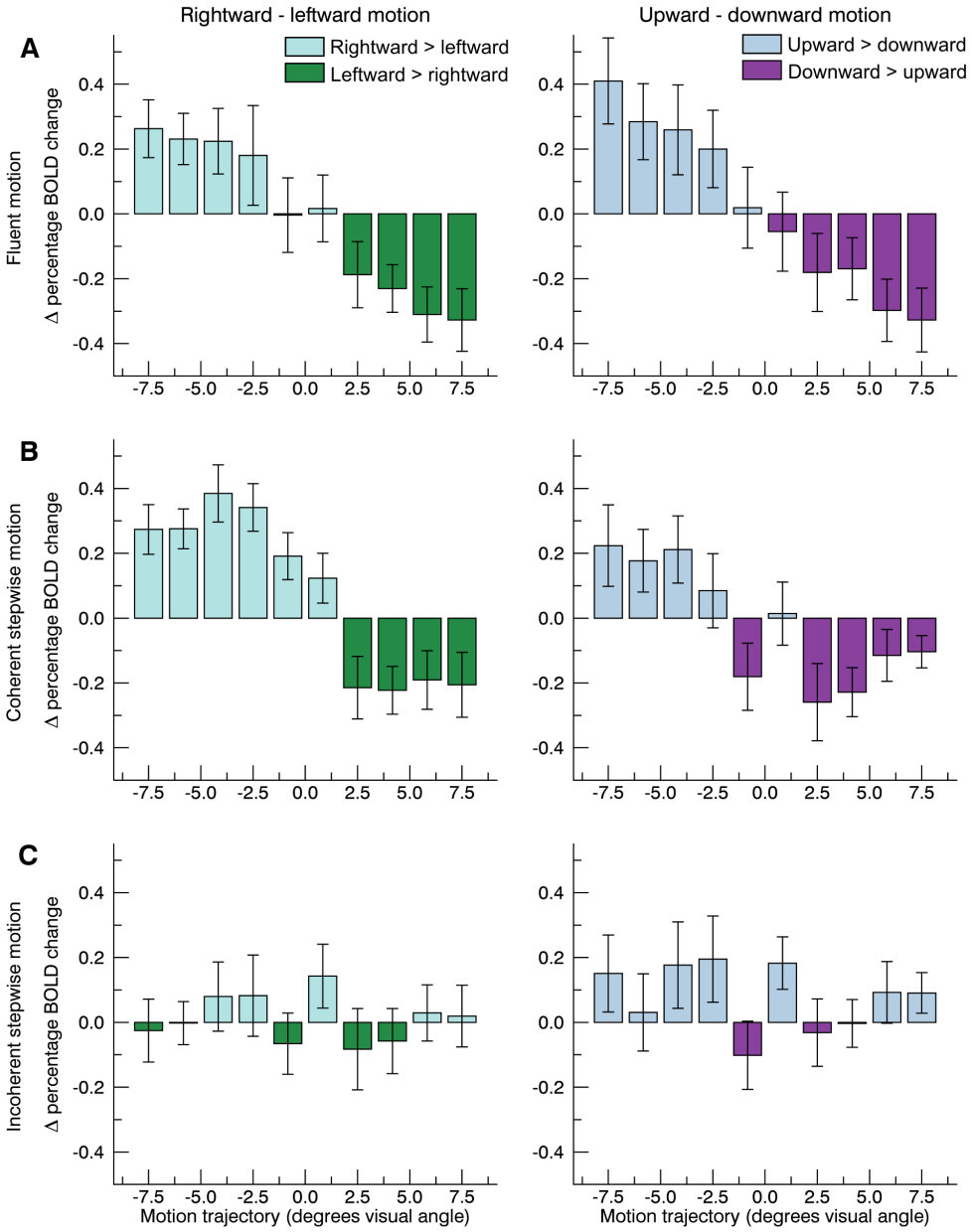

Figure 3. Results subtraction opposite motion directions. *Figure displays results after subtraction of BOLD amplitudes from opposite motion directions. Different coloring of the bars in the bar plots, shows which motion direction resulted in larger BOLD amplitudes across the visual field. During fluent motion (A), BOLD amplitudes were largest when the bar stimulus was near the onset of the motion path (e.g. rightward motion left hemifield). Differences between opposite motion directions decrease to zero near the middle of the motion trajectory. The same pattern was found for coherent stepwise bar motion (B). However, during incoherent stepwise bar motion (C), differences between opposite motion directions all reside around the zero difference line, showing no effect of motion novelty. Error bars denote the standard error across subjects.*

Coherent and incoherent stepwise motion

For coherent stepwise motion, we found a similar pattern of results as for fluently moving bar. Estimated BOLD amplitudes were enhanced near the onset as compared to the end of the motion trajectory. Furthermore, subtraction of opposite motion directions resulted in a gradual signal decrease across the motion trajectory (Figure 3B). The slope of activity decrease across the trajectory differed significantly from zero ($T_{(11)}$= -5.004, p<.001), confirming that coherent stepwise motion produces a predictable apparent motion trace. For incoherent stepwise motion, we did not observe the activity decrease along the bar's trajectory (Figure 3C), resulting in a slope that did not differ significantly from 0 ($T_{(11)}$= -.487, p=.636). Consequently, we found a significant difference between the slopes (Figure 5) of coherent and incoherent stepwise motion ($T_{(11)}$=7.243, p<.001). The slopes from fluent and coherent stepwise motion were not significantly different ($T_{(11)}$=1.983, p=.073). These results show that enhanced BOLD activity at the onset relative to the end of a motion trajectory depends on the coherence of a moving stimulus.

Change in shape of the BOLD response along the trajectory

We found that estimated BOLD amplitudes steadily decreased from onset to offset of motion trajectories during coherent motion. Upon closer inspection, we observed that the

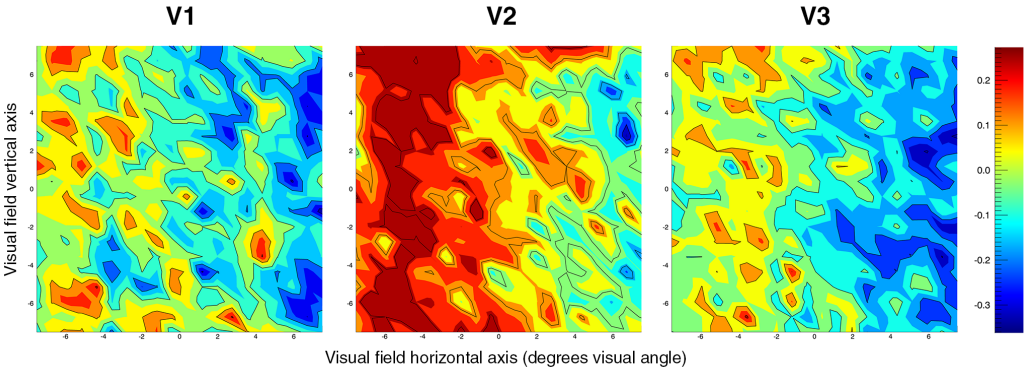

Figure 4. Contour plot fluent motion. *Figure displays the amplitude during a fluently moving bar stimulus (corrected for stimulus lag) across representations of the full stimulus area in V1, V2 and V3. Results were averaged across all motion directions and rotated to align onsets and offsets of the motion trajectories, corresponding to rightward motion. All visual areas show enhanced BOLD activity on the left side of the stimulus area, i.e. near the onset of the bar stimulus trajectory. BOLD amplitudes decrease for visual field representations towards the offset (right side stimulus area) of the motion trajectory. Effects were found along the full length of the bar stimulus, i.e. from top to bottom of the visual field representations.*

entire shape of the BOLD signal changed along the trajectory of the fluent moving bar. At the onset of a motion trajectory, the BOLD signal does not exhibit an initial dip. However, as the bar progressed towards the end of its trajectory, an initial dip with increasing size becomes apparent (Figure 6). To test whether the change in the amplitude of the initial dip was significant, we fitted a first order polynomial to the amplitude of the initial dip across the stimulus trajectory. We estimated the peak of the initial dip at each bar location by taking the lowest percentage of BOLD change during the first 3 functional images (corrected for stimulus lag) and again subtracting amplitudes from opposite motion directions to compensate for confounding effects of eccentricity. We found that the regression coefficients differed significantly from zero ($T_{(11)}$=5.614, p<.001), indicating that the initial dip indeed gradually increased in amplitude over the course of the bar's trajectory. This finding indicates that the shape of the BOLD signal depends on the novelty of visual motion input.

Discussion

We investigated if human early visual cortex anticipates the motion trajectory of a single moving stimulus. We hypothesized that fMRI BOLD activity would gradually decrease in correspondence to the increased predictability with respect to the motion stimulus. We have found that BOLD signals were enhanced at the onset of a moving bar's trajectory

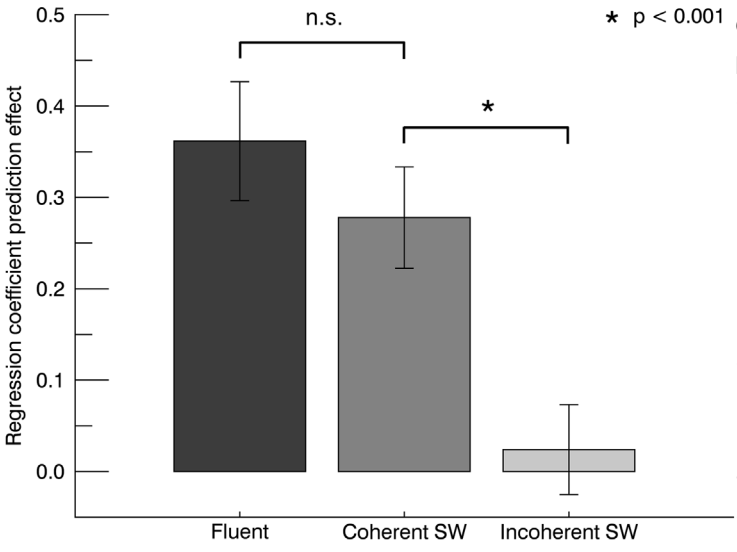

Figure 5. Regression coefficients motion prediction. *The regression coefficients are shown derived from the regression of a linear decreasing function with the subtraction of BOLD amplitudes from opposite motion directions. The larger the regression coefficient, the larger was the motion novelty effect (i.e. enhanced BOLD amplitudes for novel visual motion). Error bars denote the standard error across subjects.*

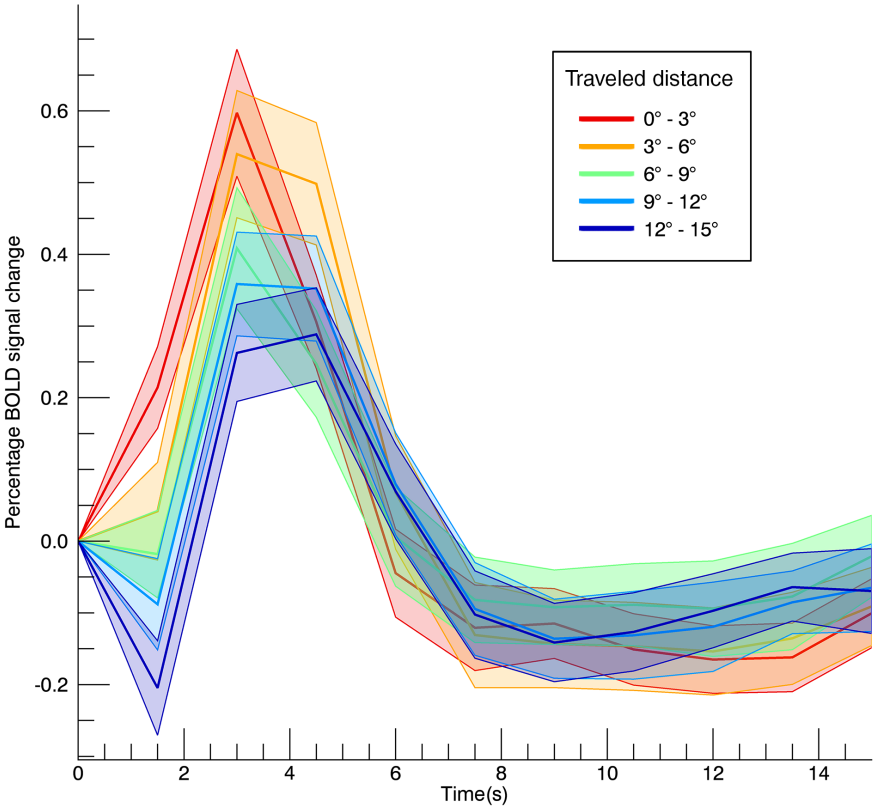

Figure 6. BOLD signal fluent motion. *The figure shows separate BOLD curves for different distances that the fluent moving bar had traveled (colors). When the bar was still close to the onset of its trajectory (i.e. shortest traveled distance; red curve), there is no initial dip and the amplitude is largest of all curves. However, when the bar had traveled the maximum distance (blue curve), there was a large initial dip and the BOLD amplitude is lowest of all curves. Both the BOLD amplitude and initial dip changed gradually as the bar stimulus moved along its trajectory. Areas of lighter shade represent standard error across subjects.*

relative to the end of the motion trajectory. Furthermore, changes in the BOLD amplitude occurred gradually along the motion trajectory and were also accompanied by gradual changes in amplitude of the initial dip. Additionally, we demonstrated that the changes in BOLD signal were in fact dependent on low-level motion features. When a black bar stimulus was presented at 20 discrete steps (i.e. stepwise, or apparent motion), BOLD responses showed a prediction pattern similar to the fluently moving bar. However, when the contrast of the bar switched between black and white at each discrete motion location, prediction effects completely disappeared.

In the current study, we present clear evidence that the BOLD response to a single moving object decreases along the motion trajectory. This finding is in line with previously reported BOLD signal enhancements at the onset of motion paths (or motion trailing edge) using various random dot kinematograms[5–9]. Classical receptive field (RF) effects could theoretically induce directional motion biases, as visual motion input at the onset of a motion trajectory may stimulate the center of a neuron's RF without first stimulating the neuron's surround, which may enhance neural transients[18,19]. The spatial extent at which the signal decrease occurs makes it unlikely that classical RF effects are underlying current findings. The BOLD signal decreased across the full motion trajectory (i.e. 15° visual angle, see also Figure 6), which clearly exceeds classical (population) receptive field sizes in human early visual cortex, ranging from approximately 1° visual angle in V1 to 3° visual angle in V3 at the outermost eccentricities of the current stimulus area[10,20]. Classical RF effects may well contribute to signal enhancement directly near the onset of a motion trajectory, but offer no plausible explanation for the linear decrease in BOLD signal over the range of 15° visual angle.

If the BOLD signal changes along the trajectory of a moving bar are not explained by classical RF effects, then by what other mechanism? There are several mechanisms that may affect visual motion processing through extraclassical (i.e. contextual) RF effects. Cortical motion signals may be summated over space and time[21,22]. Furthermore, the temporal summation is thought to be quite slow leading to a blurred cortical representation of the motion trajectory[23,24], which might subsequently be nullified by motion deblurring mechanisms[17,25,26]. Despite that these traditional motion processing mechanisms could affect the entire motion trajectory, they offer no satisfactory explanation to the gradual decrease in BOLD activity. Stimulus characteristics did not change along the trajectory, meaning that motion vector averages or blurred representations should be roughly equal along the entire trajectory. The gradual decrease in BOLD signal is more likely related to prediction mechanisms[2,27], stating the suppression of predictable neural input. We postulate that neural activity induced by a moving stimulus is increasingly suppressed along its trajectory, as predictability of future fieldmap positions increases with increased traveled distance of the stimulus. This notion of predictive motion processing is in accordance with other reports of decreases in neural activity for predictable visual input[3,28].

It is not only the amplitude of the BOLD signal that changes along a motion trajectory, but also the initial dip of the BOLD signal. When the bar stimulus was near the onset of its motion trajectory, BOLD signals did not exhibit an initial dip. However, an initial dip emerged and increased as the bar stimulus moved closer towards the end of its trajectory. This dip is thought to reflect the immediate decrease in oxyhemoglobin, following oxygen consumption as a result of neuronal activity[29,30]. However, it seems unlikely that initial oxygen consumption in response to the signaling of a moving stimulus increases as the stimulus keeps moving, while stimulus characteristics remain unchanged. In addition, it has been suggested that the cortical area that exhibits an initial dip has a tight spatial link to the cortical area where neuronal activity actually takes place in comparison to a coarse spatial distribution of the positive BOLD amplitude[29,31]. Spatial specificity of the initial dip may be established through predictive coding mechanisms, similar compared to increased fieldmap predictability of moving stimuli. We argue that these results indicate that, at least under some conditions, the initial dip is associated with a neuronal mechanism, perhaps suppression. A neuronal account, directly associated with specific stimulus features, could perhaps also contribute to the question why the initial dip is not always detected in fMRI BOLD studies[32,33].

The observed pattern of results indicates that the predictive mechanism is part of a low-level bottom-up mechanism. While fluent and apparent coherent motion produced similar motion anticipation patterns, confirming previous assertions of a similar neural basis underlying both types of visual motion processing[14,34], the BOLD activity pattern related to motion anticipation disappeared during incoherent stepwise motion. Reverse-phi phenomena could possibly have contributed to the disruption of motion coherence during the presented contrast switches[35,36]. This indicates that the occurrence of the motion prediction effect is dependent on low-level motion coherence of the stimulus. Also note that population RFs were stimulated in the same consecutive order during incoherent and coherent stepwise motion. It is therefore possible that incoherent stepwise motion caused a second-order motion trace, the trajectory of which was predictable from the participant's point of view. The observed mechanism is thus dependent on low, but not high-level anticipatory processes. Arguably the most simple neurophysiological mechanism that can account for the observed findings is that stimulated motion detectors in early visual cortex induce a temporary hyperpolarization of cell membranes at fieldmap locations in

the direction of motion, which attenuates neural responses to contrast changes when the stimulus arrives at its anticipated location. Such anticipatory inhibition might occur through (lateral) long range horizontal connections.

There are several potentially confounding issues that need to be considered. First, there is the possibility of eye movements, which can influence BOLD activity in visual cortex[37,38]. However, a previous study has shown that increased BOLD activity for novel motion information is not related to the direction of micro-saccades[5]. Second, (covert) shifts in spatial attention could theoretically confound the observed findings, by locally enhancing BOLD activity at the onset of the stimulus[39,40]. However, participants were engaged in a demanding attention task at central fixation, on which they had good but not perfect performance. In addition, effects of spatial attention would also apply to the incoherent stepwise motion, which displayed the same black bar during the initial stimulus presentation compared to coherent stepwise motion, but did not show enhanced responses near the onset of the stimulus. Finally, BOLD effects of motion prediction have been shown to be unrelated to the number of visual field locations where novel motion appeared[8], thereby dismissing shifts in visuo-spatial attention to novel motion information as a viable explanation for observed effects.

In summary, we present evidence that human early visual cortical areas V1, V2, and V3 anticipate the trajectory of a single moving bar stimulus. Relatively enhanced BOLD responses were measured near the onset of the motion trajectory, which linearly decreased as the bar stimulus moved towards the end of the motion trajectory. This effect was accompanied by an increase of an initial dip in the BOLD response. These findings can be attributed to the anticipation of a coherently moving object. We propose that early visual cortex actively anticipates upcoming motion input by means of a predictive coding related suppression mechanism.

References

1. Mumford, D. On the computational architecture of the neocortex. Biol. Cybern. 66, 241–251 (1992).
2. Rao, R. P. & Ballard, D. H. Predictive coding in the visual cortex: a functional interpretation of some extra-classical receptive-field effects. Nat. Neurosci. 2, 79–87 (1999).
3. Alink, A., Schwiedrzik, C. M., Kohler, A., Singer, W. & Muckli, L. Stimulus predictability reduces responses in primary visual cortex. J. Neurosci. 30, 2960–6 (2010).
4. Wacongne, C., Changeux, J.-P. & Dehaene, S. A neuronal model of predictive coding accounting for the mismatch negativity. J. Neurosci. 32, 3665–78 (2012).
5. Raemaekers, M., Lankheet, M. J. M., Moorman, S., Kourtzi, Z. & van Wezel, R. J. A. Directional anisotropy of motion responses in retinotopic cortex. Hum. Brain Mapp. 30, 3970–80 (2009).
6. Schellekens, W., Van Wezel, R. J. A., Petridou, N., Ramsey, N. F. & Raemaekers, M. Integration of Motion Responses Underlying Directional Motion Anisotropy in Human Early Visual Cortical Areas. PLoS One 8, e67468 (2013).
7. Maloney, R. T., Watson, T. L. & Clifford, C. W. G. Determinants of motion response anisotropies in human early visual cortex: The role of configuration and eccentricity. Neuroimage 100, 564–79 (2014).
8. Schellekens, W., van Wezel, R. J. A. Petridou, N., Ramsey, N. F. & Raemaekers, M. Predictive coding for motion stimuli in human early visual cortex. Brain Struct. Funct. (2014). doi:10.1007/s00429-014-0942-2
9. Wang, H. X., Merriam, E. P., Freeman, J. & Heeger, D. J. Motion Direction Biases and Decoding in Human Visual Cortex. J. Neurosci. 34, 12601–12615 (2014).
10. Dumoulin, S. O. & Wandell, B. a. Population receptive field estimates in human visual cortex. Neuroimage 39, 647–60 (2008).
11. Swindale, N. V. How many maps are there in visual cortex? Cereb. Cortex 10, 633–643 (2000).
12. Mijović, B. et al. The dynamics of contour integration: A simultaneous EEG-fMRI study. Neuroimage 88C, 10–21 (2013).
13. Buxton, R. B., Uludağ, K., Dubowitz, D. J. & Liu, T. T. Modeling the hemodynamic response to brain activation. Neuroimage 23 Suppl 1, S220–33 (2004).
14. Muckli, L., Kohler, A., Kriegeskorte, N. & Singer, W. Primary visual cortex activity along the apparent-motion trace reflects illusory perception. PLoS Biol. 3, e265 (2005).
15. Van de Moortele, P.-F. et al. T1 weighted brain images at 7 Tesla unbiased for proton density, T2* contrast and RF coil receive B1 sensitivity with simultaneous vessel visualization. Neuroimage 46, 432–446 (2009).
16. Van Essen, D. C. et al. An integrated software suite for surface-based analyses of cerebral cortex. J. Am. Med. Inform. Assoc. 8, 443–59 (2001).
17. Arnold, D. H., Thompson, M. & Johnston, A. Motion and position coding. Vision Res. 47, 2403–10 (2007).
18. Allman, J., Miezin, F. & Mcguinness, E. Stimulus Specific Responses from beyond the Classical Receptive Field: Neurophysiological Mechanisms for Local-Global Comparisons in Visual Neurons. Annu. Rev. Neurosci. 8, 407–430 (1985).
19. Borg-Graham, L. J., Monier, C. & Frégnac, Y. Visual input evokes transient and strong shunting inhibition in visual cortical neurons. Nature 393, 369–73 (1998).
20. Smith, A. T., Singh, K. D., Williams, A. L. & Greenlee, M. W. Estimating receptive field size from fMRI data in human striate and extrastriate visual cortex. Cereb. Cortex 11, 1182–90 (2001).
21. Webb, B. S., Ledgeway, T. & McGraw, P. V. Cortical pooling algorithms for judging global motion direction. Proc. Natl. Acad. Sci. U. S. A. 104, 3532–7 (2007).
22. Amano, K., Edwards, M., Badcock, D. R. & Nishida, S. Adaptive pooling of visual motion signals by the human visual system revealed with a novel multi-element stimulus. J. Vis. 9, 1–25 (2009).
23. Burr, D. Motion smear. Nature 284, 164–165 (1980).
24. Geisler, W. S. Motion streaks provide a spatial code for motion direction. Nature 400, 65–9 (1999).
25. Hammett, S. T., Georgeson, M. a & Gorea, a. Motion blur and motion sharpening: temporal smear and local contrast non-linearity. Vision Res. 38, 2099–108 (1998).
26. Wallis, T. S. a & Arnold, D. H. Motion-induced blindness and motion streak suppression. Curr. Biol. 19, 325–9 (2009).
27. Friston, K. The free-energy principle: a unified brain theory? Nat. Rev. Neurosci. 11, 127–38 (2010).
28. Den Ouden, H. E. M., Daunizeau, J., Roiser, J., Friston, K. J. & Stephan, K. E. Striatal prediction error modulates cortical coupling. J. Neurosci. 30, 3210–9 (2010).
29. Thompson, J. K., Peterson, M. R. & Freeman, R. D. Single-neuron activity and tissue oxygenation in the cerebral cortex. Science 299, 1070–2 (2003).
30. Yacoub, E. et al. Investigation of the initial dip in fMRI at 7 Tesla. NMR Biomed. 14, 408–12 (2001).

31. Kim, D. S., Duong, T. Q. & Kim, S. G. High-resolution mapping of iso-orientation columns by fMRI. Nat. Neurosci. 3, 164–9 (2000).
32. Hu, X. & Yacoub, E. The story of the initial dip in fMRI. Neuroimage 62, 1103–8 (2012).
33. Silva, a C., Lee, S. P., Iadecola, C. & Kim, S. G. Early temporal characteristics of cerebral blood flow and deoxyhemoglobin changes during somatosensory stimulation. J. Cereb. Blood Flow Metab. 20, 201–6 (2000).
34. Goebel, R., Khorram-Sefat, D., Muckli, L., Hacker, H. & Singer, W. The constructive nature of vision: direct evidence from functional magnetic resonance imaging studies of apparent motion and motion imagery. Eur. J. Neurosci. 10, 1563–73 (1998).
35. Bours, R. J. E., Kroes, M. C. W. & Lankheet, M. J. Sensitivity for reverse-phi motion. Vision Res. 49, 1–9 (2009).
36. Mo, C.-H. & Koch, C. Modeling reverse-phi motion-selective neurons in cortex: double synaptic-veto mechanism. Neural Comput. 15, 735–759 (2003).
37. Corbetta, M. et al. A common network of functional areas for attention and eye movements. Neuron 21, 761–73 (1998).
38. Melcher, D. & Morrone, M. C. Spatiotopic temporal integration of visual motion across saccadic eye movements. Nat. Neurosci. 6, 877–881 (2003).
39. Tootell, R. B. et al. The retinotopy of visual spatial attention. Neuron 21, 1409–22 (1998).
40. Jack, A. I., Shulman, G. L., Snyder, A. Z., McAvoy, M. & Corbetta, M. Separate modulations of human V1 associated with spatial attention and task structure. Neuron 51, 135–47 (2006).

Chapter 6

Summary and Discussion

Summary

The current thesis describes studies on visual motion integration in human early visual cortex of which a summary is presented below. Specifically, mechanisms for motion prediction are investigated using 7 Tesla BOLD fMRI. Despite numerous models on motion integration, the exact computations that are required to integrate visual motion input over substantial spatial distances remain unknown. It is known that many neurons in visual cortex are motion sensitive. Early visual cortex responds strongly to motion stimuli, such as random dot kinematograms[1,2]. However, the amplitudes of BOLD responses vary across representations of a motion stimulus in combination with specific motion directions[3–7] (i.e. directional motion bias). Relatively enhanced BOLD responses have been found for centripetal motion in the periphery of the visual field and for centrifugal motion near para-foveal visual field representations. Directional motion biases have also been reported to disappear when moving dots are occluded from sight at certain points along the dots' trajectories[3]. These findings suggest that the biased motion responses are directly related to motion integration mechanisms at the earliest stages of processing.

Whether the integration mechanisms rely on spatial or spatiotemporal integration of visual motion information is investigated in **Chapter 2**. By decorrelating random moving dot patterns either at fixed points in space or time, the presence or absence of directional motion biases could reveal the necessary information needed by the visual system to integrate visual motion signals. The study shows that directional motion biases did not disappear, when the stimulus was disrupted at fixed points in time (temporal decorrelations). However, biased motion responses significantly decreased or even disappeared when the coherence of moving dots was disrupted at fixed points in space (spatial decorrelations). The temporal decorrelations occurred every 500ms and in that time window individual dots had traveled just as far as they did in the spatial decorrelation condition. However, the length of the full uninterrupted motion trajectory was always equal to the entire stimulus width during temporal decorrelations, while the trajectory was divided into small parts during spatial decorrelations. Thus, the neural response pattern in V1, V2, and V3 to motion stimuli depends on the spatial length of an uninterrupted motion trajectory. These results, however, do not provide an answer as to why directional motion biases are consistently found within a particular visual field representation in combination with a particular motion direction. Upon examining the

results in an alternate manner, it appeared that directional motion biases were always located near a motion stimulus' trailing edge. Enhanced BOLD activity for centripetal motion in the periphery of the visual field corresponded to novel moving dots entering the stimulus area. Directional motion biases for centrifugal motion in para-foveal visual field representations were located directly after a stimulus mask surrounding the fixation dot (i.e. fixation aperture). The fixation aperture allowed the presentation of an attention task, but at the same time it occluded moving dots from sight. Hence, it created a second trailing edge when moving dots reappeared from behind the fixation aperture. Directional motion biases might therefore reflect a spatial motion integration related to the encoding of stimulus novelty.

In **Chapter 3**, the effect of stimulus novelty on directional motion biases was investigated. Neural responses in early visual cortex may represent stimulus novelty, suggesting that the visual system predicts motion input. Such interpretation is in agreement with predictive coding mechanisms, that describe the active prediction of neural input and subsequent signal inhibition[8–10]. The predictive coding hypothesis was tested by presenting moving random dot patterns over specific portions of the visual field (target area), while the stimulus' trailing and leading edges (i.e. onset and offset of motion trajectories respectively) varied with respect to the target area. As a result, BOLD amplitudes were enhanced when the stimulus' trailing edge was near the target area, compared to conditions when the stimulus' leading edge was near the target area. The actual cortical representations of the trailing and leading edges were excluded from analysis to control for classical receptive field effects, possibly causing large transient responses for novel dots appearing directly in the center of a motion detector's receptive field. Additionally, the experiments revealed no difference in BOLD response between any of the motion directions (i.e. centripetal, centrifugal, or tangential motion directions) when trailing and leading edges were equally distant from the target area. These results indicate that motion direction itself is not the immediate cause of biased BOLD responses to motion stimuli. Instead, BOLD responses seem to depend on the relative spatial distance to trailing edges and therefore stimulus novelty. Additional experimental conditions controlled for several other explanations, such as flexible retinotopy[11] and visuo-spatial attention[12]. The effects of trailing and leading edges were absent, when the motion stimulus was presented directly adjacent to the target area. This finding rules out putative shifts in retinotopic visual field

representation. A control experiment showed that the BOLD pattern related to motion novelty was unaffected by a threefold increase in the number of trailing and leading edges presented within the visual field, which excludes covert shifts in visuo-spatial attention as a viable alternative explanation. Thus, directional motion biases depend on the novelty of moving dots, causing enhanced BOLD activity near the stimulus trailing edge, where the prediction error is largest.

The visual system appears to predict motion trajectories across visual space. In **Chapter 4**, we investigated several possible consequences of visual motion prediction in early visual cortex. If the amplitude of the BOLD signal is directly proportional to the prediction error, then we expect the BOLD signal to gradually decrease along representations of the motion trajectory. Classical receptive field effects might additionally arise at the exact location of the trailing edge. Furthermore, the progressive integration of motion responses across visual space is likely accommodated by long range horizontal connections within the retinotopic representations of V1, V2 and V3: objects that move to an adjacent location in visual space produce neural signals in adjacent locations on the cortex. However, cortical retinotopy is not fully continuous (e.g. cortical disjunction of left/right hemifields). Differences in prediction effects were therefore expected near locations where moving dots bridged cortical boundaries. Predictions to moving dots were additionally expected to be sensitive to the manner of dot displacement (i.e. the duration and velocity of visual motion). Longer motion durations would result in lower prediction errors and motion predictions might scale with motion velocity. Different motion displacement parameters are thus expected to influence the slope of the gradual decrease in prediction error across the full length of the motion stimulus. As hypothesized, a gradual decrease in BOLD signal was measured as dots moved further away from the stimulus' trailing edge. This finding is a clear indication of motion prediction mechanisms in early visual cortex, especially since expected contributions of classical receptive field effects near the trailing edge were not confirmed. Furthermore, predictive encoding of motion input is likely achieved through horizontal connections since the pattern of motion predictions appears to be reset when dots cross cortical boundaries. However, effects of motion displacement on the prediction-induced signal decrease were equivocal. Motion duration resulted in an opposite effect as hypothesized, while motion velocity exerted no effect at all. The lack of influence of motion displacement parameters on motion prediction suggests that the

trajectory of moving dots is not literally predicted. The visual system might instead mimic predictions to motion input by means of an automatic heuristic suppression.

The previous chapters describe predictive integration of motion responses during perception of random dot kinematograms with high spatial contrast. The results might therefore be specific to integration mechanisms for global motion processing[13]. In **Chapter 5**, predictive processing of motion input is investigated for just a single moving bar stimulus. Similar to random dot kinematograms, a single fluently moving bar stimulus resulted in a gradual decrease in BOLD amplitudes from onset to offset of the bar's trajectory. Interestingly, not only the BOLD amplitude decreased as the bar progressed across visual space, the initial dip of the BOLD response became more pronounced. The initial dip is thought to reflect the immediate increase in de-oxyhemoglobin following neural stimulation. However in this context, the initial dip might be taken to reveal an active suppression of neural activity. To test whether the signal decrease was in fact caused by a predictive motion integration mechanism two separate experiments were conducted with stepwise moving bar stimuli. The first stimulus consisted of a bar stimulus presented at 20 discrete consecutive locations, while the contrast of the bar stimulus remained constant (coherent stepwise motion). The second stepwise bar stimulus was similar with respect to the first stepwise stimulus, except the bar's contrast switched between black and white at every other location (incoherent stepwise motion). The coherent stepwise bar stimulus produced a similar prediction pattern as the fluent moving bar stimulus. However, the incoherent stepwise bar stimulus did not reveal any prediction pattern at all. These results indicate that early visual cortical areas anticipate the trajectory of a single motion stimulus by means of actively suppressing predictable low-level motion features.

Discussion

The current thesis explores visual motion processing mechanisms using 7 Tesla fMRI. We have investigated whether local cortical changes in the BOLD signal could reveal the underlying mechanisms, used by the visual system to integrate visual motion input to create stable and coherent motion percepts. We have consistently found enhanced BOLD signals near the onset of motion trajectories and suppressed BOLD signals towards the end of motion trajectories. These signal anisotropies are not confined to the visual field representations of motion on- and offsets, but gradually decrease as motion

stimuli progress across the visual field. We have found this to be true for both random dot kinematograms and single moving objects. The gradual decrease in BOLD activity plausibly exposes the neural mechanisms at work, when the visual system is confronted with visual motion input.

Classical receptive field effects

One could argue that the presence of directional motion biases can already be explained by classical receptive field effects. Neurons coding for visual field locations of a motion stimuli's trailing edge (i.e. the onset of motion trajectories) might receive new visual input directly in the center of their receptive fields due to the stimulus aperture. The aperture occludes motion information up to point of entrance within the stimulus area, possibly allowing new motion information to appear directly in a neuron's receptive field. This stands in contrast to neuronal input at other portions of a motion stimulus, where motion gradually moves into the center of a receptive field. More specifically, the initial stimulation of a neuron's OFF-surround might be absent directly at the trailing edge, whereas OFF-surrounds will be stimulated prior to the stimulation of the ON-center for the remainder of the motion trajectory. The different dynamics of neuronal stimulation near the trailing edge could produce large transient responses in comparison to the stimulation of neurons further down the motion trajectory[14–16.] Hence, classical receptive field effects could at least have contributed to the enhanced BOLD signals at the trailing edges measured during current experiments. However, there are certain limitations to the contribution of classical receptive field effects. In early visual cortex (i.e. V1, V2 and V3) receptive field sizes are relatively small even for peripheral visual field locations. Receptive field sizes in V1 corresponding to the extremities of stimulus locations used in current experiments rarely exceed 1° visual angle. Receptive field sizes in extra-striate areas V2 and V3 are larger, but still rarely exceed 3° visual angle in diameter[17,18]. If classical receptive fields effects enhance neural activity, it would thus be limited to a small restricted area near the representation of the trailing edge. Contrastingly, in Chapters 3,4 & 5 we report a gradual signal decrease over the full length of motion trajectories stretching over 15° visual angle. The reported gradual signal decrease exceeds the range of classical receptive field effects substantially. Furthermore, we specifically investigated possible contributions of classical receptive field effects in Chapter 4. The hypothesized model of classical receptive field effects was unable to sufficiently explain the observed effects.

These results indicate that classical receptive field effects did not sufficiently contribute to measured patterns of BOLD responses.

Visuo-spatial attention

The decrease in amplitudes of BOLD responses from trailing to leading edge is most likely accomplished through extraclassical receptive field effects. Extraclassical receptive field effects cover a wide variety of possible mechanisms, including (covert) shifts in spatial attention. It is not unthinkable that the appearance of novel motion information at the trailing edge draws the attention of the observer. Accordingly, spatial attention has been shown to locally enhance BOLD responses[12,19,20]. It is therefore possible that the observed BOLD signal enhancements at motion trailing edges do not reflect motion processing mechanisms, but rather shifts in spatial attention. However, there are several reasons why spatial attention is an unsatisfactory explanation. Firstly, all experiments were conducted, while participants fixated at the center of the screen where an attention task was presented. Participants were instructed to only carry out the attention task and ignore any of the presented motion patterns. The attention task showed that participants in approximately 80% of the time had pressed the corresponding button on a button box, given 1 of 4 possible attention cues. This is a clear indication that participants were attending the center of the screen. Secondly, the control experiment presented in Chapter 3 was conducted to investigate effects of shifts in visuo-spatial attention. The experiment showed that a threefold increase in the number of trailing and leading edges (2 vs. 6) had no effect on enhanced BOLD activity near trailing edges. If visuo-spatial attention had caused enhanced BOLD activity at the locations of motion signal appearance, dividing one's attention over three times the number of trailing edges would likely have attenuated the effect. Finally, in Chapter 5 we showed that a single coherent stepwise moving bar also produced BOLD enhancements near the onset of its trajectory, whereas the incoherent stepwise bar stimulus did not. Importantly, the presentation of the bar stimulus at its initial location was equal for both types of stepwise moving bar stimuli. Visuo-spatial attention would have been drawn equally towards the initial bar location for both stimuli. The observed pattern of BOLD responses during coherent motion (i.e. both dot patterns and bar stimuli) is therefore not likely confounded by extraclassical receptive field effects related to visuo-spatial attention. Rather, the results indicate that extraclassical receptive field effects related to motion processing offer the best explanation.

Cortical visual motion processing

Early visual cortex contains many motion sensitive neurons, plausibly signaling motion input in accordance with the Reichardt motion sensor model[21,22]. The experiments presented in the current thesis clearly show that the BOLD responses to motion input differ with respect to the visual field representation of the motion stimulus in combination with the motion direction. One could argue that these are caused by a priori biased preferences for radial motion directions[23,24]. This would be in line with the direction of translation of visual sceneries during self-locomotion. In Chapter 2 we accordingly report biased BOLD responses for radial versus tangential motion directions during the presentation of a coherent motion stimulus. However, in Chapter 3 we explicitly disprove that biased BOLD responses solely rely on the presented motion direction. At certain fieldmap locations we showed that biased motion responses fully depend on the relative distance between the visual field location and trailing edge of the motion stimulus regardless of motion direction. Furthermore, the dependence of the BOLD signal decrease along the motion trajectory on an uninterrupted motion stimulus is in support of mechanisms for motion integration.

Several studies have suggested that motion integration entails the summation (or pooling) of detector activity over space and time[25,26]. The summation of motion detector activity could affect motion signals along the entire motion trajectory. In addition, if motion information is pooled over extensive portions of the visual field, then a smear, or motion blur, of detector activity across cortical representations might be expected[27]. Motion blur has actually been suggested to aid visual motion integration over larger spatial distances. The visual system might benefit from the blurry representation of a motion trajectory to determine the global motion direction[28]. However, there is no direct physical indication of motion trailing edges being more smeared out over cortical activity than the leading edges. The summation of motion signals would roughly be equal along the entire trajectory, given that an object moves coherently in one direction at a constant velocity. Motion pooling or blur cannot explain the enhanced activity at the trailing edge, nor the gradual decrease in BOLD activity along a motion trajectory. Furthermore, several psychophysical studies have reported that motion stimuli actually appear sharpened to human observers, rather than blurred[29,30]. To account for this mismatch the visual system arguably enforces an additional motion deblurring mechanism to accomplish sharpened

percepts of moving objects[28,31,32]. The deblurring of cortical motion signals might not be isotropic along a motion trajectory and trailing edges have been suggested to receive relatively more deblurring[11,33]. Excessively deblurred trailing edges might then result in differential motion signals. However, motion deblurring mechanism are thought to be essentially suppressive[31], which does not fit well with the enhanced BOLD activity at the trailing edge as currently reported. Furthermore, motion deblurring as an explanation for current findings is also unable to explain the gradual signal decrease in amplitudes of BOLD responses with distance from the trailing edge, given there is no reason to expect different blurring of objects that translate linearly at constant velocity.

Predictive coding

From the studies presented in this thesis, it is clear the BOLD activity is enhanced at the onset of a motion stimulus, and gradually decreases along its trajectory. This finding most likely represents a prediction mechanism with respect to visual input. At the onset of motion trajectories motion information enters the visual field. Since this coincides with the first instance of motion detection, visual neurons cannot predict the occurrence of any motion signal or change in contrast. However, as the moving stimulus progresses across visual space, increasingly more motion detectors signal the stimulus and its future trajectory becomes increasingly more likely. Could it be that motion responses in early visual cortex are adjusted in direct proportion to this likelihood of detection? If so, the visual system might be actively predicting its future input. Predictive coding is a mechanism by which predictions could be estimated and utilized to encode neural input[8,34]. In predictive coding, neurons would only signal input that was not predicted and therefore directly reflect the prediction error. Our results are in agreement with predictive coding, for novel motion information entering the stimulus area cannot be predicted resulting in a large prediction error, which is reflected by a relatively enhanced BOLD signal. As objects move along their trajectory, the prediction error decreases, which accounts for the gradual decrease in BOLD activity towards the end of motion trajectories.

There are, however, several aspects of predictive coding that are not in agreement with current findings. Commonly accepted models of predictive coding describe modulation of neural responses as a top-down feedback system. Predictions are estimated for all visual input and the mismatch between visual input and prediction is fed back to the detector. It

has also been suggested that visual area V2 accommodates predictions for the primary visual cortex[8]. In current studies, prediction effects of motion input have been obtained from all included visual areas (i.e. V1, V2, and V3). The low temporal resolution of the BOLD signal prevents direct inferences on the order of processing among early visual cortical areas. Nevertheless, predictive BOLD patterns were generally largest in extra-striate visual areas V2 and V3 (Chapters 2, 3 & 5). It appears contradictory that large effects of input prediction in extra-striate visual cortex are not fed back to the primary visual cortex, if predictive coding is realized as feedback processes from high- to low-level cortical areas. Chapter 5 accordingly shows that prediction effects must already occur at the earliest stages in visual processing. Effects of visual motion prediction were not found during disruptions of low-level motion coherence, while the stimulus was predictable from the participant's, and thus a high-level, point of view. Additionally, there is a pragmatic objection to the ontological account of predictions. If the visual system would estimate a prediction for each individual neuron, it would essentially create a buffer of the entire cortical visual field representation. Since receptive field sizes in early visual cortex are relatively small, buffering the entire visual field seems rather costly and inefficient. Instead, we found specific signs that the visual system does not literally accommodate input predictions. When a random dot pattern is re-scrambled every 500ms, as was the case during temporal decorrelations in Chapter 2, motion input would match predictions to a lesser extent. However, temporal decorrelations still resulted in enhanced BOLD activity for novel motion input similar to a fully coherent motion stimulus. Furthermore, in Chapter 4 it was hypothesized that actual predictions to moving dots would be sensitive to different motion durations and velocities. Prediction accuracy was expected to increase for longer motion durations and the spatial extent of predictions was expected to scale with velocity. However, varying motion stimulus durations resulted in the opposite effect and motion velocity had no effect on the signal decrease at all. These provide strong indications that the visual system does not literally predict the motion trajectories of moving dots.

Motion prediction through automatic suppression

If the visual system does not create predictions for every motion sensitive neuron, then how does the pattern of BOLD responses, which is in accord with a prediction mechanism, come about? Rather than entertaining actual predictions the visual system might mimic

predictions. Actual input predictions may be too expensive and it might suffice for the visual system to find solutions that are 'good enough'[35]. Hence, we propose a mechanism where motion detector activity is automatically suppressed along a motion trajectory. Whenever a motion detector is activated, it would automatically suppress adjacent detectors that represent sequential visual field locations of the motion trajectory. The amount of inhibition a motion detector applies to neighboring detectors could be inversely proportional to its own firing rate. Motion detectors that maximally respond to their preferred visual input would suppress adjacent motion detectors of similar input preference only marginally. These suppressed motion detectors therefore respond submaximally to their preferred visual input, which increases the amount of suppression that is applied to sequential neighboring motion detectors. By doing so, automatic suppression would increasingly inhibit detector activity along the motion trajectory. The probability of detecting input is heuristically determined and conveyed to the appropriate neurons that encode the future locations of the moving stimulus. Automatic suppression is therefore likely mediated through horizontal connections, which have been shown to connect neurons with similar input preferences[35,36]. Additional evidence for contributions of horizontal connections to the prediction-dependent BOLD signal is provided by experiments described in Chapter 4. After moving dots crossed horizontal or vertical meridians (i.e. cardinal axes of the visual field), the BOLD amplitude in extra-striate cortex increased considerably. The cardinal axes correspond to the locations where the extra-striate cortical representation of the visual field is physically separated. This means that no horizontal connections are present that could transfer the prediction-induced suppression signal, which could result in the observed signal increase at physically separated cortical visual field representations. The suppression of detector activity occurs by a temporary hyperpolarization of the cell's membrane. The hyperpolarization might be directly observable in the BOLD signal. We observed in Chapter 5 that the entire shape of the BOLD response changed in relation to the novelty of the moving bar stimulus. Specifically, an initial dip emerged and became larger as the bar progressed along its trajectory. The initial dip is traditionally believed to reflect the immediate decrease in oxyhemoglobin/de-oxyhemobglobin ratio, following neural stimulation. However, there is no reason to expect that this initial effect would change with traveled distance of a moving stimulus. The variation in size of the initial dip cannot be taken to merely reflect cerebrovascular effects. Plausibly, the increasing initial dip reflects the increasing hyperpolarization of detectors along the stimulus trajectory.

The visual system would benefit greatly from an automatic suppression mechanism. It allows for determining the onset and offset of motion trajectories of individual as well as many simultaneously perceived motion stimuli. Integration of prior motion information provides additional information on the reliability of perceived visual input. Automatic suppression is therefore able to differentiate between actual motion signals and interfering noise signals for instance due to spontaneous neural activity[37,38]. A gradual signal decrease across spatially distant cortical locations may stand out under noisy or motion-rich visual conditions, thereby guiding neural computations towards probable solutions. Hence, the visual system with automatic motion suppression is adequately equipped to integrate real motion signals over cortical space coming from the same external source. This would allow for a kind of 'grouping' effect, which eventually allows human observers to perceive any moving object as stable, rather than as fragmented snapshots. Finally, it is worth noting that automatic suppression maintains a flexible attitude towards changes in visual input. A moving object that suddenly changes its direction will activate motion detectors sensitive to the new motion direction which were previously not stimulated. The newly stimulated motion detectors were not suppressed in any way and should therefore produce differential neural signals. Different neural responses to novel motion input might also be used in guiding attention towards changes in the visual field. Such neural behavior would likely have had evolutionary benefits for the detection of danger or predators.

Future directions

The current thesis presents compelling evidence that human early visual cortex anticipates visual motion input. During all experiments, participants were instructed to remain focused on an attention task at the center of the screen. Hence, the observed effects cannot be directly linked to certain psychophysical effects. There have been several studies that show lower detection thresholds for Gabor patterns near the leading edge of motion stimuli[39,40]. Possibly, the lower detection thresholds emerge as a side-effect of automatic suppression towards the leading edge, resulting in a surplus of available resources for signal detection. However, the low detection thresholds were found for areas beyond the location of a motion stimulus, which leaves the actual perceptual effects of automatic suppression on motion stimuli uninvestigated. An interesting line of investigation would

be to provide a psychophysical assessment of the influence of automatic suppression on motion direction discrimination under conditions with low motion coherence.

Additionally, assessment of the role of separate cortical layers in automatic suppression would be of great relevance. Using high-field fMRI, it has become possible to measure BOLD activity at submillimeter voxel sizes[41,42]. The thickness of gray matter in visual cortex is relatively modest compared to other brain areas (~2mm). Having voxel sizes smaller than 1mm isotropic, would provide a way to profile the pattern of BOLD activity across the different cortical layers during visual motion experiments. Plausibly, each cortical layer occupies a different part of the processing chain, while anticipating motion input.

Finally, the role of upstream cortical areas in automatic suppression for motion anticipation was not investigated. To obtain a full picture of the involved mechanisms, it is essential to identify the role of areas like MT and MST in motion anticipation mechanisms. A previous study has shown that enhanced BOLD activity for novel motion information was not measured in area MT[3], despite its well-known relation to motion processing[43,44]. Arguably, receptive field sizes in MT are too large to differentiate between specific parts of the motion trajectory. Alternatively, information from lower-level areas (e.g. V1 & V2) is converged in a certain manner that negates motion anticipation effects. Thus, finding out whether MT is subjected to motion anticipation effects could reveal essential information on the role of upstream areas for visual motion processing that leads to motion perception.

Conclusion

The current thesis shows that fMRI BOLD responses to motion stimuli reveal enhanced neural activity for novel visual motion input and suppressed neural activity for previously detected visual motion input. We have been able to refute several viable explanations that could account for the observed effects, such as classical receptive field effects, spatial attention and mechanisms specific to visual motion processing. The changes in neural activity are best explained by a prediction mechanism. However, the current results explicitly deviate from more standard models of predictive coding. We advocate a heuristic account of predictive coding where motion detector activity is automatically suppressed along the direction of motion. The automatic suppression allows the visual system to anticipate previously detected motion input in an efficient manner. As a result,

automatic suppression for motion anticipation produces unique signals for unique sources of visual motion. It enables the visual system to glue space, time and external source back together, underlying the formation of stable visual percepts of the highly dynamic visual sceneries that lie before our eyes.

References

1. Huk, A. C. & Heeger, D. J. Pattern-motion responses in human visual cortex. Nat. Neurosci. 5, 72–5 (2002).
2. Smith, A. T., Greenlee, M. W., Singh, K. D., Kraemer, F. M. & Hennig, J. The processing of first- and second-order motion in human visual cortex assessed by functional magnetic resonance imaging (fMRI). J. Neurosci. 18, 3816–30 (1998).
3. Raemaekers, M., Lankheet, M. J. M., Moorman, S., Kourtzi, Z. & van Wezel, R. J. A. Directional anisotropy of motion responses in retinotopic cortex. Hum. Brain Mapp. 30, 3970–80 (2009).
4. Clifford, C. W. G., Mannion, D. J. & McDonald, J. S. Radial biases in the processing of motion and motion-defined contours by human visual cortex. J. Neurophysiol. 102, 2974–81 (2009).
5. Maloney, R. T., Watson, T. L. & Clifford, C. W. G. Determinants of motion response anisotropies in human early visual cortex: The role of configuration and eccentricity. Neuroimage 100, 564–79 (2014).
6. Wang, H. X., Merriam, E. P., Freeman, J. & Heeger, D. J. Motion Direction Biases and Decoding in Human Visual Cortex. J. Neurosci. 34, 12601–12615 (2014).
7. Beckett, A., Peirce, J. W., Sanchez-Panchuelo, R.-M. M., Francis, S. & Schluppeck, D. Contribution of large scale biases in decoding of direction-of-motion from high-resolution fMRI data in human early visual cortex. Neuroimage 63, 1623–32 (2012).
8. Rao, R. P. & Ballard, D. H. Predictive coding in the visual cortex: a functional interpretation of some extraclassical receptive-field effects. Nat. Neurosci. 2, 79–87 (1999).
9. Mumford, D. On the computational architecture of the neocortex. Biol. Cybern. 66, 241–251 (1992).
10. Friston, K. A theory of cortical responses. Philos. Trans. R. Soc. Lond. B. Biol. Sci. 360, 815–36 (2005).
11. Whitney, D. et al. Flexible retinotopy: motion-dependent position coding in the visual cortex. Science 302, 878–81 (2003).
12. Tootell, R. B. et al. The retinotopy of visual spatial attention. Neuron 21, 1409–22 (1998).
13. Bartels, A., Zeki, S. & Logothetis, N. K. Natural vision reveals regional specialization to local motion and to contrast-invariant, global flow in the human brain. Cereb. Cortex 18, 705–17 (2008).
14. Borg-Graham, L. J., Monier, C. & Frégnac, Y. Visual input evokes transient and strong shunting inhibition in visual cortical neurons. Nature 393, 369–73 (1998).
15. Gieselmann, M. a & Thiele, a. Comparison of spatial integration and surround suppression characteristics in spiking activity and the local field potential in macaque V1. Eur. J. Neurosci. 28, 447–59 (2008).
16. Allman, J., Miezin, F. & Mcguinness, E. Stimulus Specific Responses from beyond the Classical Receptive Field: Neurophysiological Mechanisms for Local-Global Comparisons in Visual Neurons. Annu. Rev. Neurosci. 8, 407–430 (1985).
17. Dumoulin, S. O. & Wandell, B. a. Population receptive field estimates in human visual cortex. Neuroimage 39, 647–60 (2008).
18. Gattass, R., Sousa, A. P. & Rosa, M. G. Visual topography of V1 in the Cebus monkey. J. Comp. Neurol. 259, 529–548 (1987).
19. Liu, T., Pestilli, F. & Carrasco, M. Transient attention enhances perceptual performance and fMRI response in human visual cortex. Neuron 45, 469–477 (2005).
20. Watanabe, T. et al. Attention-regulated activity in human primary visual cortex. Journal of neurophysiology 79, 2218–2221 (1998).
21. Van Santen, J. P. H. Van & Sperling, G. Elaborated Reichardt detectors. J. Opt. Soc. Am. A. 2, 300–21 (1985).
22. Reichardt, W. Autocorrelation, a principle for the evaluation of sensory information by the central nervous system. Sens. Commun. 303–317 (1961).
23. Albright, T. D. Centrifugal directional bias in the middle temporal visual area (MT) of the macaque. Vis. Neurosci. 2, 177–188 (1989).
24. Edwards, M. & Badcock, D. R. Asymmetries in the sensitivity to motion in depth: a centripetal bias. Perception 22, 1013–1023 (1993).
25. Webb, B. S., Ledgeway, T. & McGraw, P. V. Cortical pooling algorithms for judging global motion direction. Proc. Natl. Acad. Sci. U. S. A. 104, 3532–7 (2007).
26. Amano, K., Edwards, M., Badcock, D. R. & Nishida, S. Adaptive pooling of visual motion signals by the human visual system revealed with a novel multi-element stimulus. J. Vis. 9, 1–25 (2009).
27. Burr, D. Motion smear. Nature 284, 164–165 (1980).
28. Geisler, W. S. Motion streaks provide a spatial code for motion direction. Nature 400, 65–9 (1999).
29. Hammett, S. T., Georgeson, M. a & Gorea, a. Motion blur and motion sharpening: temporal smear and local contrast non-linearity. Vision Res. 38, 2099–108 (1998).

30. Ramachandran, V. S., Madhusudhan Rao, V. & Vidyasagar, T. R. Sharpness constancy during movement perception. Perception 3, 97–98 (1974).
31. Wallis, T. S. a & Arnold, D. H. Motion-induced blindness and motion streak suppression. Curr. Biol. 19, 325–9 (2009).
32. Anderson, C. H. & Van Essen, D. C. Shifter circuits: a computational strategy for dynamic aspects of visual processing. Proc. Natl. Acad. Sci. U. S. A. 84, 6297–6301 (1987).
33. Arnold, D. H., Thompson, M. & Johnston, A. Motion and position coding. Vision Res. 47, 2403–10 (2007).
34. Lee, T. S. & Mumford, D. Hierarchical Bayesian inference in the visual cortex. J. Opt. Soc. Am. A 20, 1434 (2003).
35. Cornelissen, F. W., Brenner, E. & Smeets, J. True color only exists in the eye of the observer. Behavioral and Brain Sciences 26, (2003).
36. Gilbert, C. D. & Wiesel, T. N. Columnar Specificity of Intrinsic Horizontal and Corticocortical Connections in Cat Visual Cortex. J. Neurosci. 9, 2432–2442 (1989).
37. Gilbert, C. D. Horizontal integration in the neocortex. Trends Neurosci. 8, 160–165 (1985).
38. Cai, D., Rangan, A. V & McLaughlin, D. W. Architectural and synaptic mechanisms underlying coherent spontaneous activity in V1. Proc. Natl. Acad. Sci. U. S. A. 102, 5868–5873 (2005).
39. Mao, B. Q., Hamzei-Sichani, F., Aronov, D., Froemke, R. C. & Yuste, R. Dynamics of spontaneous activity in neocortical slices. Neuron 32, 883–898 (2001).
40. Roach, N. W., McGraw, P. V & Johnston, A. Visual motion induces a forward prediction of spatial pattern. Curr. Biol. 21, 740–5 (2011).
41. Arnold, D. H., Marinovic, W. & Whitney, D. Visual motion modulates pattern sensitivity ahead, behind, and beside motion. Vision Res. 98, 99–106 (2014).
42. Duyn, J. H. The future of ultra-high field MRI and fMRI for study of the human brain. NeuroImage 62, 1241–1248 (2012).
43. Petridou, N. et al. Pushing the limits of high-resolution functional MRI using a simple high-density multi-element coil design. NMR Biomed. 26, 65–73 (2013).
44. Tootell, R. B. H. et al. Functional analysis of human MT and related visual cortical areas using magnetic resonance imaging. J. Neurosci. 15, 3215–30 (1995).
45. Simoncelli, E. P. & Heeger, D. J. A model of neuronal responses in visual area MT. Vision Res. 38, 743–761 (1998).

Chapter 7

Nederlandse Samenvatting

Inleiding

Onze ogen worden bijna continu blootgesteld aan visuele bewegingsprikkels. Objecten bewegen in het visuele veld en wij, de waarnemers, bewegen in de omgeving. Toch is het brein in staat om alle visuele bewegingsinformatie als dusdanig te interpreteren dat er een stabiele waarneming ontstaat. Dat is nog niet zo eenvoudig, daar individuele neuronen in vroeg-visueel corticale gebieden input ontvangen van een beperkt gedeelte van het netvlies en dus het visuele veld (i.e. een neurons receptief veld). Hoe bepaalt het brein of gedetecteerde bewegingsinformatie in een specifiek receptief veld reeds door andere neuronen is gedetecteerd of dat beweging zich nieuw in het visuele veld begeeft? Het visuele systeem staat voor de lastige opdracht om overeenkomstigheid tussen individuele visuele prikkels te bepalen, hetgeen noodzakelijk is om een stabiele waarneming te creëren van de continue veranderingen in het visuele veld. In dit proefschrift wordt onderzocht met behulp van 7 Tesla BOLD fMRI hoe vroeg-visueel corticale gebieden bewegingsinformatie integreren over de ruimte en tijd. Tevens wordt onderzocht of de integratie van bewegingsinformatie gepaard gaat met voorspellingen over toekomstige visuele bewegingsinput.

Ondanks het bestaan van talrijke modellen aangaande de verwerking van visuele bewegingsinformatie, is het onduidelijk welke berekeningen exact worden uitgevoerd om visuele bewegingsintegratie over langere afstanden te bewerkstelligen. Het is bekend dat vele neuronen in visuele cortex sterk reageren op bewegende stimuli, zoals ‘random dot kinematograms’ (bewegende willekeurige stippatronen). Echter, de amplitudes van het BOLD-signaal (i.e. neurale activatie) variëren sterk over de representaties van een bewegingsstimulus naar gelang de aangeboden bewegingsrichting (i.e. directionele bewegingsbias). Een relatief verhoogd BOLD-signaal is gevonden voor centripetale beweging in de periferie van het visuele veld en voor centrifugale beweging rond corticale representaties van de fovea. Bewegingsbiases verdwijnen echter weer, wanneer de bewegingstrajecten van een random dot kinematogram gedeeltelijk worden onttrokken van het zicht. Deze bevinding laat zien dat de aanwezigheid van directionele bewegingsbiases in vroeg-visuele cortex direct gerelateerd is aan de integratie van bewegingsinformatie.

Experimenten

Of de integratie van bewegingsinformatie alleen plaatsvindt over de ruimte of over de ruimte en tijd wordt onderzocht in **Hoofdstuk 2**. Door bewegingsstimuli te verstoren op vaste punten in de ruimte of tijd (i.e. spatiële of temporele decorrelaties) kon naar gelang de aan- of afwezigheid van bewegingsbiases onderzocht worden welke informatie vereist is voor de integratie van bewegingssignalen. De studie toont aan dat bewegingsbiases niet verdwenen, wanneer de coherentie van bewegingsstimuli op vaste punten in de tijd verstoord werden. Echter, bewegingsbiases werden aanzienlijk kleiner en verdwenen soms, wanneer de bewegingsstimuli op vaste punten in de ruimte werden verstoord. Zo is het patroon van neurale signalen in V1, V2 en V3 wanneer deelnemers beweging waarnamen afhankelijk van de lengte van een ononderbroken bewegingstraject. Deze resultaten bieden echter geen antwoord waarom bewegingsbiases consistent bij bepaalde visuele veldrepresentaties gevonden worden in combinatie met een specifieke bewegingsrichting. Wanneer de resultaten op een alternatieve manier bekeken worden, blijkt dat bewegingsbiases altijd plaatshebben bij een stimulusrand, waar bewegingsinformatie (op)nieuw het visuele veld betreedt. Bewegingsbiases representeren waarschijnlijk de ruimtelijke integratie van bewegingsinformatie op basis van de nieuwheid van de stimulus.

In **Hoofdstuk 3** is het effect van stimulusnieuwheid op bewegingsbiases verder onderzocht. Neurale signalen in vroeg-visuele cortex worden mogelijkerwijs beïnvloed door de nieuwheid van bewegingsstimuli, wat kan betekenen dat het visuele systeem voorspellingen maakt van visuele bewegingsinformatie. Een dergelijke interpretatie wordt ook beschreven in modellen van ‘voorspellende codering’, die de actieve voorspelling van neurale input en de daaropvolgende onderdrukking van neurale signalen uiteenzetten. We hebben de hypothese van voorspellende codering getest door verscheidene bewegingspatronen te projecteren op een specifieke plek in het visuele veld (i.e. doelgebied), terwijl we de presentatie van de ‘leidende’ en ‘aflopende’ kant van bewegingspatronen varieerden ten opzichte van het doelgebied waar de neurale activatie gemeten werd. Nieuwe bewegingsinformatie betrad het stimulusgebied bij de aflopende kant van de bewegingsstimulus, terwijl de bewegingsinformatie de maximale lengte had afgelegd bij de leidende kant van het bewegingspatroon. De experimenten resulteerden in verhoogde BOLD-signalen in het doelgebied, wanneer de aflopende kant van de stimulus

nabij het doelgebied geprojecteerd werd en onderdrukte BOLD-signalen wanneer de leidende kant zich nabij het doelgebied bevond. Deze resultaten werden gemeten voor alle getoonde bewegingsrichtingen (i.e. radiaal en tangentieel) en de effecten bleven uit wanneer er geen verschil in trajectlengte was tussen leidende en aflopende kant ten opzichte van het doelgebied. Deze resultaten geven aan dat de bewegingsrichting zelf geen directe oorzaak van verhoogde BOLD-signalen op bewegingsstimuli is. In plaats daarvan lijkt het BOLD-signaal als gevolg van visuele beweging af te hangen van de nieuwheid van de stimulus op de plek waar gemeten wordt. Aanvullende experimenten lieten daarnaast zien dat de effecten niet veroorzaakt werden door alternatieve verklaringen, zoals klassieke receptieve-veldeffecten of verschuivingen in ruimtelijke aandacht. Directionele bewegingsbiases zijn dus afhankelijk van de nieuwheid van bewegingsinformatie, hetgeen resulteert in verhoogde BOLD-signalen in de buurt van de aflopende kant van een bewegingsstimulus, waar de nieuwe bewegingsinformatie nog niet voorspeld kan worden. Dus de amplitude van het BOLD-signaal lijkt proportioneel te zijn aan de grootte van de voorspellingsfout.

Het visuele systeem lijkt bewegingstrajecten over de visuele ruimte te voorspellen. In **Hoofdstuk 4** onderzochten we een aantal mogelijke gevolgen van visuele bewegingsvoorspelling in vroeg-visuele cortex. Als de amplitude van het BOLD-signaal recht evenredig is met de grootte van de voorspellingsfout, dan verwachten dat het BOLD-signaal geleidelijk afneemt naar mate bewegingsstimuli grotere gedeelten van een bewegingstraject hebben afgelegd. Invloeden van klassieke receptieve-veldeffecten kunnen ook worden waargenomen direct bij de locatie van de aflopende kant van de bewegingsstimulus. Bovendien is het mogelijk dat de geleidelijke verandering van het BOLD-signaal door voorspellende codering wordt gefaciliteerd door horizontale verbindingen in de vroeg-visuele cortex: objecten die verplaatsen naar aangrenzende locaties in het visuele veld, produceren ook neurale signalen in aangrenzende locaties op de cortex, die door horizontale verbindingen met elkaar in contact staan. Echter de corticale representaties van het visuele veld zijn niet volledig continu (e.g. corticale disjunctie van linker en rechter hemiveld). Derhalve verwachtten wij verschillen in het BOLD-signaal voor locaties waar bewegingsinformatie corticale grenzen overschrijdt. Tot slot, verwachtten we dat voorspellingen van bewegingsinformatie gevoelig zouden zijn voor de duur en snelheid waarmee de stimuli door het visuele veld bewegen. Hoe

langer beweging zichtbaar is, hoe accurater de voorspelling en voorspellingen worden geacht mee te schalen met de getoonde bewegingssnelheid. Derhalve zouden de duur en snelheid van beweging de mate van verval van het BOLD-signaal langs het bewegingstraject moeten beïnvloeden als de visuele cortex daadwerkelijk voorspellingen maakt van alle getoonde bewegingsinput. Zoals we hadden verwacht, nam het BOLD-signaal geleidelijk af naar mate bewegingsstimuli verder verwijderd raakten van de aflopende kant van de stimulus. Deze bevinding is een directie indicatie van voorspellende coderingmechanismen in visuele cortex, vooral omdat er nagenoeg geen bijdrage van klassieke receptieve veldeffecten nabij de aflopende kant van de stimulus gemeten werd. Voorspellende codering van beweging wordt hoogstwaarschijnlijk mogelijk gemaakt door horizontale verbindingen, daar de geleidelijke afname van het BOLD-signaal lijkt te worden gereset wanneer bewegingsstimuli corticale grenzen overschrijden. Echter, de effecten van duur en snelheid van beweging op de afname van het BOLD-signaal waren tegenovergesteld aan de hypotheses. Het ontbreken van duidelijke effecten van duur en snelheid op veronderstelde voorspellingen suggereert dat bewegingstrajecten niet letterlijk werden voorspeld. In plaats daarvan kan het visuele systeem voorspellingen van beweging nabootsen door middel van een automatische heuristische onderdrukking van neurale activiteit.

In de vorige hoofdstukken werd bewegingsintegratie op basis van voorspellende codering beschreven tijdens de waarneming van random dot kinematograms. De resultaten kunnen dan ook specifiek gerelateerd zijn aan mechanismen voor de verwerking van globale bewegingsinformatie. In **Hoofdstuk 5** wordt onderzocht of voorspellende bewegingsintegratie ook van toepassing is op één enkele bewegende balkstimulus. Net als tijdens random dot kinematograms veroorzaakte de projectie van één enkele vloeiend bewegende balkstimulus een geleidelijke afname van het BOLD-signaal van begin tot einde van het bewegingstraject. Echter niet alleen de amplitude van het BOLD-signaal daalde geleidelijk, ook de 'initiële dip' van het BOLD signaal werd sterker negatief. De initiële dip wordt hoogstwaarschijnlijk veroorzaakt door de onmiddellijke verhoging van de-oxyhemoglobine ten gevolge van neurale stimulatie. Maar in de huidige context kan de initiële dip mogelijk ook de onderdrukking van neurale activiteit weerspiegelen. Om te testen of de daling van het BOLD-signaal daadwerkelijk veroorzaakt wordt door een voorspellend integratiemechanisme, werden er 2 extra experimenten uitgevoerd

met stapsgewijs bewegende balkstimuli. Tijdens de eerste stapsgewijze stimulus werd een balk op 20 gescheiden opeenvolgende locaties geprojecteerd, terwijl het contrast gelijk bleef (coherente stapsgewijze beweging). De tweede stapsgewijze stimulus had dezelfde eigenschappen als de eerste stapsgewijze stimulus, behalve dat het contrast van de balk veranderde (zwart/wit) op elk van de 20 gescheiden posities (incoherente stapsgewijze beweging). De coherente stapsgewijze balkstimulus resulteerde in een vergelijkbaar patroon als de vloeiend bewegende balkstimulus. Echter de incoherente stapsgewijze balkstimulus liet geen enkel spoor van voorspellende codering meer zien. Deze resultaten laten zien dat vroeg-visueel corticale gebieden het bewegingstraject van individuele objecten anticiperen door middel van het onderdrukken van voorspelbare basale stimuluseigenschappen.

Conclusies

Het huidige proefschrift laat zien dat fMRI BOLD-signalen relatief vergroot worden tijdens de waarneming van nieuwe visuele bewegingsinformatie, terwijl BOLD-signalen worden onderdrukt tijdens de presentatie van reeds gedetecteerde visuele bewegingsinformatie. We hebben een aantal mogelijke alternatieve verklaringen kunnen weerleggen, waaronder klassieke receptieve veldeffecten en verschuivingen in ruimtelijke aandacht. De veranderingen in neurale activiteit worden het best verklaard door een voorspellingsmechanisme. Echter, de huidige bevindingen wijken expliciet af van standaard voorspellende coderingsmechanismen. Wij staan een heuristische variant van voorspellende codering voor, waarbij neurale activiteit automatisch wordt onderdrukt van begin tot eind van een bewegingstraject. Heuristische voorspellende codering stelt het visuele systeem in staat om reeds gedetecteerde bewegingsinformatie te anticiperen op zeer efficiënte wijze. Op dergelijke wijze kan het visuele systeem de gefragmenteerde neurale informatie van een uiterst dynamische visuele omgeving integreren tot een stabiel en coherent geheel.

List of Abbreviations

List of abbreviations

7T 7 Tesla

AP Anterior-to-Posterior

BOLD Blood-Oxygen-Level Dependent

CB Cortical Boundary

EPI Echo Planar Imaging

FH Foot-to-Head

fMRI Functional Magnetic Resonance Imaging

FOV Field Of View

GLM General Linear Model

Hz Hertz

LP Linear Prediction

MRI Magnetic Resonance Imaging

MST Medial Superior Temporal area

MT Medial Temporal area

pRF Population Receptive Field

RCG Retinal Ganglion Cell

RF Receptive Field

ROI Region Of Interest

RL Right-to-Left

SD Standard Deviation

SNR Signal-to-Noise Ratio

TE Echo Time

TR Repetition Time

V1 Visual area 1

V2 Visual area 2

V3 Visual area 3

VA Visual Angle

List of Publications

List of publications

Journal articles

Schellekens, W., Van Wezel, R. J., Petridou, N., Ramsey, N. F., & Raemaekers, M. (2013). Integration of motion responses underlying directional motion anisotropy in human early visual cortical areas. PloS one, 8(6), e67468.

Raemaekers, M., **Schellekens, W**., van Wezel, R. J., Petridou, N., Kristo, G., & Ramsey, N. F. (2014). Patterns of resting state connectivity in human primary visual cortical areas: a 7T fMRI study. Neuroimage, 84, 911-921.

Schellekens, W., van Wezel, R. J., Petridou, N., Ramsey, N. F., & Raemaekers, M. (2014). Predictive coding for motion stimuli in human early visual cortex. Brain Structure and Function, 1-12.

Conference abstracts

Schellekens W., Ramsey N.F., Raemaekers M. (2011). Directional anisotropy in retinotopic cortex for temporally decorrelated motion. Human Brain Mapping.

Schellekens W. Ramsey N.F. Raemaekers M. (2012). Motion anisotropies depend on motion stimulus novelty. Society for Neuroscience.

Schellekens W., Ramsey N.F., Raemaekers M. (2013). Predictive coding for motion information in early visual cortex. Society for Neuroscience.

Schellekens W. Ramsey N.F., Raemaekers M. (2014). Predictions to a single motion stimulus in early visual cortex. Human Brain Mapping.

Invited talks

Schellekens W. (2013). Effects of motion displacement on motion predictability. Rutgers University, New Jersey, USA.

Schellekens W. (2013). Predictive coding for motion information in early visual cortex. Society for Neuroscience, San Diego, USA.

Schellekens W. (2014). Predictive coding for single moving objects. University of York, York. UK.

Curriculum Vitae

Curriculum Vitae

Wouter Schellekens was born on the 20th of June 1983 in Rotterdam, Netherlands. In 2001 he graduated from his high school 'Erasmiaans Gymnasium' and moved to Utrecht to begin his study on Cognitive Artificial Intelligence at the University of Utrecht. There he developed a general interest in neuroscience and learned to find simple solutions for apparently difficult problems. During his M.Sc. thesis, he conducted an fMRI-study with Dr. Mathijs Raemaekers regarding voluntary changes in the perception a of multi-stable kinetic depth sphere. After he received his M.Sc. degree, Wouter accepted a job at Fortis Insurance Netherlands as a systems architect. However, he realized shortly after that the world of banking and insurance did not suit him all that well. After working for a year at Fortis, he quit his job to travel South-America for over 6 months in anticipation of several grant proposals. Upon returning in the Netherlands he was offered a Ph.D. position in 2010 at the lab of Prof. Dr. Nick Ramsey and was reunited with Dr. Mathijs Raemaekers to investigate directional motion biases using high-field 7 Tesla fMRI. There, he was able to put all his energy and creativity in the interesting problem of signal correspondence and showed that the human brain predicts future sensory input. His scientific interests have grown beyond fMRI-studies and he hopes to contribute to the field of computational neuroscience for years to come.

Dankwoord

Eindelijk is het zover, met trots presenteer ik mijn proefschrift! Ik heb hier de afgelopen jaren hard aan gewerkt, maar besef me dat dit niet mogelijk was geweest zonder de inbreng, hulp en vriendschap van een aantal belangrijke personen. Graag neem ik hier de ruimte om deze mensen, jullie, te bedanken.

Allereerst wil ik graag beginnen met de promovendi met wie ik de afgelopen jaren heb gewerkt en mij zijn voorgegaan: Dora, Erika, Floor, Gert, Jeroen, Martin, Matthijs en Patrick. Ik koester een berg goede herinneringen aan de congressen en lab-uitjes met jullie. Het is altijd weer feest als ik jullie tegenkom en ik hoop jullie nog vaak te zien! Mijn dank gaat ook uit naar mijn huidige lieve intelligente collegae in Nick's lab: Anna, Benny, Efraïm, Elmar, Erik, Mariana, Mariska, Mark, Martijn, Max en Zac. Jullie maken het lab tot wat het is: een waar festijn om in te werken. Hulde!

Als fMRI-onderzoeker ben je afhankelijk van de grillen van MR-scanners en zeker bij de 7 Tesla scanner krijg je het nodige gelazer voor je kiezen. Gelukkig is daar altijd die rots in de branding als de scanner een rothumeur heeft: de flowmanager. Ik heb met alle flowmanagers de kamer gedeeld en genoten van de grappige, belachelijke en ook serieuze gesprekken. Lotte, Elmar (alweer, mazzelpik), Bart en Milan bedankt voor alles en *happy scanning!*

Soms raakt je hoofd vol van codegepriegel, onderzoeksconfounders of reviewergeneuzel. In dat geval helpt het om je nicotinegehalte wat op te krikken. Gelukkig stond daar onderaan het Stratenum immer een vertrouwd gezelschap. Even uitblazen, discussietje, of gewoon genieten van de zon. Arjen, Bart, Kristel en Roger bedankt voor jullie vriendschap die uiteindelijk gestoeld is op de belangrijkere zaken in het leven: bier en sigaretten.

Dan wil ik nu graag de mensen bedanken die het dichtst bij mijn onderzoek stonden. Om te beginnen met Richard. Ik heb je input en betrokkenheid altijd zeer gewaardeerd. Hopelijk komt het er nog van dat we het project uitbreiden met calcium imaging. Ik denk dat daar nog heel veel mooie vondsten op ons liggen te wachten.

Next in line ist Natalia. Thank you so much for your help with the scanning protocols. Additionally, I'd like to thank you for the wonderful times at conferences and the lab diners

at any of the Greek restaurants in Utrecht (you wouldn't have anything to do with that, right?). I know where to find you when I'm in need of an excellent MR-physicist.

Dan wil ik nu diegene bedanken die zonder twijfel het dichtst bij mijn onderzoek stond. Mathijs, zonder jou was dit ongetwijfeld uitgelopen op één groot fiasco. Ik moet je bedanken dat je mij aan deze promotieplek hebt geholpen, voor die bergen fMRI-kennis, hoe je mij hebt begeleid deze jaren, hoe je mij hebt weerhouden om reviewers met een knuppel te lijf te gaan en waarschijnlijk nog wel veel meer. Het was absoluut mijn genoegen om jou als copromotor te hebben en ik hoop dat we nog vaak mogen samenwerken!

Dan gaat mijn dank uit naar mijn promotor. Nick, heel erg bedankt dat je mij de kans hebt gegeven om te promoveren (het was misschien een gokje). Ik heb met heel veel plezier in jouw lab gewerkt en mag dat gelukkig nog even blijven doen. Jouw kennis en kijk op de wetenschap heeft mij zonder enige twijfel vooruit geholpen. Ook heb ik altijd onze meetings gewaardeerd: kort en duidelijk met soms een klein uitstapje naar randzaken zoals squash (misschien komt onze langverwachte squashpot er nog van…). Nick, bedankt voor je vertrouwen en begeleiding!

Ik wil ook graag al mijn vrienden bedanken uit Utrecht en Rotterdam. Er zijn echter 4 jokers die ik in het bijzonder wil bedanken: Leon, Marcus, Matthijs en Merlijn. Eigenlijk hoef ik hier weinig woorden aan vuil te maken. Jullie zijn een mooi stel gasten. *Nimmer allein!*

Lieve zusjes, Anne, Esther en Sarah, na jarenlang jengelend en gillend mijn oren op de proef te hebben gesteld, zijn jullie uitgegroeid tot 3 prachtdames, die net iets minder jengelen en gillen. Ik kan altijd op jullie bouwen en ben trots dat jullie mijn zusjes zijn.

Ad en Anne, jullie mogen natuurlijk ook niet ontbreken in dit dankwoord. Het is altijd fijn om bij jullie thuis te komen; lekker eten en fijne gesprekken. Daarnaast is het ook te gek om fMRI-krantenknipsels op de mat te vinden! Gauw kom ik weer een weekje genieten in Frankrijk.

Lieve pa, Chris, het zal je allicht verbazen, maar het is gelukt. Echter, bij dit boekje was je ongetwijfeld ook in slaap gevallen op de bank. Ik had graag gewild dat je er nog bij had kunnen zijn. Ik heb veel van je geleerd en dit hele gebeuren was natuurlijk niet mogelijk geweest zonder jou, waarvoor dank.

Lieve moeders, Sas, je bent er altijd voor me geweest en nog steeds kan ik je lastigvallen met van alles en nog wat. Je hebt me altijd overal in gesteund: van judotoernooien in één of ander Brabants gat, tot een schier ongrijpbare studie. Dit proefschrift was onmogelijk geweest zonder jouw liefde en support. Mam, je bent mijn held!

En dan als laatste, Jiska. Onlangs ben je al in het dankwoord van een paar boeken verschenen (van een ander literair kaliber allicht) en je zei dat je misschien de muze van de hedendaagse literatuur zou kunnen worden. Dat kan zomaar gebeuren, zolang je maar weet dat je de mijne al bent. Lieve Jis, bedankt voor de pret, de feestjes, samen ("regenboogzwaai"), de slaapmutsjes, Jaap, dansen in de keuken en al onze dingen!